ELECTRONIC PROPERTIES OF DNA FROM SELECTED *Pleurotus* SPECIES USING DNA-SPECIFIC SCHOTTKY DIODES

NASTARAN RIZAN

FACULTY OF SCIENCE
UNIVERSITI MALAYA
KUALA LUMPUR

2021

ELECTRONIC PROPERTIES OF DNA FROM SELECTED *Pleurotus* SPECIES USING DNA-SPECIFIC SCHOTTKY DIODES

NASTARAN RIZAN

THESIS SUBMITTED IN FULFILMENT OF THE REQUIREMENTS FOR THE DEGREE OF DOCTOR OF PHILOSOPHY

INSTITUTE OF BIOLOGICAL SCIENCES
FACULTY OF SCIENCE
UNIVERSITI MALAYA
KUALA LUMPUR

2021

UNIVERSITI MALAYA

ORIGINAL LITERARY WORK DECLARATION

Name of Candidate: **NASTARAN RIZAN**

Matric No: **17035248/1**

Name of Degree: **DOCTOR OF PHILOSOPHY**

Title of Thesis ("this Work"):

ELECTRONIC PROPERTIES OF DNA FROM SELECTED *PLEUROTUS* SPECIES USING DNA-SPECIFIC SCHOTTKY DIODES

Field of Study: **BIOTECHNOLOGY**

I do solemnly and sincerely declare that:

(1) I am the sole author/writer of this Work;
(2) This Work is original;
(3) Any use of any work in which copyright exists was done by way of fair dealing and for permitted purposes and any excerpt or extract from, or reference to or reproduction of any copyright work has been disclosed expressly and sufficiently and the title of the Work and its authorship have been acknowledged in this Work;
(4) I do not have any actual knowledge nor do I ought reasonably to know that the making of this work constitutes an infringement of any copyright work;
(5) I hereby assign all and every rights in the copyright to this Work to the University of Malaya ("UM"), who henceforth shall be owner of the copyright in this Work and that any reproduction or use in any form or by any means whatsoever is prohibited without the written consent of UM having been first had and obtained;
(6) I am fully aware that if in the course of making this Work I have infringed any copyright whether intentionally or otherwise, I may be subject to legal action or any other action as may be determined by UM.

Candidate's Signature Date:

Subscribed and solemnly declared before,

Witness's Signature Date:

Name:

Designation:

ELECTRONIC PROPERTIES OF DNA FROM SELECTED *PLEUROTUS* SPECIES USING DNA-SPECIFIC SCHOTTKY DIODES

ABSTRACT

The exciting discovery of the semiconducting-like properties of deoxyribonucleic acid (DNA) and its potential applications in molecular genetics and diagnostics in recent times has resulted in a paradigm shift in biophysics research. In this aspect, recent studies are being conducted towards detecting charge transfer mechanism to understand the electronic properties of DNA based on its sequence-specific electronic response. This current research aims to contribute towards this effort by fabricating and developing DNA-specific Schottky barrier diodes for characterizing and identifying mushrooms using current-voltage (*I-V*) profiles. Selected electronic properties such as ideality factor, barrier height, shunt resistance, series resistance, turn-on voltage, knee-voltage, breakdown voltage and breakdown current were calculated. The data was further utilized to quantify the identification process as compared to conventional morphological and molecular characterization techniques. Conventional techniques are used in order to study biodiversity, but sometimes it can be misleading and unreliable and is not sufficiently useful for the identification of mushrooms genera especially for identification of closely related species in genus *Pleurotus*. In this research, genomic DNA as well as amplified specific regions (internal transcribed spacer, large subunit ribosomal DNA and large subunit of ribosomal polymerase II) of selected species of *Pleurotus* were subjected to *I-V* measurements. Both genomic and amplified DNA showed distinct profiles corresponding to each species. However, comparison of *I-V* profiles of genomic and amplified DNA suggested that genomic DNA is a better choice for electronic identification of species. This is mainly due to more base pair differences between genomic DNA of different species. High similarity in the conserved regions showed a closer yet distinguishable electronic profile for each species. The electronic profiles, both

in the negative and positive bias regions were however found to be highly characteristic according to the base-pair sequences. However, DNA charge transfer are significantly regulated by pH fluctuations which influences the stability of the double helix structure and strongly attenuated its electronic profile. To investigate the pH influence, genomic DNAs integrated within an aluminium (Al)-indium tin oxide (ITO) Schottky junction was prepared and its electronic profiles studied. Although DNA is known to be reasonably stable in aqueous solution, environmental factors can also affect the helical structure resulting in significantly attenuated electronic profiles. DNA molecules are not stable when stored for long periods in solution form at room temperature (RT) prompting much interests for solvents in which DNA structures exhibit long-term stability. Ionic liquid (IL), 1-butyl-3-methylimidazolium acetate ([BMIM][Ace]) is a potential solvent that ensure long-term stability of DNA. Therefore, the effect of IL on genomic DNAs was investigated by using the *I-V* profiles. Furthermore, various solid-state parameters calculated allow us to understand the charge transfer mechanism in DNA molecules as a function of pH conditions and IL, which could act as a potential indicator for various stages of DNA functionality.

Keywords: Fungal Deoxyribonucleic acid (DNA), semiconductor, solid-state parameters, Schottky diodes, DNA electronics.

SIFAT ELEKTRONIK DNA DARI SPESIS *PLEUROTUS* TERPILIH MENGGUNAKAN DIGITAL SCHOTTKY DNA-SPECIFIC

ABSTRAK

Penemuan menarik mengenai sifat semikonduktor asid deoksiribonukleik (DNA) dan potensi penggunaannya dalam genetik molekul dan diagnostik sejak kebelakangan ini telah menghasilkan perubahan paradigma dalam penyelidikan biofizik. Dalam aspek ini, kajian terkini dilakukan untuk mengesan mekanisme pemindahan cas untuk memahami sifat elektronik DNA berdasarkan tindak balas elektronik urutan khusus. Penyelidikan semasa ini bertujuan untuk menyumbang ke arah usaha tersebut dengan membuat dan mengembangkan diod penghalang Schottky khusus DNA untuk mencirikan dan mengenalpasti cendawan menggunakan profil voltan arus (*I-V*). Sifat elektronik yang dipilih seperti faktor idealiti, ketinggian penghalang, rintangan shunt, rintangan siri, voltan putar, voltan lutut, voltan kerosakan dan arus kerosakan telah dikira. Data tersebut selanjutnya digunakan untuk mengukur proses identifikasi berbanding teknik pencirian morfologi dan molekul konvensional. Teknik konvensional digunakan untuk mengkaji biodiversiti, tetapi kadang-kadang boleh mengelirukan dan sukar dipercayai serta kurang berguna untuk mengenalpasti genera cendawan terutama dalam mengenalpasti spesies yang berkait rapat dalam genus *Pleurotus*. Dalam penyelidikan ini, DNA genomik serta profil tertentu yang dipertingkatkan (transkripsi peregang dalaman, DNA ribosom subunit besar dan subunit polimerase ribosom II) dari spesies *Pleurotus* terpilih dilaksanakan pengukuran *I-V*. Kedua-dua DNA genomik dan penguat menunjukkan profil yang berbeza yang sesuai dengan setiap spesies. Walau bagaimanapun, perbandingan profil *I-V* genomik dan DNA yang dipertingkat menunjukkan bahawa DNA genom adalah pilihan yang lebih baik untuk mengenal pasti spesies secara elektronik. Ini terutama disebabkan oleh perbezaan pasangan asas antara DNA genomik dari pelbagai spesies. Persamaan yang tinggi di kawasan terpelihara menunjukkan cirian profil elektronik yang hampir

namun dapat dibezakan untuk setiap spesies. Profil elektronik, baik di kawasan bias negatif mahu pun positif bagaimanapun didapati sangat mengikut cirian urutan pasangan asas mereka. Walau bagaimanapun, pemindahan cas DNA diatur secara signifikan oleh perubahan pH yang mempengaruhi kestabilan struktur heliks berganda dan melemahkan profil elektroniknya. Untuk menyiasat pengaruh pH, DNA genom yang disatukan dalam persimpangan aluminium (Al) -indium timah oksida (ITO) Schottky telah disiapkan dan profil elektroniknya telah dikaji. Walaupun DNA diketahui cukup stabil dalam akueus, faktor persekitaran juga dapat mempengaruhi struktur heliks yang mengakibatkan profil elektronik dilemahkan dengan ketara. Ketidakstabilan molekul DNA apabila disimpan untuk jangka masa panjang dalam larutan akueus pada suhu bilik (RT) mendorong kajian agar struktur DNA menunjukkan kestabilan jangka panjang. Cecair ionik (IL), 1-butil-3-metilimidazolium asetat ([BMIM] [Ace]) adalah suatu pelarut berpotensi untuk memastikan kestabilan DNA jangka panjang. Oleh itu, kesan IL pada DNA genomik juga dikaji dengan menggunakan profil *I-V*. Selanjutnya, pelbagai parameter keadaan pepejal yang dikira memungkinkan kita memahami mekanisme pemindahan cas dalam molekul DNA sebagai fungsi keadaan pH dan IL, yang dapat bertindak sebagai petunjuk berpotensi untuk pelbagai tahap fungsi DNA.

Kata kunci: Asid Deoksiribonukleik (DNA) kulat, semikonduktor, parameter keadaan pepejal, diod Schottky, elektronik DNA.

ACKNOWLEDGEMENTS

I would like to express my gratitude to all those who gave me a helping hand to complete this thesis. Special thanks go to my supervisors, Associate Professor Doctor Vengadesh Periasamy, Associate Professor Doctor. Tan Yee Shin and Associate Professor Doctor Hairul Anuar Bin Tajuddin, who have been a source of motivation, guidance and affection for me during all this phase. No words can express your supports and constant helps to achieve my dream.

To my parents and my parents-in-law for playing a vital role and standing by my side with their endless encouragement. Thank you for your encouragement and your support. My husband, Arash Bayat Shahbazi who has always understood me, encouraged me and became my support system. Thank you for understanding me during my worst days. My sister and her husband for supporting me with their kind love and care. I am indebted to all of you.

I deem it my utmost pleasure to avail this opportunity to express the heartiest gratitude and a deep sense of obligation to Emeritus Professor Doctor Phang Siew Moi for her guidance and technical support. I gladly express my regards to Professor Dr Mitsumasa Iwamoto, Department of Physical Electronics, Tokyo Institute of Technology for his sincere support. My sincere gratitude to Assistant Professor Doctor Georgepeter Gnana kumar, Department of Physical Chemistry, Madurai-Kamaraj University, Madurai, India for his sincere support. I am thankful for the support and help of my research mates especially Chua Su Boon and all my friends especially Shadi Pourmehdi, Hamidreza Mansouri, Hoora Mazaheri, Kiarash Koushfar, Shinto Amiri, Zahra Shafieidoost, Hossein Siamaknejad, Yasaman Anisi, Ehsan Brousan, Tile, Tiam, Sormeh and Mishka.

TABLE OF CONTENTS

LIST OF FIGURES

LIST OF TABLES

LIST OF SYMBOLS AND ABBREVIATIONS

I-V	:	current-voltage
AFM	:	Atomic Force Microscopy
Al	:	Aluminium
aq/DNA	:	DNA in aqueous solution
[BMIM][Ace]	:	1-butyl-3-methylimidazolium acetate
bp	:	base pairs
COI	:	cytochrome c oxidase I
DNA	:	deoxyribonucleic acid
EB	:	ethidium bromide
H^+	:	hydrogen ion
PF_6^-	:	Hexafluorophosphate
IL	:	Ionic liquid
IL/DNA	:	DNA dissolved in [BMIM][Ace]
InP	:	indium phosphide semiconductor
ITO	:	indium tin oxide
ITS	:	internal-transcribed spacer
LED	:	light-emitting diode
LSU	:	nuclear large subunit
LEEPS	:	low-energy electron point source
MS	:	metal-semiconductor
OFET	:	organic field effect transistors
OH-	:	hydroxide ion
OI	:	organic-on-inorganic
PCR	:	polymerase chain reaction

PN	:	propylammonium nitrate
RDP	:	Ribosomal Database Project
RH	:	relative humidity
RNA	:	ribonucleic acid
RPB1		large subunit of RNA polymerase II
RPB2	:	RNA polymerase 2 second largest subunit
RT	:	room temperature
SMU	:	Source Measurement Unit
SSU	:	small subunit
T	:	temperature
TBE	:	Tris-Borate EDTA
TEF1-α	:	translational elongation factor 1-α
UV-VIS	:	Ultra-Violet Visible

LIST OF APPENDIX

CHAPTER 1: INTRODUCTION

1.1 Background of Study

The benefits of consuming mushrooms include important nutritive as well as medical value and have been widely used as human food since ancient times (Samiya et al., 2011). Through the passage of time, there was an increase in awareness regarding the benefits of mushrooms (Cheung, 1999), which was included into many food cultures around the world. Although mushrooms contain low amounts of calories and fat, they are rich in proteins and fibers (Deepalakshmi & Mirunalini, 2014; Manzi et al., 2001). Mushroom contains bioactive secondary metabolites with biological activities such as antibiotics, antivirals, antimycotics, antiprotozoans, cytotoxics and immunosuppressives, which make them extremely important for medicine, pharmaceutical and food industry applications. Many secondary metabolites act as virulence factors in plant and human pathogenic fungi; others act as protectants against other organisms or abiotic stress (e.g. UV shields).

Classification of mushroom to species level plays significant role in ecology, taxonomy, genomics and bioprospecting applications. Scientific names are important in communicating knowledge about mushroom. These names allow researchers to identify other closely related species or to prioritize taxonomically related strains when a productive species may attenuate production of key bioactive compounds. The impact to identify mushrooms on industrial, agrochemical or pharmaceutical products is enormous and continues to grow and would be a critical task (Stajich et al., 2009; Huzefa et al., 2017).

Due to the nutritive values of mushrooms, remarkable progress took place in the morphological and molecular characterization techniques (Staniaszeket al., 2002). The use of these techniques is necessary in order to study biodiversity but sometimes it can be misleading, inaccurate and are not sufficiently for the identification into species level.

Many of these methods have failed when it comes to identification of closely related species of genus *Pleurotus* (Iqbal et al., 2010). *Pleurotus* is a genus of gilled mushrooms which includes one of the most widely edible oyster mushrooms; *Pleurotus pulmonarius, P. floridanus* and *P. eryngii* are some of the common oyster mushroom (Philip & Shu-Ting, 2004). *Pleurotus* genus cannot be grouped easily using morphological factors because phenotypic variation in mushrooms can be affected by substrate and environmental factors (Avin et al., 2012). The taxonomy of *Pleurotus* species, even with all the efforts to identify it, has remained ambiguous (Junior et al., 2010).

According to Zervakis & Balis (1996), the taxonomic disagreements in the genus *Pleurotus* have risen for the following reasons; initial misidentification, absence of type specimens, instability of morphological characters due to environmental changes, limited reports on physiological characteristics and lack of mating compatibility studies. Therefore, to illuminate the taxonomic position of species in the genus *Pleurotus* (earlier determined mainly by morphological features), many researchers started to classify these mushrooms using molecular techniques (Bao et al., 2004). However, the use of molecular methods to differentiate between closely related species are also difficult because of the high similarity in conserved regions which may lead to misidentification (Pereira et al, 2008).

Production of smaller device and denser circuits are one of the mainstream attempts since the past few decades due to its increasing importance in the operation of electronic devices (Porath et al., 2006). Many researchers have utilized nanotechnology in order to build electronics segment and nano dimensional circuits. Therefore, integrating more segments in electronic devices provides more efficient devices as compared to conventional technology when it comes to nano-scale processing (Artés et al., 2014). In order to overcome the limitations in electronic devices, deoxyribonucleic acid (DNA) has

been employed in recent years due to the discovery of its ability of electrical conduction. There is much interest in the use of DNA molecules to build electronic devices which are smaller, faster and with higher energy efficiency for different fields (Porath et al., 2006).

In spite of numerous theoretical and experimental studies that has been done, the electronic properties of different DNA molecules remain unclear, demonstrated by the wide variety of conducting or non-conducting behaviors (Endres et al., 2004). However, it is well-understood that particles such as electrons and holes are the main cause of current flow in DNA (Fink & Schönenberger, 1999). The electrical conductivity of the DNA molecules depends on some strong environmental conditions such as variation with temperature, chemical composition of the solution, humidity, quality of the metallic contacts and others.

Dried DNA molecules were used in many previous researches in order to test their conductivity by applying a voltage between two gold electrodes (Heim et al., 2004; Gomez-Navarro et al., 2002; Braun et al., 1998). The outcomes of the experiments have reported that DNA can be considered as an insulator, ohmic, non-ohmic conductor (Fink & Schönenberger, 1999; Braun et al., 1998) or as a semiconductor (Porath et al., 2000). Later, several theoretical models were suggested to explain the direct conductivity measurement experiments. These concluded that DNA behaves as a 1-dimensional (1D) disordered system where a variable range of hopping mechanisms occur with dependence of localization lengths with temperature (Bagci & Krokhin, 2007). Figure 1.1 shows the schematic charge transfer in a molecule of DNA in terms of tunneling and hopping under thermoelectric effect as was reported in one study (Li et al., 2016).

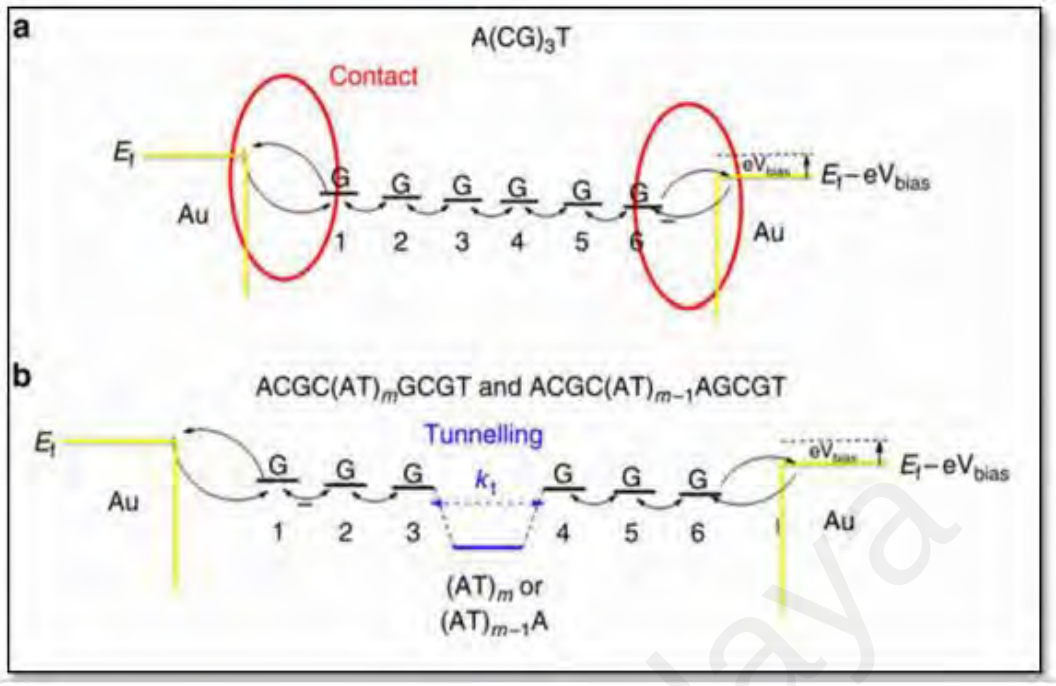

Figure 1.1: Schematic charge transfer in a molecule of DNA (a) illustrates the charge transport in A(CG)nT and (b) meanwhile shows the charge transport in ACGC (AT)mGCGT and ACGC(AT)m−1AGCGT (Source: Li, Xiang, Palma, Asai, & Tao, 2016).

Figure 1.1(a) illustrates the charge transport in A(CG)nT, where a hole is injected from the left electrode into the first G, then hops along the molecule with each G as a hopping site and eventually reaches the right electrode. The charge transfer rates at the contacts (red part) are energy dependent, which is a dominant contribution to the Seebeck coefficient. Figure 1.1(b) meanwhile shows the charge transport in ACGC (AT)mGCGT and ACGC(AT)m−1AGCGT, where a tunneling barrier (marked blue) arises from the AT block (Li et al., 2016).

The interface between biosystems and nanomaterials appears as one of the most diverse and dynamic areas of science and technology. Linear polymers such as DNA provide such molecules and the study of their conductive properties is therefore of high importance in designing molecular electronic devices. Specific DNA sequence detection is a major issue in life science. An important knowledge in this field was accomplished during the last two decades with the design of DNA biosensors (García-Martinez et al., 2011). The development of DNA biosensor has attracted considerable attention due to

their potential applications including clinical diagnostics, forensic study, gene analysis, environmental monitoring and food controls. Among the methods for DNA detection, electrochemical techniques offer great advantages with simplicity, rapidness, relatively low cost and high sensitivity (Jin et al., 2013).

Biosensors technology can be defined as a device that includes a combination of biological sensing elements with a transducer. Both of the components are supposed to integrate together for the purpose of producing a digital electronic signal, which is proportional to the concentration of a set of chemicals or a specific chemical stimulus. Therefore, the merging of the two contrasting disciplines combine the sensitivity and specificity of biological systems with the computing power of a microprocessor. This technology offers a powerful tool to be used as an alternative choice in analytic science (Turner et al., 1987). Biosensors essentially involve a biological component in the form of organisms, tissues, cells, organelles, membranes, enzymes, antibodies or nucleic acids. For the right functioning of this technique, the activity of this biological moiety needs to be preserved (Tembe et al., 2006).

DNA is a smart electronic material that could be easily configured for tuning specific electronic properties due to its complementary base pair specificity. And in recent years, the use of this new solid-state material has gained importance, especially in DNA electronics (Di Ventra & Zwolak, 2004; Bhalla et al., 2003) for developing effective DNA-based sensors (Al-Ta'ii, Amin, & Periasamy, 2015; Al-Ta'ii, Periasamy, & Amin, 2015; Al-Ta'ii, Periasamy, & Amin, 2016) Organic semiconductors are considered as alternative materials to conventional inorganics in electronic devices due to their low cost and the ease of processing. Therefore, the utilization of DNA molecules in biosensors demonstrates that DNA could be a good alternative due to its specific features such as nanometer-scale molecular film, adjustable length, self-assembly and self-replicate

properties besides the ability of adopting various states and conformations. There are other advantages in using DNA for these devices. The important and interesting issue in DNA based devices is their semiconductive behavior or response in the presence of external electric and magnetic fields (Sun & Kiang, 2005). DNA as a molecular wire plays an important role in exhibition of nonlinear behaviors in current-voltage (*I-V*) characteristic curves. Once DNA is sandwiched between metal layers, these wires enable charge transport phenomena similar to a transistor.

The nature of the conductive properties of duplex DNA has attracted substantial interest. Over the past two decades, a wide-ranging collection of experiments has both revealed the fundamental details of DNA-mediated charge transfer (CT) and illustrated its potential for sensing applications (Gorodetsky et al., 2009). In many published studies, the *I–V* data of double-stranded DNA molecules show a unique symmetrical S-shaped semiconducting curve with a non-conducting region near zero voltage (Sainz & Alfonso, 2012).

Unique DNA fingerprints corresponding to the specific base pairs content and sequence can be employed as a sensitive genomic identification tool. These characteristic electronic behaviors could find use in taxonomy, which is essential to biological science and is the basis of information exchange. Improved taxonomic awareness of edible mushrooms can help research on cultivation technology and breeding. For instance, awareness of the current taxonomy will assist to focus breeding strategy avoiding crosses between two apparent ‘species’ (strains bearing different names) that are taxonomically identical. The plasticity of basidioma morphology of different species, especially those distributed in different regions of the world and the inaccurate identification of commercial isolates has led to numerous names for the same species and incidences of misidentification (Buchanan, 1993).

The proposed method in this thesis involves acquiring electronic signature signals from semiconducting DNA molecules from different species of a closely related mushroom genus. Primarily, this involves the fabrication of a metal-semiconductor (DNA)-metal Schottky barrier diode, which quantitatively response to different DNA sequences when biased negative or positive. This variation in responses, which originates from DNA electronics were due to different base pair sequence giving rise to highly specific current profiles with bias voltage. The characteristic of *I-V* profiles was observed for both the negative and positive bias voltages from where various electronic parameters were measured. These quantified parameters were then used to effectively identify and detect the different mushrooms investigated in this research.

The challenge however is related to the sensitivity of DNA molecules due to physical factors such as variations in ionic strength, pH, temperature, solvent and other factors (Privalov & Ptitsyn, 1969). Varying pH conditions, for example, have been found to impart significantly higher biochemical fluctuations in terms of DNA functionality in cellular environments (Ageno et al., 1969; Luck et al., 1970; Wang et al., 2014; Lando et al., 1994; Costantino & Vitagliano, 1966; Williams et al., 2001; Cheng & Pettitt, 1992).

DNA is a molecule composed of two strands bound together by hydrogen bonds. Changes in pH conditions could denature DNA causing separation of these strands (Bhalla et al., 2003; Privalov & Ptitsyn, 1969; Gates, 2009). Denaturation is a process where nucleic acids lose the secondary, tertiary and quaternary structures which are present in their native states by applying some external stress or compounds such as strong acid or base, concentrated inorganic salt, organic solvent (e.g., alcohol or chloroform), radiation or heat (Gates, 2009; Todd, 1954; Watson & Crick, 1953). Generally, changes in the environmental conditions such as pH seem to have a significant effect on the charge conduction source of DNA and pathways (Rodríguez-Laguna et al.,

2015; Rychła et al., 2011; Watson et al., 1996; Lawrence & Smith, 1974). Denaturation of DNA is due to strong acidic or basic conditions and depends on the concentration of chemicals and the type of DNA (Segel, 1976). In this research, the pH-dependent DNA-specific Schottky junction structures were utilized to further understand the functionality of DNA conductivity and other parameters under various pH conditions.

Although DNA is considered stable in aqueous solutions, numerous studies have documented DNA stability in different non-aqueous and mixed solvents. These studies indicate that DNA is not stable and loses its double-helical structure when dissolved in formamide, methanol or dimethyl sulfoxide (Bonner & Klibanov, 2000; Hammouda & Worcester, 2006). Duplex DNA is conventionally stored at low temperature for short and long-term applications and the effect of storage temperature has been previously reported (Legoff et al., 2006; Vijayaraghavan et al., 2010; Röder et al., 2010). And in another study, DNA molecules in aqueous solution stored for more than one month at ambient temperatures were found to be unstable due to their inherent chemical instability and degradation by contaminating nucleases (Sasaki et al., 2007). Development of a new solvent capable of stabilizing and maintaining DNA for longer periods of storage at room temperature (RT) is therefore increasingly justified.

Ionic liquids (ILs) have proven to be the preferred solvents in many reactions over the past decade to replace conventional organic solvents and aqueous solution. They contain combination of cations and anions, and can be environmentally friendly green solvents due to their certain physico-chemical features such as low vapour pressure (close to zero), non-flammability, high chemical and thermal stability, low toxicity, high ionic conductivity, controllable hydrophobicity and hydrophilicity (Armand et al., 2009; Welton, 1999; Trincao et al., 2004; Fujita et al., 2007; Fujita & Ohno, 2010; Earle & Seddon, 2000; Huddleston et al., 2001; He et al., 2006). ILs have been used in various

applications based on their properties including in electrochemistry, organic synthesis, extraction/separation, materials science and other applications. Given their nature, they have been described as “designer” solvents because of its tunable features that can be customized for a diverse range of reactions (Avery et al., 2002; Huddleston et al., 1998; Smietana & Mioskowski, 2001; Fukumoto et al., 2005; Leone et al., 2001; Wasserscheid & Keim, 2000; Anderson et al., 2002; Chun et al., 2001; Blanchard & Brennecke, 2001; Kim et al., 2004; Zhou & Antonietti, 2003; Taubert, 2004; Scheeren et al., 2003).

In this research, DNA molecules from different species of oyster mushroom are mixed with [BMIM][Ace]and integrated within the Aluminium (Al)-DNA-ITO junction forming IL/DNA-Schottky junction diodes. The fluctuation of the electronic properties of DNA molecules in 1-butyl-3-methylimidazolium acetate ([BMIM][Ace]) was then interrogated upon application of increasing bias potentials to study the effect of IL as a solvent at RT.

1.2 Problem Statement

The taxonomic identification of mushrooms is a critical and essential topic that requires standardization to ensure reproducibility, especially in discovering bioactive secondary metabolites that could be used for drug discovery. However, this task needs accurate and advanced techniques for species identification that have ability to represent important information about a species and its potential biochemical properties. More importantly, this provides more insights into development of efficient screening programs that can be used for discovery of natural products. In addition, far more information can be achieved regarding the ecology, genomics, phylogenetic relationships and transcriptomics among the mushrooms. The use of morphology in identification of the fungal species is very important and can be helpful to understand the evolution of morphological characters. Moreover, it plays an important role in fungal taxonomic

studies in order to classify mushrooms at the ordinal or familial level but may not be useful for classification of species level (Wang et al., 2016).

There are different molecular diagnostic tools available for identification and detection of mushrooms. Unfortunately, all these molecular methods have their drawbacks. Their limitations include high detection limit and lower sensitivity, complex offline preparation procedures, labor-intensive incubation and purification steps, usage of carcinogenic chemicals such as ethidium bromide, technical and laboratory standards upgraded to a well-equipped laboratory (for DNA assays), technical expertise and time-consuming measurements. There are a number of biosensor methods already available for detection (Durmanov et al., 2017; Natarajan et al., 2017; Samanman et al., 2011). These methods are either electrochemical-based sensors requiring extended preparation steps, involves complicated processes or metal nanoparticles for functionalization which increases the cost of operation and/or involve chemicals.

Although DNA are known to be reasonably stable in aqueous solution, various environmental factors such as pH fluctuations and long periods of storage at RT can affect the stability of the double helix structure resulting in significantly attenuated electronic profiles. Therefore, in this research the effect of pH and ILs on basidiomycetes DNAs integrated within an Al-ITO Schottky junction will also be investigated to find the proper pH and also a solvent in which DNA structures exhibit long-term stability.

1.3 Aims and Objectives

The general objectives of this research are to fabricate the metal-semiconductor (DNA)-metal Schottky barrier diodes, which quantitatively response to different DNA sequences when biased negative or positive and to study its application in detection of macrofungi DNA. Therefore, the following research objectives will be addressed in this thesis;

- To investigate the phylogenetic relationship among *Pleurotus* spp using molecular methods.
- To fabricate DNA-specific Schottky diodes.
- To conduct *I-V* characterization studies of the DNA samples and calculation of various quantitative electronic parameters of the DNA-metal junctions using genomic and PCR-amplified DNA sequences.
- To evaluate the changes in genomic DNA conductivity by changing the pH of the DNA solution.
- To evaluate the effect of IL on the long-term structural and chemical stability of genomic DNA integrated within the Schottky-like junction and gel electrophoresis analysis of PCR-amplified DNA samples stored at different temperatures and time intervals.

1.4 Thesis Outline

The rest of the thesis is divided into five chapters and the content and functions of which are;

Chapter 2: Literature Review. This chapter comprises of a detailed study of the background of DNA, the basic structure of these nucleic acid and its role in DNA electronics. This chapter also includes a comprehensive literature review of semiconductor physics, p-n and Schottky diodes, and previous techniques employed for mushroom identification. Moreover, an insight into conventional characterization techniques and their working principles are also presented.

Chapter 3: Materials and Methods. The different materials and experimental methods employed in this research with detailed samples preparation techniques, procedures and testing conditions were extensively explained in this chapter.

Chapter 4: Results and Discussions. This chapter is dedicated to results and discussions based upon the findings of the experimental work. This chapter focuses on the analysis of the results related to the fabrication of the Al-DNA Schottky barrier diode. There are three main highlights of this chapter; the discussion on the *I-V* characterization for mushroom genomic and amplified DNA, effect of pH on the conductivity of DNA and effect of IL on the long-term structural and the chemical stability of DNA.

Chapter 5: Conclusions and Future Works. A summary of the research findings is presented in this chapter besides providing some discussion on the future outlook of this research.

CHAPTER 2: LITERATURE REVIEW

2.1 Introduction to Mushrooms

2.1.1 Edible Mushroom

Mushrooms are important food source not only for its nutritional value but also for its unique taste. Common edible mushrooms that are available to consumers everyday includes the oyster mushrooms (*Pleurotus ostreatus*), ear mushrooms (*Auricularia nigricans*), straw mushrooms (*Volvariella volvacea*) and shitake mushroom (*Lentinula edodes*) (Mortimer et al., 2012) to name a few. Mushrooms also act as an unusual source for cosmetics because they contain a number of biologically active compounds (Hyde et al., 2010). The benefits of using mushroom as medicinal have been explored since ancient China and Japan (Bao et al., 2001).

Mushroom cultivations plays important role in today‘s agriculture, but research on breeding and production of mushroom cannot catch up with other crops (Sadler, 2003). The reason includes minimal understanding of the genetics and breeding system of mushroom. Recent ongoing mushroom whole genome sequencing will contribute to understanding of the organization and functions of gene that will eventually lead to assisted selection breeding systems. Thus, superior strain of commercial mushroom with high yield and productivity can be produced (Bipasha, 2011).

2.1.2 Identification of genus *Pleutorus*

Taxonomic identification is the most common analysis and hypothesis-testing endeavor in science. Errors of identification are often related to the inherent problem of small organisms with morphologies that are difficult to distinguish without research-grade microscopes and taxonomic expertise in this field. Molecular identification has been used in biodiversity and conservation. Morphological and molecular identification of mushrooms are current practice to identify mushroom taxa. However, automated

identification technology does not allow for the simultaneous analysis of thousands of samples (Manoylov, 2014).

The concept of "species" is perhaps the most debated subject in evolutionary biology as demonstrated by the existence of more than twenty definitions founded on different methods and criteria (Hey, 2001). The difficulty in assigning an organism to a biologically meaningful category should be well considered before the use of any molecular identification tool. Researchers are aware of the evolutionary history and taxonomic position of the specimen by understanding the order of branching and ages of divergence (phylogeny) of the organisms and familiarized with the nomenclature. Terms such as "strain", "variant", "subspecies" or "breed" could be highly subjective in some circumstances and be used as synonyms by different investigators to describe the same biological entity. All methods for the identification of species that rely on DNA or protein sequence analysis presuppose the neutral theory of molecular evolution, in which different lineages diverge over evolutionary times by the accumulation of molecular changes (Kimura, 1968).

These methods are based on the assumption that individuals from a same species carry specific DNA (or protein) sequences that are different from those found in individuals from other species. However, the distribution of a given molecular variant in time and in space will be influenced by the reproductive success of individuals, migratory events and random genetic drift (Loewe & Hill, 2010). Therefore, it should be realized that a continuous genetic variability does exist among individuals of a species. The level of intraspecies diversity in the locus under study has to be properly assessed before undertaking any taxonomic identification in order to guarantee that there is no overlap between intraspecies variation and interspecies divergence. Furthermore, different loci have variable rates of evolution owing to the action of processes such as mutation and

recombination. Therefore, to choose the appropriate loci is vital to the success of the identification (Wyler & Naciri, 2016). If possible, a representative sample of individuals should be genotyped, preferentially from different geographic locations or from different hosts, in cases of internal parasites.

The genus *Pleurotus* are widely exploited for converting lignocellulosic by-products into edible mushrooms of high nutritional and medicinal value (Chang, 2008). Precise identification of wild mushroom isolates/taxa and elucidation of their relationships are essential prerequisites for the development of biotechnological applications. The genus *Pleurotus* is one of the most taxonomically challenging groups of macrofungi comprising several species and sub-specific entities with complex affinities, whose delimitation is problematic due to great diversity in morphology taxonomy, biodiversity and ecology. (Martin et al., 2011; Araujo, 2014; Xu, 2016). Therefore, developing an efficient species recognition system which is applicable for all macrofungi seems difficult. (Zervakis, 2004). Therefore, rapid and reliable identification of *Pleurotus* is critical for many research areas such as taxonomy, biodiversity, ecology, conservation and health.

The genus *Pleurotus* exhibits a wide variety of sizes, shapes and colors, which showing different habitats, functions and life strategies. Such heterogeneity makes the identification a complex and difficult process. Classical morphology-based identification is suffering from phenotypic plasticity and genetic variability, which may lead to misinterpretations. Morphological characters can be contentious or problematic even for trained mycologists, as they may not always provide accurate groupings within an evolutionary framework, mainly at the species level (Geiser, 2004). Morphological characters can often be misleading due to hybridization, cryptic speciation and convergent evolution (Huzefa et al., 2017; Brun & Silar, 2010). Therefore, molecular data is complementing morphological data for species delimitation and identification, taxonomic

classification and phylogenetic inference. Molecular data are based on the variability in DNA sequences of closely related species and have been applied to determine mushroom species since 1990s (White et al., 1990; Bruns et al., 1991).

The term DNA barcoding was coined in 2003 as a molecular technique, which uses a short, variable and standardized DNA region for species identification and phylogeny (Hebert et al., 2003; Dulla et al., 2016). DNA barcoding is used not only to identify an unknown sample by comparing the sequence to the reference DNA library (Liimatainen, 2013) but also to resolve phylogenetic relationships with other taxa (Stielow et al., 2015; Raja et al., 2017). However, deciding the potential region(s) as DNA barcode is a crucial step to identify biological specimens and to assign them to a given species. Utility and success of the marker or barcode substantially depends on the rate of evolution, sequence length, polymerase chain reaction (PCR) and sequencing success, presence of universal primer pairs, existence of a barcode gap (the difference between inter- and intra-specific genetic distances within a group of organisms), and nucleotide variations among sequences and conserved flanking regions (Yang & Rannala, 2012; Giudicelli et al., 2015). The ideal genetic marker includes a small part of DNA 500-800 bp length, with high inter and low intra-species sequence divergence, and specific primers delimiting the region (Stielow et al., 2015).

Several DNA markers are commonly proposed for genus *Pleurotus* includes internal transcribed spacer (ITS), large subunit ribosomal DNA (LSU), small subunit (SSU), the cytochrome oxidase subunit 1 (COX1, COI), largest subunit of ribosomal polymerase II (RPB1), second largest subunit of RNA polymerase II (RPB2), translational elongation factor 1-α (TEF1-α) and, β-tubuli (Tekpinar & Kalmer, 2019). Each of these regions may be used alone or with different combinations to determine mushrooms into genus/species level and phylogenetic relations.

The ITS region is found in all living forms and preserved evolutionarily for a long time. It has important biological significance in ribosomal RNA (rRNA) processing. rRNA forms specific secondary structures which are needed for correct recognition of special ribosomal sites and provide the binding sites for ribosomal proteins during ribosome maturation (Rossman, 2007). Although most of the studies have indicated ITS region as the universal barcode marker for mushrooms (Smith et al., 2013; Harrower et al., 2011; Schoch et al., 2014), ITS data in the International Nucleotide Sequence Database (INSD: GenBank, EMBL and DDBJ) revealed that this region is not equally variable in all groups of mushrooms (Nilsson et al., 2008). Even though the region was indicated as successful of identification for most of basidiomycetous genera, (Ordynets et al., 2018; Wang et al., 2004; Lindner & Banik, 2011; Vydryakova et al., 2012) but some overlapping of basepairs was observed between intraspecific and interspecific variations. Therefore, ITS marker may not be enough to delimit species for all the genera reliably without careful morphological examination.

In addition, the genera with high variability in the sequence of ITS region needed additional DNA markers in addition to morphological characters to understand infrageneric relationships of the genus for reliable identification and reevaluation of the taxonomy (Ge et al., 2018). The presence of polymorphisms originating either from differences within nuclei (heterogeneity among repeats) or from differences between nuclei (dikaryotic and multinucleate mushrooms) is another disadvantage for the region (Aanen et al., 2001). This polymorphism causes complications and difficulties during direct sequencing of the products because of existing of multiple ITS copies. Eberhardt et al. (2009) considered ambiguous base calls (double peaks) as a signal originated from the presence of different ITS copies in the genome. They indicated that double peaks in the forward and reverse sequences were induced due to single base pair mutations. Other researchers also mentioned this situation and pointed out the importance of specifying

sequencing procedure; direct sequencing or sequencing after cloning the PCR amplification (Eberhardt et al., 2009; Kiss, 2012; Chen et al., 2016; Mark et al., 2016). ITS amplicons shorter than 500 bp may be a problem due to the lack of sufficient variability. Although the region can reliably determine mushrooms to the genus level, identification to the species level is sometimes poor for certain group of mushrooms (Crous et al., 2015).

Although the ITS region has been proposed as a standard barcode for mushrooms (Schoch et al., 2012a), other regions of the rRNA also gaining interest. The nLSU (28S nuclear ribosomal large subunit rRNA) gene located immediately downstream of the ITS region is widely used to elucidate questions in mushroom phylogeny (Bruns et al., 1991). Especially two hypervariable domains of LSU, D1 and D2, flanked by relatively conserved regions in most mushrooms are widely preferred for studies (Raja et al., 2017).

The LSU region, by itself (Vizzini et al., 2010; Liu et al., 2012; Acar et al., 2017) or generally combined with other regions such as ITS (Taylor et al., 2008; Geml et al., 2009; Schoch et al., 2012a; Brown et al., 2014; Millanes et al., 2016; Telleria et al., 2017; Vizzini et al., 2018) is used for identification of mushroom into genus/species level. Length of the studied region is important to get reliable results. Long sequences produce greater taxonomic resolution but they may also stimulate higher rates of sequencing errors and chimera formation (Heeger et al., 2018). Liu and co-workers (2012) showed that long sequences of LSU gene provided higher classification accuracy, especially for the finer-scale taxa such as genus. Porras-Alfaro et al. (2014) proved this result by indicating that long sequences provide a higher discriminatory power than short sequences for both of the ITS and LSU regions.

The LSU region encountered less problems during amplification, sequencing, alignment, or editing (Schoch et al., 2012a) but variable length and low-quality LSU

sequences are common in the database. The lack of an accurate and validated sequence database is one of the most important limitations in taxonomic analysis of mushrooms. Ribosomal Database Project (RDP) (Cole et al., 2014) database has been established for LSU region. However, the coverage of the database generally remains poor for several mushrooms (Ohsowski et al., 2014; Frenken et al., 2017). Length of the region is another important character to obtain accurate result even though determining how long the region is difficult to predict. Furthermore, this region is generally considered to be less variable than the ITS and this situation may limit taxonomic resolution at the species levels and diversity analysis. LSU was indicated as the most conservative and insufficient marker to distinguish species reliably (Zhao et al., 2011a). However, the gene may be combined with RNA polymerase II genes, RPB1 and RPB2, to improve phylogenetic inference of relationships even at lower taxonomic ranks (Frøslev et al., 2005).

Although rRNA genes are the most commonly used loci in molecular systematic studies of mushrooms, limited resolving power of nuclear LSU may be observed for some mushroom phyla. Studies has obviously demonstrated that the use of protein-coding genes are valuable to determine deep phylogenetic relationships with high support for topologies inferred based on rRNA genes in mushrooms (Liu et al., 1999; Matheny et al., 2002; Tanabe et al., 2004). The main advantage of using protein-coding gene is the presence of a single copy in the mushroom genome and avoiding the pitfalls of paralogs. RNA polymerase II is an enzyme responsible for transcription of protein-coding genes into pre-mRNA transcripts (Matheny et al., 2002). The variable region between conserved domains six and seven of the RPB2 (encoding the second largest subunit of RNA polymerase II) genes have a large number of parsimony-informative sites so that they might be phylogenetically useful to study mushrooms at lower taxonomic levels (Liu et al., 1999; Matheny et al., 2002; Tanabe et al., 2002).

In general, protein markers such as RPB1 and RPB2 are used to identify to family and genus level but PCR, sequencing and alignment failings limit their potential as universal barcodes. Matheny (2005) inferred easy alignment of the regions even though samples are found in different families. There are inconsistent remarks about success of PCR and sequencing procedures. Some studies pointed out that success rate of PCR and sequencing efficiency are less for RPB1 and/or RPB2 genes (Schoch et al., 2012a; Carlson et al., 2014; Liu et al., 2006) while others expressed high (Zhao et al., 2011a; Zhao et al., 2011b) or sufficient success (Frøslev et al., 2005; Matheny et al., 2007; Stockinger et al., 2014) for RPB1 and/or RPB2 genes. The other problem about the genes is the copy number in the genome which affects PCR and sequencing successes. Although only one copy for both RPB1 and RPB2 genes is expected in most of the mushroom species, two RPB1 genes with slightly different sequences and two similar RPB2 copies were detected in some mushrooms (Liu et al., 2006).

Some studies showed that the RPB1 and RPB2 gene having slow rate of sequence divergence are only useful for higher-level phylogenetic studies (Stiller & Hall, 1997; Tanabe et al., 2002). Tanabe and colleagues (2004) identified a few indels (insertions/deletions) in the middle part of the RPB2 gene of several mushrooms and deletions in the sequence of almost all studied Basidiomycota. Therefore, unexpected phylogenetic relationships were observed in the phylogenetic tree constructed based on RPB2 gene such as the nesting of some Basidiomycota within the Ascomycota clade even though their monophyly was demonstrated via phylogenetic analyses (Tanabe et al., 2002; Tanabe et al, 2004). This unexpected relationship may be originated from the lack of an accurate and validated sequence database (Rosenberg & Kumar, 2001; Tanabe et al., 2004).

2.2 Introduction to Deoxyribonucleic Acid

Watson and Crick conceived the double helix structure of DNA in 1953 (Watson & Crick, 1953) using X-ray diffraction patterns obtained by Franklin Rosalind and Maurice Wilkins (Klug, 2004). Being a biopolymer, it consists of monomer units called nucleotides (Calladine, Drew, Luisi, & Travers, 2004), where each nucleotide in turn is comprised of five-carbon sugar ring (deoxyribose), a nitrogen-holder base connected to the sugar and phosphate backbone. The polymer is known as "polynucleotide". DNA is formulated into structures in cells called chromosomes (Ohayon et al., 2011).

In general, DNA has double helix structure consisting of four nitrogen bases, adenine (A) pairs with thymine (T) and guanine (G) pairs with cytosine (C). The arrangement of these bases is what determines the DNA's genetic code. This order also referred to as DNA sequence, forms the genes which directs the cells how to produce protein. These base pairs are connected to each other through strong hydrogen bonds. Sugar and phosphate groups are linked internally by ester bonds forming the helix backbone of the structure. DNA macromolecules present a net negative charge as the outside groups are phosphates (Klug, 2004).

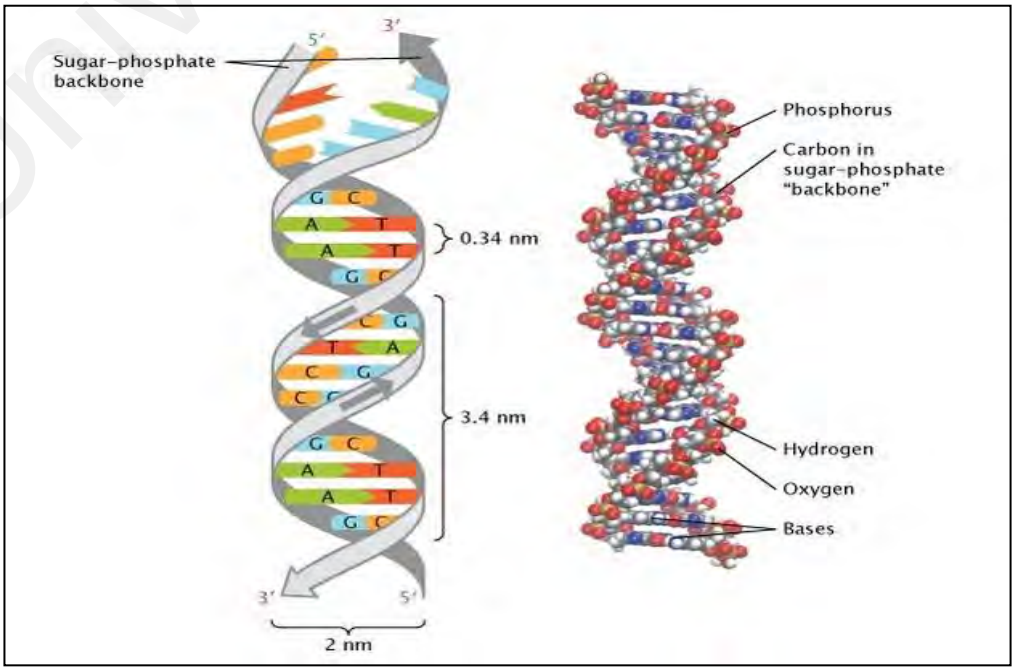

Figure 2.1: The double helix model of DNA (source: Pray, 2008).

As showed in Figure 2.1, the DNA molecule is made up of two strands which are anti-parallel. The strands are label 5' and 3' indicating the directionality of the strands. The numbers 5' and 3' refers to the carbon number of the DNA backbone. In nucleic acids, 3' refer to the 3rd carbon in the sugar ribose or deoxyribose linked to the hydroxyl group and the 5' refer to the 5th carbon linked to the phosphate group.

The nucleotides are attached together to form two long strands which are spiral to create a double helix structure. Sometimes drawn in the form of a ladder, the phosphate and sugar are the sides and the bases are the rungs of the ladder forming a base pair. The nitrogen bases are complementary, which is either an adenine-thymine pair (Figure 2.2a) formed by a two-hydrogen bond or a cytosine-guanine pair (Figure 2.2 b) which formed a three-hydrogen bond. The size of DNA is usually expressed in the number of base pairs (bp), which ranges from tens of base pairs to billions depending on the development level of the species. Diameter of the helix is about 2 nm and the distance between the two base pairs is 3.4 nm (Fitch, 2002).

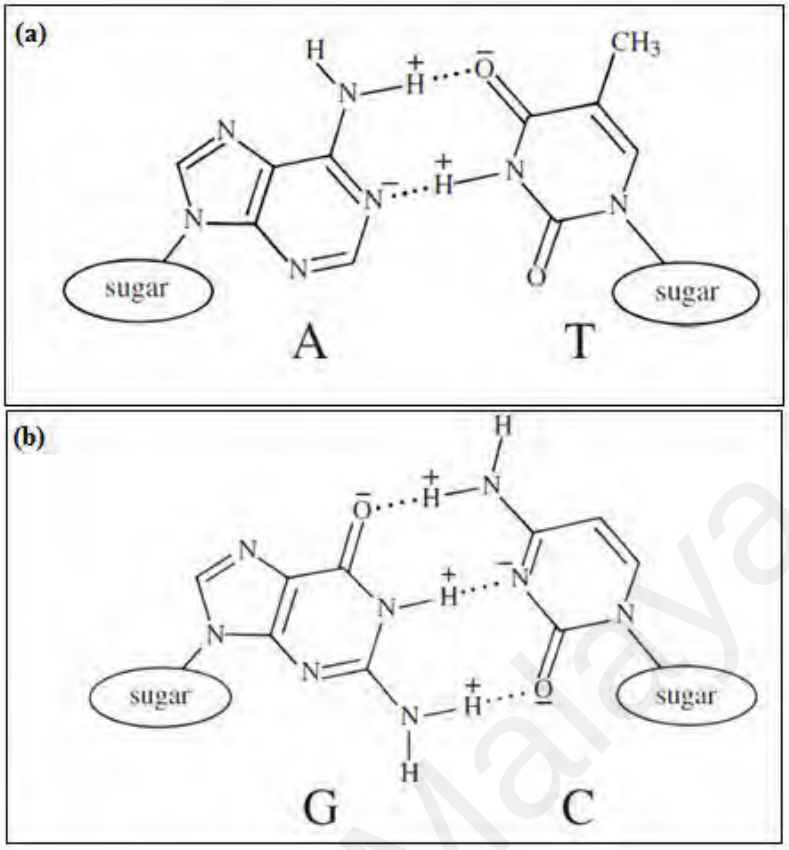

Figure 2.2: (a) Adenine-thymine base pair with two hydrogen bonding and (b) guanine-cytosine base pair with three hydrogen bonding (Source: Calladine et al., 2004).

DNA is considered to be the basic building block of life (Pray, 2008; Sun & Kiang, 2005). The first observation on DNA was by the biochemist Johannes Friedrich Miescher in 1869 who discovered a new matter extracted from the cell nucleus that he named nuclein, which is what we know today as nucleic acids. The method he used was through isolating the white blood cells made readily available from pus of fresh surgical bandages obtained from the local surgical clinics. Eventually, Miescher had managed to produce a precipitate of DNA which he named as nuclein (Zon, 2015). By studying the composition of the precipitate, Miescher tried to investigate the elements in nuclein and he discovered that there were large amounts of phosphorus in addition to other elements such as carbon, oxygen, hydrogen and nitrogen (Dahm, 2005). At that time, Miescher had guessed that this material has a fundamental role in hereditary due to its presence in other cells. He postulated that his discovery of this new substance was equally important to proteins.

Prior to the discovery of the double helix structure, two notable findings paved the way to understand this elusive molecule. Previously, it was believed that proteins served the function of carrying genetic information. The connection between nucleic acid and genes was not discovered for a long time after Miescher's research until the contribution of Oswald Theodore Avery Jr. in 1944 (Avery et al., 1944). In the paper published, Oswald Avery together with his co-workers Colin Macleod and Maclyn McCarty designed an experiment known as the Avery-MacLeod-McCarty experiment to report that DNA was the substance that causes bacterial transformation. On top of that, it was discovered that the previously harmless bacteria could pass the new trait to the next generation. The substance which moved carried the genetic information and was the nucleic acids, which led Avery and his colleagues to suggest that DNA rather than proteins are the hereditary material of the bacteria and possibly other biological organisms. Upon reading Oswald Avery's research on the gene, Erwin Chargaff, an American scientist furthered this research by discovering two rules which helped to shed light on the DNA structure (Chargaff, 1971).

By that time, scientists knew that the DNA molecule was made up of four bases or components; adenine (A), thymine (T), guanine (G) and cytosine (C). However, the components were organized so simply that many people thought the proteins and not the DNA carried the genes, even after Avery's publication. Erwin Chargaff had used techniques such as paper chromatography and ultra-violet (UV-Vis) spectroscopy to measure the precise amounts of bases in a DNA sample. In 1950, Chargaff published his researches (Chargaff, 1950) consisting of two findings. Firstly, he found a pattern where the number of adenines would match with thymines, at the same time, guanines would match with cytosines. Furthermore, he observed that the number of guanine/cytosine and adenine/thymine varied among different species but remained the same for the same

species. This observation, known as Chargaff's rules, laid the grounds that DNA sequences are variable and species-specific.

The base pairing restriction plays an important role when DNA is being replicated. The helical structure will be unzipped to form two long stretches of single strand DNA (Alberts et al., 2002). Each half will be used as a template for a new complementary strand. The cells will then arrange corresponding free bases into the single strand and after this process two exact copies of the original DNA molecule are produced. This method is used in biological labs in a process known as PCR as illustrated in Figure 2.3 (Lents, 2010).

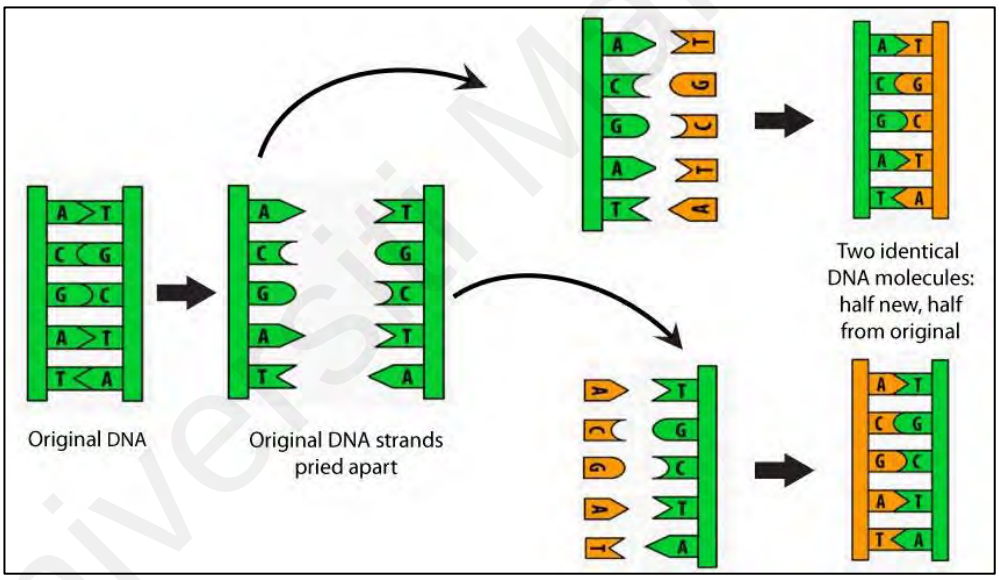

Figure 2.3: Schematic diagram of the PCR process (Source: Lents, 2010).

The special properties of DNA make it so effective in the construction and fabrication of nanostructures and devices. It can be considered as a device element itself besides the possibility to use it for the assembly of interconnects, computational elements and devices. There are some advantages to use DNA for these constructions. Firstly, DNA has intermolecular interactions, which are the most readily programmable properties that make it effective as the genetic material. In this context, the base A always pairs with T and G pairs with C, making it ideal for programmed self-assembly. Secondly, DNA of

arbitrary sequences can be available through convenient solid support synthesis. Depending on the requirements of the biotechnology industry, it is possible to apply reliable chemistries to produce modifications, such as linking functions, biotin groups and fluorescent labels. Thirdly, DNA molecules can be modified and manipulated by various enzymes that include DNA ligases, kinases, restriction endonucleases and exonucleases (Sun & Kiang, 2005).

2.3 Effect of pH on the Structure of DNA

The concentrations of hydroxide ion and pH have a direct correlation, meaning the pH increases by the concentration of hydroxide ion (Leveling, 2002; Coleman et al., 2013). Conceptually, the stability of double-stranded nucleic acids refers to helix-coil transitions which can be characterized by physical and chemical techniques (Riley et al., 1966; Michelson et al., 1967). According to Cheng & Pettitt (1992), the stability of nucleic acids may be characterized by compositional, environmental and molecular weight dependent components. The pH of solution affects the duplex stability and conductivity of DNA (Leveling, 2002).

2.3.1 The Effects of Alkaline pH on the Structure of DNA

Adding strong bases such as NaOH dramatically increases the pH (pH>7), thus decreasing the hydrogen ion concentration of the solution and denaturing double-stranded DNA. At high pH, the solution contains more hydroxide ions (OH^-) than hydrogen ions (H^+) (Kharel & Hashinaga, 1999). Unlike ribonucleic acid (RNA), DNA does not contain hydroxyl group at the 2' position. This suggest that DNA are not easily hydrolyzed leading to higher stability of DNA in alkaline solutions. However, high concentration of negatively charged hydroxide ions (higher pH (pH >10)) can attract hydrogen ions from DNA for neutralization process. At lower alkaline pH (7-8) conditions will not adversely affect the nucleic acid structure and might only denature some binding proteins or cause

breakage of a few hydrogen bonds of the base pairing. At higher pH (>10) conditions, there is extensive deprotonation and changes in the tautomeric state of the bases resulting in unstable base pairing (Samanta & Medintz, 2016; Privalov & Ptitsyn, 1969; Ageno et al., 1969). Thus, the hydrogen bonds between the strands are broken denaturing the double-stranded DNA. In other reports, the alkaline lysis method is used in isolation of plasmid DNA from bacterial cell (Coleman et al., 2013; Nelson & Cox, 2008; Perrin & Nielson, 1997; Ehrlich & Doty, 1958; Chen et al., 2009; Poltronieri et al., 2008).

2.3.2 The Effects of Acidic pH on the Structure of DNA

The mechanism of protonation of DNA phosphodiester groups in acidic condition (very low pH) is well known. Protonation is reported to decrease the stability of a double helix (Sorokin et al., 1986; Lando et al., 1994; Costantino & Vitagliano, 1966). At low pH values (pH<7), depurination occurs as a result of hydrolysis where purine bases are released from the nucleic acids by hydrolysis of *N*-glycosidic bonds. At high acidic conditions (pH<3), the phosphodiester bonding of the DNA is disrupted, which cleaves the DNA into nucleosides and nucleotides (complete hydrolysis). The hydrolysis and depurination proceed by acid-catalysed S_N1 reaction mechanism. Nucleophilic centres on guanine and adenine are in N1, N3, N7 and N6 positions, in which electrophilic acid attacks occurs on N7.

As such, at extremely low pH, DNA is digested completely into smaller nucleosides. At much lower pH conditions (nearing pH 2), for example in the stomach, most of the bacterial load were reduced prior to digestion and therefore allow only decontaminated food to be passed further (Lando et al., 1994; Williams et al., 2001; Bergerová et al., 2011; An et al., 2014; Suzuki et al., 1994; Lindahl & Nyberg, 1972).

2.4 Semiconductor Physics

2.4.1 Introduction

Semiconductors are a group of materials having conductivity properties between conductors and insulators. The basic classifications of semiconductors according to the Periodic Table are the elemental semiconductor materials. These materials are found in group IV, and the compound semiconductor materials are formed by special combinations of group III and group V elements. In general, semiconductors are a single-crystal material. The electrical properties of a single-crystal material can be determined by the chemical composition as well as the arrangement of atoms in the solid. The growth or the formation of the single-crystal material plays a significant role in semiconductor technology.

The electrical properties for different elements can be explained in term of energy band. In solid materials, electron energy levels form bands of allowed energies separated by forbidden bands. Electrons in a completely filled band cannot move since all the states are occupied, therefore the only way to move would be to "jump" into next higher partly filled bands since there are free states available (Neamen, 2003). The solids band structure can be classified into three types (Figure 2.4); 1) Insulators: Forbidden region between highest filled band (valence band) and lowest empty or partly filled band (conduction band) is very wide. The energy band gap for insulators is in the order of 3 to 6 eV or larger. That means, the electrons on valance band have to obtain energy more than 3 eV to jump to the conduction band. 2) Semiconductors: Material for which gap between valence band and conduction band is small, about 0.1 to 1 eV. 3) Conductors: Valence band only partially filled or if it is filled the next allowed empty band overlaps with it. It is known that conductor elements have an overlapping of valence and conduction bands, which enables the valance electrons to transfer to the conduction band easily.

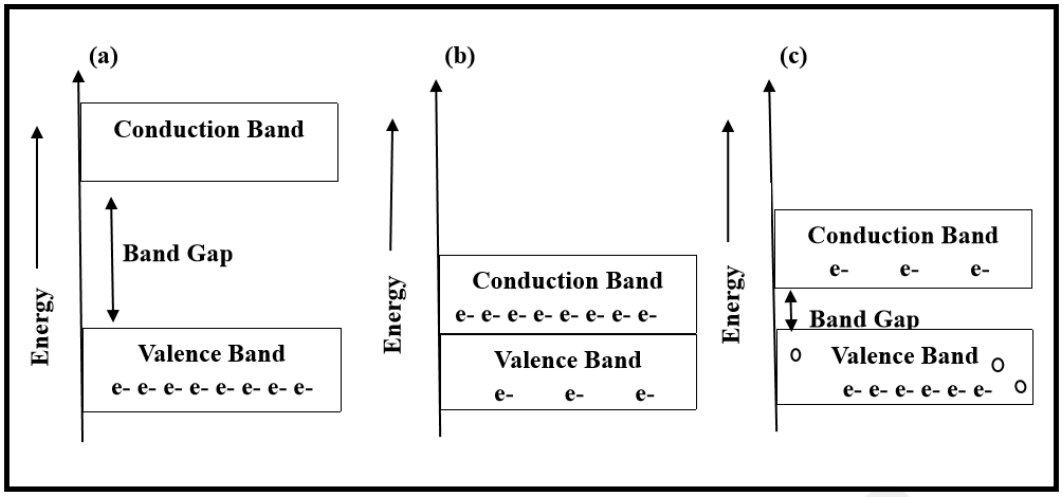

Figure 2.4: Schematic of band gap in (a) insulator, (b) conductor and (c) semiconductor.

Silicon (Si) and Germanium (Ge) are the most common semiconductor element, where gap width in Si is 1.1 eV and Ge is 0.7 eV (Vidyasagar, 2019). It is demonstrated that at temperature (T)=0, there are no significant number of electrons in the conduction band and therefore the semiconductor does not conduct (lack of free charge carriers). At T>0, some fraction of electrons has sufficient thermal kinetic energy to overcome the gap and jump to the conduction band. The number of electrons rises with temperature, which allows fraction of the valence electrons in the material to move into the conduction band by given a certain amount of energy. For instance, at 20°C (293 K), Si has $0.9x10^{10}$ conduction electrons cm^{-3} and at 50°C (323 K), there are $7.4x10^{10}$ conduction electrons cm^{-3} (Yacobi, 2003).

Si atoms bind to each other with covalent bonds. Each Si atom is surrounded by eight valence electrons that are in their lowest energy state and are directly involved in the covalent bonding at T=0 K. The valance electrons exist in the valance band, while the conduction band is empty. When the temperature is increased above 0 K, a few valence band electrons gain thermal energy which may be enough to break the covalent bond. Therefore, the electrons will jump into the conduction band. The semiconductor is neutrally charged. So, when the electrons break away from their covalent bonding

position, positive charges or "empty states" are created in the original covalent bonding position in the valence band. This movement of the valence electron into the empty state is actually equivalent to the movement of the positively charged empty state itself.

The semiconductor crystal now has another equally important charge carrier that can give rise to a current. This charge carrier is called a hole, considered as the second type of charge carrier in semiconductor in addition to the electron. Accordingly, the number of electrons in the conduction band and the number of holes in the valence band determined the current in semiconductors. In summary, electrons moving to conduction band leave “hole” (covalent bond with missing electron) behind. Under influence of applied electric field, neighboring electrons can jump into the hole and create a new hole. Holes can therefore move under the influence of an applied electric field, just like electrons and both contribute to conduction. As a result, the density of these charge carriers is considered to be one of the important characteristics of semiconductors.

Semiconductors are crystal structure-like materials. It can be intrinsic by nature, which means that its crystal structure is pure with no impurities or defects. An intrinsic semiconductor at absolute zero temperature is shown in Figure 2.5(a). When the temperature is raised and some heat energy is supplied to it, some of the valence electrons are lifted to the conduction band leaving behind holes in the valence band as shown below in Figure 2.5(b). This behaviour of the semiconductor shows that they have a negative temperature coefficient of resistance. This means that with the increase in temperature, the resistivity of the material decreases and the conductivity increases.

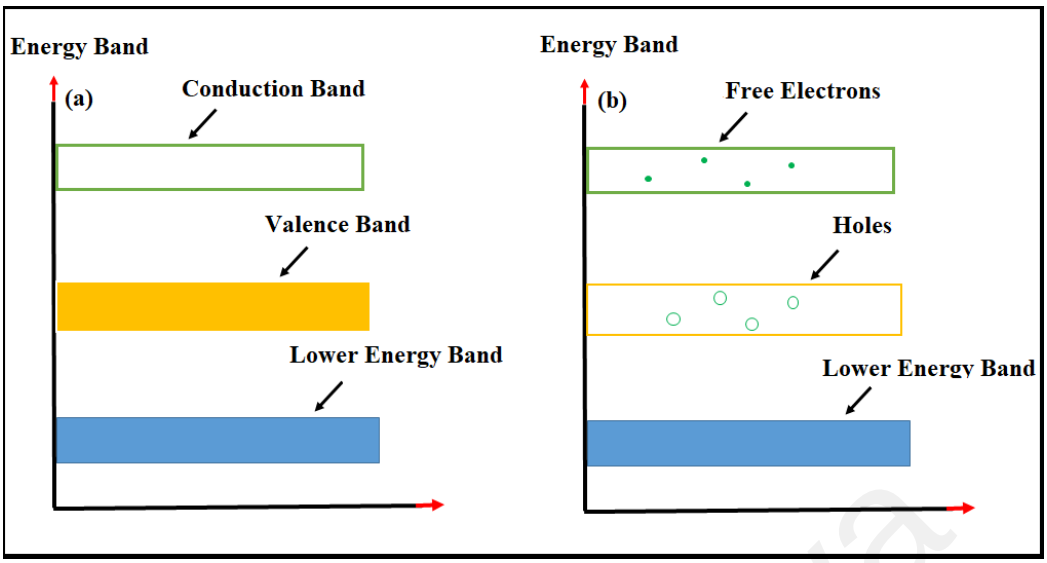

Figure 2.5: Schematics showing the charge distribution in intrinsic semiconductors. (a) valence band is completely filled and the conduction band is completely empty and (b) the electrons reaching at the conduction band move randomly. The holes created in the crystal also free to move anywhere.

A semiconductor to which an impurity at controlled rate is added to make it conductive is known as an extrinsic semiconductor. An intrinsic semiconductor is capable of conducting a small current even at RT, but it is not useful for the preparation of various electronic devices. Thus, to make it conductive a small amount of suitable impurity is added to the material. The electrical properties of semiconductor can be changed by adding some impurities to the crystal structure. This process is called doping and it is carried out in order to increase the number of free electrons or holes and therefore improve the semiconductor's electrical properties. To get the desirable level of doping, a controlled amount of specific dopant atoms must be added. The dominant charge carrier in a semiconductor depends on the type of the dopant atoms and as such it may consist of electrons or holes.

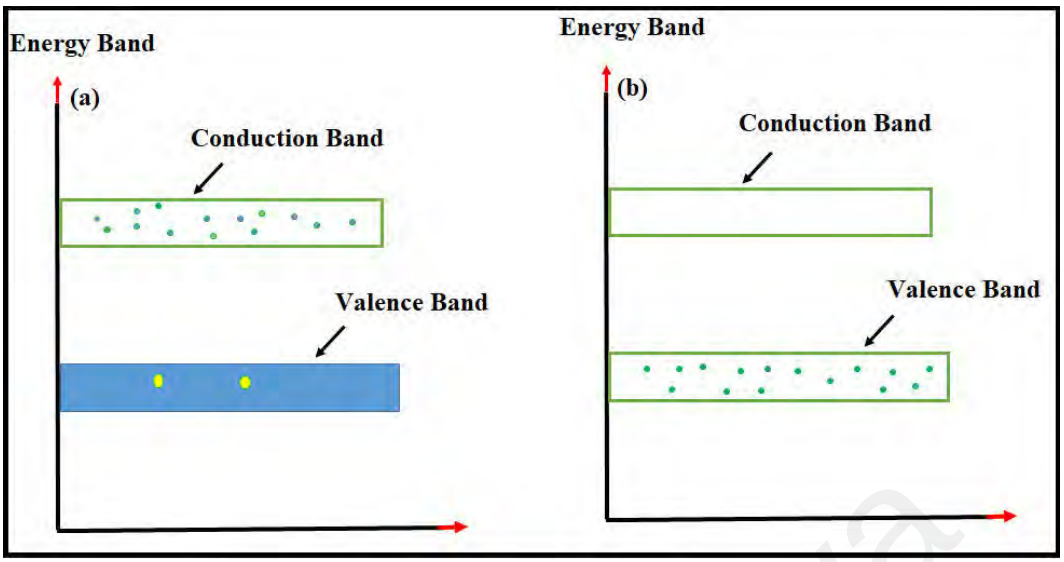

Figure 2.6: Schematics showing the charge distribution in extrinsic semiconductors. (a) The energy diagram of the n-type semiconductor and (b) The energy band diagram of a p-type semiconductor.

In this case, the Fermi energy becomes a function of the type and concentration of the impurities since the dopant atoms change the distribution of electrons among the available energy states (Neamen, 2003; Kittel, 1995; Yacobi, 2003; Feynman, 1963; Shockley, 1950). Depending upon the type of impurity added, the extrinsic semiconductor may be classified as n-type or p-type semiconductor. The energy diagram of the n-type semiconductor is shown in the Figure 2.6(a). A large number of free electrons are available in the conduction band because of the addition of the pentavalent impurity. These electrons are free electrons which did not fit in the covalent bonds of the crystal. However, a minute quantity of free electrons is available in the conduction band forming hole-electron pairs

The following points are important in the n-type semiconductor; 1) The addition of pentavalent impurity results in a large number of free electrons. 2) When thermal energy at RT is imparted to the semiconductor, a hole-electron pair is generated and as a result, a minute quantity of free electrons is available. These electrons leave behind holes in the valence band. 3) In n-type semiconductor," n" stands for negative material as the number of free electrons provided by the pentavalent impurity is greater than the number of holes.

The energy band diagram of a p-type semiconductor is shown in Figure 2.6(b). A large number of holes or vacant space in the covalent bond is created in the crystal with the addition of the trivalent impurity. A small or minute quantity of free electrons is also available in the conduction band. They are produced when thermal energy at RT is imparted to the germanium crystal forming electron-hole pairs. But the holes are more in number as compared to the electrons in the conduction band. It is because of the predominance of holes over electrons that the material is called as a p-type semiconductor. The word “p” stands for positive material.

If the dopant atom is an element from group V in the periodic table, such as phosphorus, the process will create n-type semiconductor. That means the majority carriers are electrons. To explain this, group V elements have five valence electrons; four of them will contribute to the covalent bonding with the semiconductor atoms (for example Si), leaving the fifth electron more loosely bound to the phosphorus atom. This fifth electron is called donor. The energy required to elevate the donor electron into the conduction band is considerably less than that for the electrons involved in the covalent bonding. As such, a small amount of energy, such as thermal energy, enables the donor electron to elevate into the conduction band leaving behind a positively charged phosphorus ion. The electron in the conduction band can now move through the crystal generating a current, while the positively charged ion is fixed in the crystal.

This type of impurities is called donor impurity atom since it includes adding electrons to the conduction band without creating holes in the valence band. This is the reason why the resulting material is referred to as n-type semiconductor (n for the negatively charged electron), which means that the density of electrons is greater than the holes. In the n-type semiconductor, a large number of free electrons are available in the conduction band

which is donated by the impurity atoms. Figure 2.7 shows the conduction process of an n-type semiconductor.

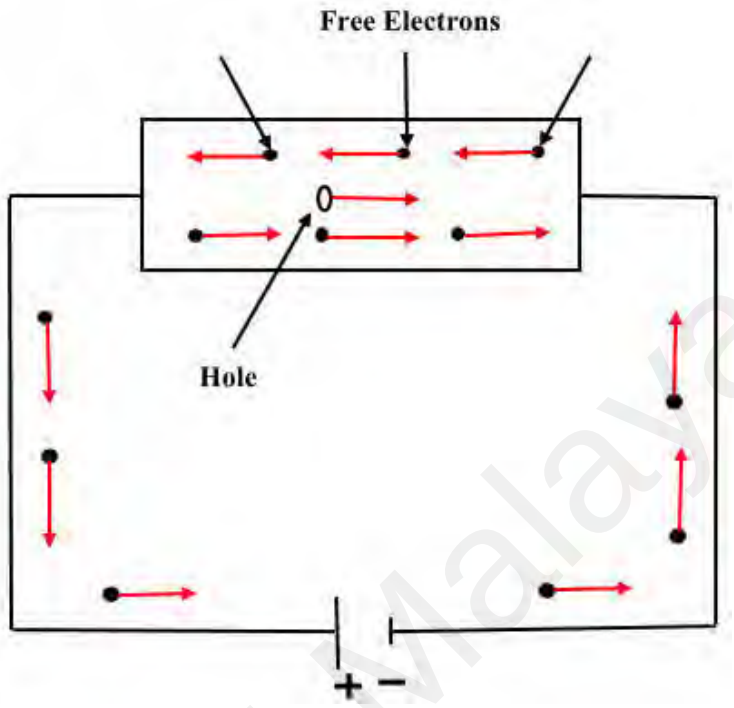

Figure 2.7: Schematic showing the donor (n-type) impurities: Conduction through n-type semiconductor.

When a potential difference is applied across this type of semiconductor, the free electrons are directed towards the positive terminals. It carries an electric current. As the flow of current through the crystal is constituted by free electrons which are carriers of negative charge, therefore, this type of conductivity is known as negative or n-type conductivity. The electron-hole pairs are formed at RT. These holes which are available in small quantity in valence band also consist of a small amount of current. For practical purposes, this current is neglected.

If the added atom is from group III, such as boron (B), added to Si, the semiconductor will be p-type. That's because group III elements have three valence electrons. In this case of B, the three electrons are combined with covalent bonding, but one covalent bonding position will be empty. There will be an electron that comes to occupy this "empty" position. However, the electron occupying this "empty" position does not have

sufficient energy to be in the conduction band, so its energy is far smaller than the conduction band energy. Therefore, valence electrons may gain a small amount of thermal energy and move about in the crystal (valence electron positions become vacated).

These vacated electron positions can be thought of as holes in the semiconductor material. The hole can move through the crystal generating a current, while the negatively charged B atom is fixed in the crystal. The group III atom accepts an electron from the valence band and so is referred to as an acceptor impurity atom and the semiconductor now is called p-type (p for the positively charged hole), which means that the density of holes is greater than the density of the electrons (Neamen, 2003). In p-type semiconductors, the large number of holes is created by the trivalent impurity. Figure 2.8 shows the conduction process of a p-type semiconductor when a potential difference is applied across this type of semiconductor.

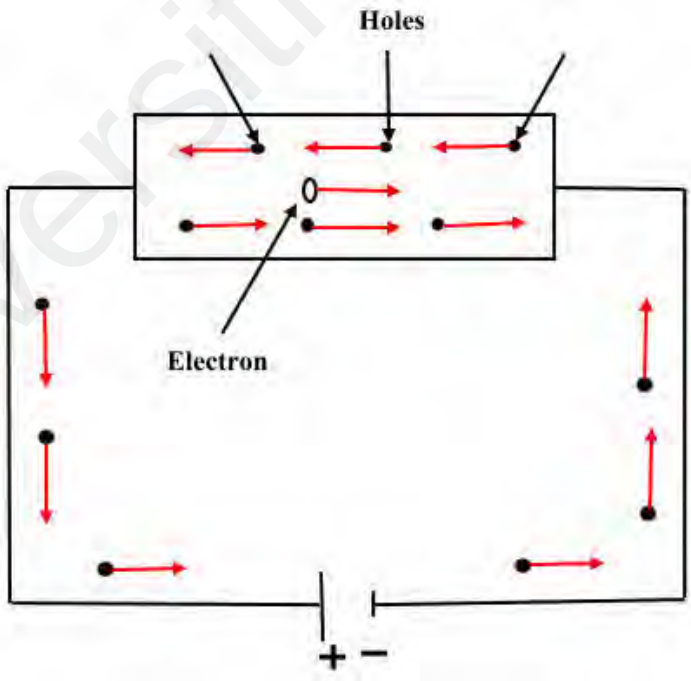

Figure 2.8: Schematic showing the acceptor (p-type) impurities; conduction through p- type semiconductor.

In electronics, connecting the p and n-type together creates junction that is called p-n junction diode (Figure 2.9). A p-n junction diode is a two terminal device that allows

electric current in one direction and blocks electric current in the other direction. The junction is mostly used in electronic devices and has characteristics that are used in rectifiers and switching circuits. This is due to the connection of p and n semiconductors makes the junction with (ideally zero) resistance to the flow of current in one direction and high (ideally infinite) resistance in the other direction. The concept of a diode is established leading to rectifying *I-V* profiles where the profiles seem to be of an exponential function rather than linear. In p-n junctions, impurity changes abruptly from p-type to n-type and so charged ions are left behind (cannot move around).

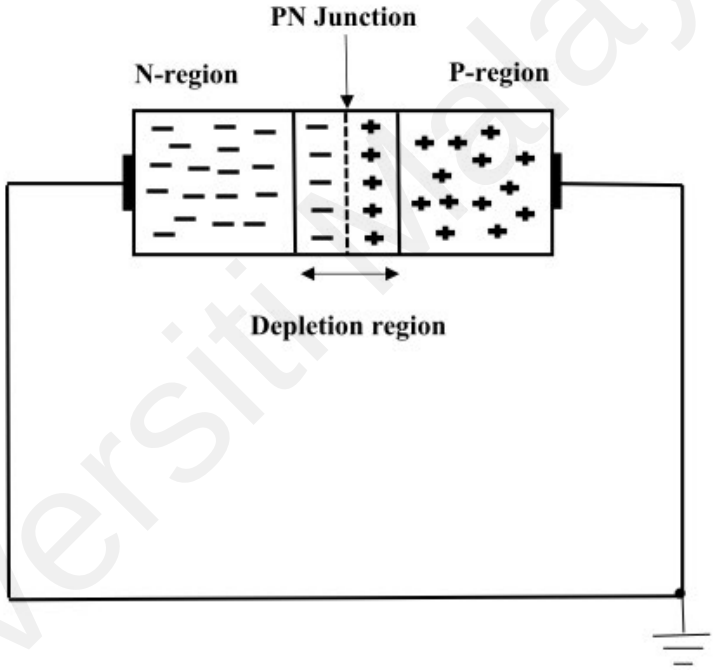

Figure 2.9: Schematic showing the p-n junction.

Diffusion refers to the process of movement of charge carriers due to concentration gradient along the semiconductor that is from the higher to the lower concentration. In absence of electric field across the junction, holes diffuse towards and across the boundary into n-type and "capture" electrons. Negative ions are left on the p-side (net negative charge on p-side of the junction) and positive ions are left on the n-side (net positive charge on n-side of the junction). The established electric field across the junction now prevents further diffusion. Due to that, there will be a region at the junction called

space charge region or depletion region. At this region, electrons diffuse across boundary and fall into holes (recombination of majority carriers), which will form a depletion region (region without free charge carriers) around the boundary (Shockley, 1949).

When the p-type of the junction is connected with the positive terminal of dc voltage and the n-type is connected with the negative terminal of the voltage, the depletion layer becomes narrower and this is called forward bias (p-side more positive than n-side). On the contrary, when the p-type is connected with the negative terminal of the dc voltage while n-type with the positive, the depletion region becomes wider and is called reverse bias (n-side more positive than p-side).

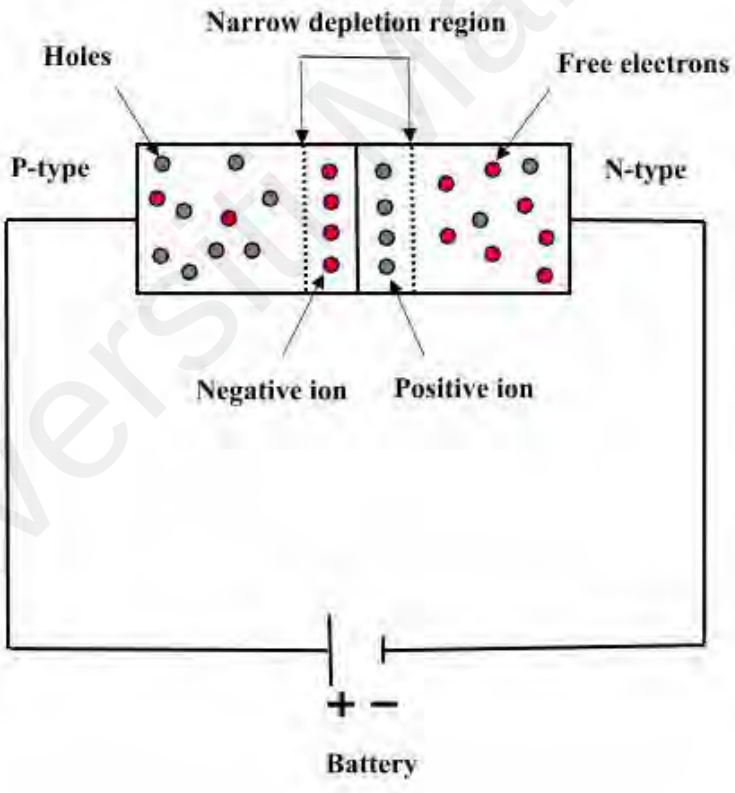

Figure 2.10: Forward biased diode; in forward bias condition, the diode allows electric current.

In forward bias diode (Figure 2.10), the direction of the electric field is from p-side towards n-side and p-type charge carriers (positive holes) in p-side are pushed towards and across the p-n boundary while n-type carriers (negative electrons) in n-side are pushed

towards and across the n-p boundary. Therefore, current flows across the p-n boundary (Neamen, 2003). In reverse biased diode (Figure 2.11), applied voltage makes n-side more positive than p-side. Therefore, electric field direction is from the n-side towards the p-side, which pushes charge carriers away from the p-n boundary (Neamen, 2003; Kittel, 1995; Yacobi, 2003; Feynman, 1963).

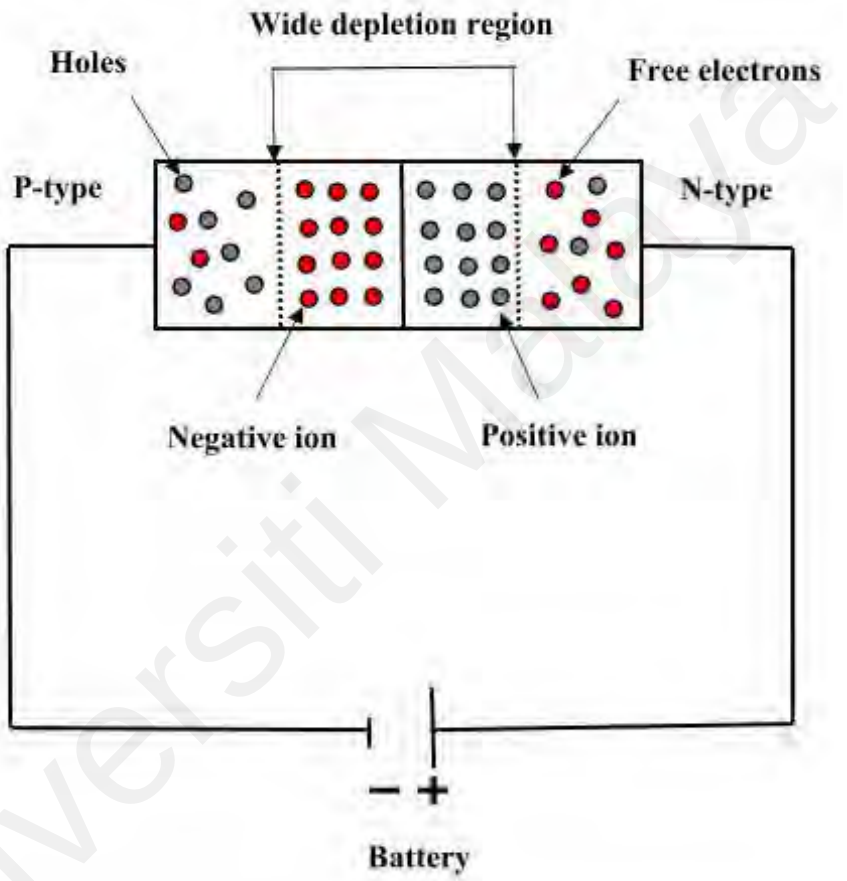

Figure 2.11: Reverse biased diode; in reverse bias condition, the diode does not allow electric current.

2.4.2 The *I-V* Profile of a Diode

Diodes are electronic devices which allows current to flow in one direction only. Common *I-V* graphs of diodes depict an exponential growth in the current with a small increase in the voltage, also known as a rectification behavior. When connected in a way where the diode allows current to flow, the diode is said to be forward-biased and on the other hand, it is known as reverse-biased when it restricts current flow. Figure 2.12

illustrates the *I-V* graph of a conventional semiconductor diode, with the common diode parameters included.

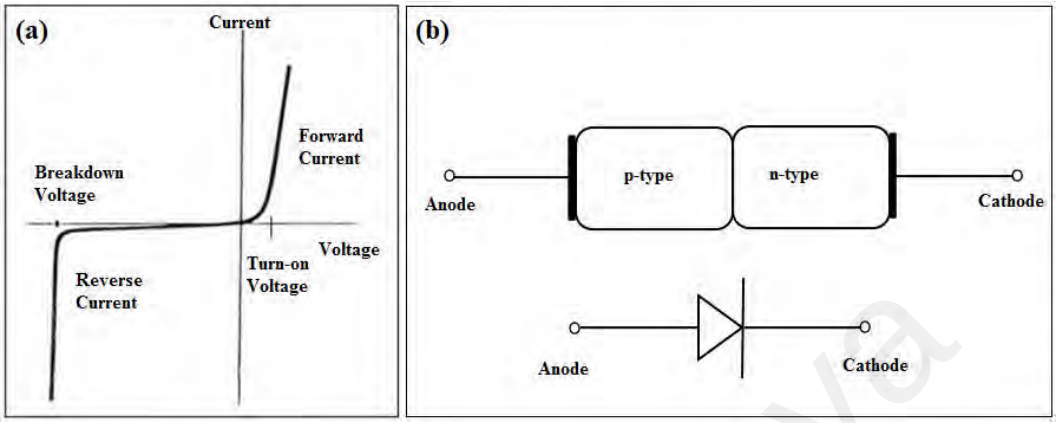

Figure 2.12: Schematics showing the (a) *I-V* characteristics for a typical p-n junction diode and (b) symbol of a typical p-n junction diode.

One of the most well-known form of diodes, the light-emitting diode (LED) are found in numerous uses and has proven to be extremely suitable to replace the aging technology of fluorescent lamps due to its efficiency of electric conduction. There are other electronic junctions and other types of diodes that have specific structures and functions. Schottky diode is one of these diodes that have a significant role in the electronics world.

2.4.3 Schottky Diodes

Schottky diode's construction is quite different than that of the conventional p-n junction. It has a structure of metal-semiconductor junction. The semiconductor is usually n-type Si (sometimes p-type Si is also used), while the metal can be of different choices such as molybdenum, chrome, platinum or tungsten. In metal, holes are the minority carrier and they are considered to be insignificant. Therefore, these two materials have electrons as the majority carriers. When the materials are joined together, the electrons in the n-type Si semiconductor flow into the metal and this creates a heavy flow of majority carriers. The injected carriers have a very high kinetic energy level compared to the metal's electrons. Those additional carriers in the metal cause a "negative wall" at the boundary between the semiconductor and the metal. This wall is called "surface barrier".

It prevents any further flow of current. That is, any electrons (negatively charged) in the Si material face a carrier-free region and a “negative wall” at the surface of the metal (Natarajan, 2012).

When a forward bias is applied through the diode, the strength of the negative barrier will be reduced, since the applied positive potential will attract the electrons in that region. This cause a return to the heavy flow of electrons through the boundary, the magnitude can be controlled by controlling the applied bias potential. Comparing the barrier heights for Schottky and p-n junctions, the barrier height for Schottky diode is less than that of the p-n junction device in both the forward and reverse-bias regions. That means higher current at the same applied bias in the forward and reverse-bias region for Schottky diode (Chen, 2014) as shown in Figure 2.13.

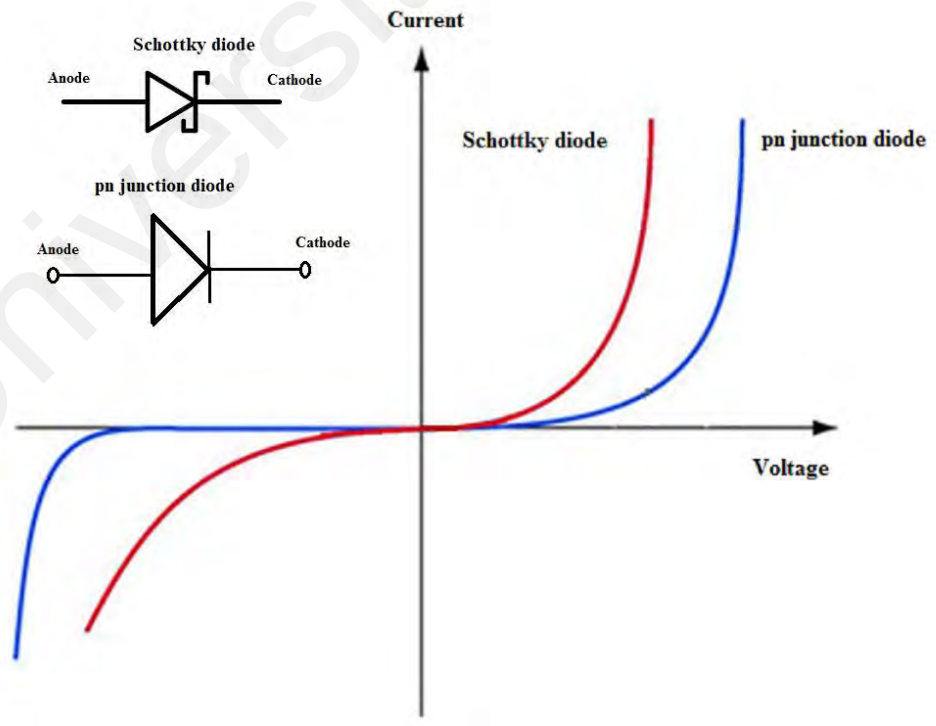

Figure 2.13: A comparison of symbols and *I-V* graphs for Schottky diode and p-n junction diode.

From the characteristic *I-V* graph above, it is clear that the current voltage curve is similar for both types of diodes in that, the currents rise exponentially with forward bias. However, the current is much larger for Schottky diode than the typical p-n junction, which means a smaller forward bias is required to produce a given diode current. This property makes the Schottky diode a good choice for rectifying and as such it is preferred as a rectifier in low-voltage and high-current applications. Even a small value of forward-voltage drop across the p-n junction diode will produce a large loss of power. Actually, Schottky barrier height is a function of the metal and the semiconductor. It depends on the work function of the metal and the electron affinity of the semiconductor and therefore both are different for different metals or semiconductors (Neamen, 2003).

There are many applications of Schottky diodes such as in operation at high frequency range, in AC (alternating current) to DC (direct current) converters, radar systems, mixers and detectors in communications equipment, analogue-to-digital converters and others (Robert & Louis, 1995).

2.4.4 Acquisition of *I-V* Characteristic Profiles and Calculation of Electronic Parameters

I-V characteristic of the forward bias region was used to obtain electrical parameters such as ideality factor, barrier height and series resistance of Schottky diode. Two different method were taken to calculate the values of the electrical parameter, and the values were compared to the most reliable model. The first method is to calculate the electrical parameter with the assumptions that the current in the Schottky diode is based on thermionic emission, and the effects of series resistance ignored for low forward bias region.

The equation for voltage and current (method 1) can be expressed as (Tuğluoğlu & Karadeniz, 2012; Tahir et al., 2012);

$$I = I_0 e^{\frac{qV}{nkT}}[1 - e^{\frac{-qV}{kT}}] \quad (1)$$

for$V > \frac{3kT}{q}$, equation (1) becomes as;

$$I = I_0 e^{\frac{qV}{nkT}} \quad (2)$$

where *n* is the ideality factor, *q* is the electronic charge, *k* is the Boltzmann constant, *T* is the temperature in Kelvin and I_o the reverse saturation current can be expressed as;

$$I_0 = AA^*T^2 e^{\frac{-q\emptyset_b}{kT}} \quad (3)$$

where *A* is the effective diode area, A^* is the effective Richardson constant which is equal to 1.3×10^5 A/cm^{2}K^2 for ITO (Joseph, Colwell, & Kaper, 1982; Gupta & Yakuphanoglu, 2012; Güllü, Pakma, & Türüt, 2012; Selçuk, Ocak, Aras, & Orhan, 2014; Al-Ta'ii, Amin, & Periasamy, 2015) and $\emptyset_b$ is the zero-bias barrier height. The I_o can be obtained by extrapolating the straight line of *ln I versus V* to intercept the axis at zero voltage.

$$\ln I = \ln I_o + \frac{q}{nkT}V \quad (4)$$

$$\emptyset_b = \frac{kT}{q}\ln\left(\frac{AA^*T^2}{I_0}\right) \quad (5)$$

Further, the deviation of Schottky diode form ideal thermionic emission model can be evaluated by calculating the ideality factor, *n* which can be extracted from the gradient of the straight-line *ln I* versus *V* plot and can be written from equation (2) as;

$$n = \frac{q}{kT}\left(\frac{\partial V}{\partial(\ln I)}\right) \quad (6)$$

To verify the values obtained for ideality factor and barrier height, Cheung and Cheung's method (Method 2) (Cheung & Cheung, 1986) which includes the effect of series resistance was adopted. The equation can be expressed as;

$$\frac{dV}{d\ln I} = n\frac{kT}{q} + IR_s \quad (7)$$

Using *dV/dln(I)* versus *I* graph, the axis intercept at zero current was obtained to calculate the ideality factor of the Schottky diode. The *H(I)* function meanwhile was obtained by using the Cheung and Cheung's method;

$$H(I) = V + n\frac{kT}{q}\ln\left(\frac{I}{AA^*T^2}\right) \quad (8)$$

$$H(I) = n\emptyset_b + IR_s \quad (9)$$

From the plots of *H(I)* versus *I*, *y*-axis intercepts were used to estimate the barrier height values of the Schottky junctions.

2.5 DNA Electronics

2.5.1 Conductivity in DNA

Scientists have been interested to understand how charges transfer through molecules for decades. The process of electron movement plays a significant role in most biological processes and chemical reactions. Photosynthesis, cellular respiration, DNA oxidative damage and most of the enzyme-catalysed reactions are few examples of these biological processes. Thus, studying the basic points and laws of electron transfer process is essential. In addition, understanding these things allow us to use them in interesting technological applications. Most of the biosensors or other diagnostic tools depend on detecting the biomolecules using different biological techniques coupled with optical detection. However, these techniques have some shortcomings like high cost, time consuming and needs labile natural products.

In electron transfer, there are two major mechanisms that can describe the reactions of electrons in biomolecules; hopping and tunneling. For tunneling process, quantum mechanics provided some explanations for the question of how charges can transfer between small nanosized biomolecules. However, according to classical mechanics, most

of the biomolecules are assumed to be insulators and they should constitute an impenetrable energy barrier for a charge (Artés et al., 2014).

DNA defines genetic information in living organic cells and besides this essential role, it has been a subject of investigation in the past few decades because of two important properties, which are the electronic and self-assembly properties. These two properties are very important for utilizing DNA in electronic devices. With the self-assembly property, DNA can be used to form novel nanostructures. Silver and palladium nanowires were fabricated using DNA molecules as templates. The possibility of electrical conductivity in DNA was first put forward by Eley and Spivey in 1962 not long after Watson and Crick's discovery of the DNA model (Eley & Spivey, 1962). At that time, researchers could not pursue the charge behavior and dynamics of the electrical mechanism as DNA was difficult to obtain and synthetic DNA was not available yet.

In electronic aspects, DNA has been suggested as a conductor because of the π-band formation of base pairs (Güllü et al., 2008; Güllü, 2010). Previously, a few researches did not confirm to this theory of charge transport in DNA. Insulating properties of DNA are based on series of experiments that investigate whether this result is because of external conditions like the type of substrate, the base pair sequence of the DNA, the distance between the electrodes and the contact material or due to the internal electronic properties of DNA (Storm et al., 2001). The outcomes of these experiments emphasize the absence of the electrical conductivity for double-stranded DNA molecules located between nano electrodes. No evidence of any electronic conductivity was observed for DNA at single-molecular scale with lengths larger than 40 nm and various pair sequences.

Other study by Braun et al., (1998) considered DNA as a template for silver nanoparticles after a bridge of DNA was formed between two electrodes of gold. Two sets of 12-mers of DNA were used to attach with the gold electrodes by using disulphide

functionalization. A connection is then made by hybridizing two distant surface-bound oligonucleotides with a 16 μm long and fluorescently labelled λ-DNA that contains two 12-base sticky ends, where each of the ends is complementary to one of the two different sequences attached to the gold electrodes. Then the growth of silver on DNA template with dimensions of (12 x 100) μm was carried out. Results of this research shows that the resistance was much higher (10^{13} Ω) in the case of using silver nanoparticle on DNA template, while the resistance is smaller by 100 times when DNA bridge or deposited silver were used without the DNA molecules. The *I-V* characteristics therefore demonstrated that λ-DNA behaves as an insulator (Braun et al., 1998).

In 1990s, Murphy and co-workers demonstrated the electric conduction in DNA according to the observed fluorescence quenching in DNA (Murphy et al., 1993). These studies of using DNA as conductors or non-conductors caused charge transport in DNA become a debatable subject. Therefore, in the past few decades, many researches in experimental aspects have been carried out to clarify the conduction properties of DNA (Fink & Schönenberger, 1999; Braun et al., 1998; Bhalla et al., 2003; Ventra & Zwolak, 2004). In spite of a lot of research in this area, the charge transport mechanism of DNA is remained inconclusive. In general, it is now understood that experiments with different initial conditions like humidity, DNA length, type of base pairs sequence, DNA storage condition, temperature and quality of contacts of DNA to the electrodes and surface adsorption could cause DNA to act as an insulator, semiconductor or conductor (Lin, Jiang, & Lu, 2005; Ventra & Zwolak, 2004).

Studies have also demonstrated that the electrons can transfer in DNA over distances of a few nanometers (Ventra & Zwolak, 2004; Storm et al., 2001). These researches were based on the characterization of electronic coupling through the DNA molecule when donor and acceptor groups were attached at both ends of the molecule. On the other hand,

some direct transport experiments indicate the possibility of transport for much larger length (in order of microns).

DNA bases have been shown to participate and mediate electron transfer when electrochemical and optical techniques were used (Kelley & Barton, 1999). Although there is no clear idea about the electron transfer process in DNA, scientists believe that this process is very important in many biological processes. For instant, oxidative DNA damage and the repair mechanisms linked to many life-threatening human diseases (D'Errico et al., 2008). Probably, the differences in the experimental conditions (such as different lengths or different base-pair arrangement of DNA) affect the results of conductance range in terms of several orders of magnitude. That might be the reason why DNA has been reported to be insulating, semiconducting, conducting and even superconducting (Genereux & Barton, 2010). In spite of the variations in the early reports of DNA conductance, the electron transfer mechanism in small oligonucleotides followed a transition from tunneling to hopping depending on the length and the sequence of the oligonucleotide (Venkatramani et al., 2011; Xu et al., 2004; Giese et al., 2001).

Charge transfer rate measured in double-stranded DNA by using redox probes (Giese et al., 2001) showed change in electron transfer mechanism when the number of A/T base pairs were increased from 1 to 16 in the sequence. The charge transfer rate has been studied indirectly as a function of length by using optical measurement in order to measure the ratios of different redox products that exist in the oligonucleotides. Tunneling and hopping processes coexist for the electron transfer between G/C base pairs in the DNA molecules. When the number of base pairs that separates the donor and the acceptor is less than four, the electron transfer rate can be explained by a super exchange tunneling process where the tunneling barrier is considered to be the A/T base-pair bridge. However, when that number is larger than or equal to four, the dependence on the length

becomes weaker and indicates a hopping electron transfer process (linear dependence with distance). As adenine has the second lowest ionization potential compared to the four bases, the adenines in this hopping electron transfer serves as intermediate states where the charge can be localized (Artés et al., 2014).

2.5.2 Previous Studies on Conduction in DNA

Fink & Schönenberger (1999) reported the first direct measurement of the conducting properties of DNA. It was found that DNA is a good conductor, where the *I-V* results represent resistance comparable to polymer conductors. This experiment was conducted in vacuum to eliminate other possible conducting factors, and a low-energy electron point source (LEEPS) microscope was used to image the DNA. A tungsten tip was used to apply a bias across the DNA and the measured resistance for a 600 nm portion of DNA was 2.5 MΩ. However, other researches (Beyer & Gölzhäuser, 2010) have suggested that the LEEPS imaging technique might have leached charges onto the samples and contributed towards the conducting behavior.

One of these researches by De Pablo and co-workers performed measurements on the resistance of λ-DNA by depositing DNA on a mica surface with a gold electrode (De Pablo et al., 2000). A gold-covered Atomic Force Microscopy (AFM) tip was used as a second contact. At different distances from the electrode, a lower resistivity limit of 10^4 Ωcm was measured for the DNA molecule. This suggested that λ-DNA is an insulator, directly contradicting the previous results by Fink and Schonenberger (1999). De Pablo et al (2000) suggested that the dispute can be due to the effect of the contamination from the low-energy electron beam used to image the DNA rope, which was proven when DNA samples resistivity was greatly reduced after irradiation.

Majority of other researchers however discovered that DNA resembles a large band gap semiconductor. By measuring the conductivity of poly(G)-poly(C) DNA, Porath and

co-workers discovered that the DNA oligomer did not conduct charge for biases below 1 V at RT, which is similar to the characteristics of a semiconductor with a large band gap (Porath et al., 2000). Similarly, Watanabe's team reported semiconducting behavior of a double strand DNA measured using an AFM with a carbon nanotube tip and a two-probe "nanotweezer" (Watanabe et al., 2001).

Storm and co-workers measured the conductivity of single DNA molecules and bundles of DNA molecules (Storm et al., 2001). Results indicated that while measured in ambient conditions, a lower resistance limit of 10 TΩ was found for ten mixed sequences of 1.5 μm long DNA molecules in parallel on a SiO_2 surface. There have been suggestions that compression caused by depositing DNA on surfaces changes its electronic structure. In this case, DNA height was at 0.5 nm, suggesting that compression induced by the surface decreased the conductivity.

Besides reported semiconducting, conducting or insulating behavior of DNA, Kasumov et al (2001) reported proximity-induced superconductivity in DNA. Rhenium/carbon electrodes were deposited on a mica surface and a flow of 16 μm long λ-DNA solution parallel to the electrodes was introduced. The overall resistance of the structure decreased from 1 GΩ without any DNA molecules to a few kΩ after deposition. Three different samples of varying lengths were obtained and the effect of temperature to resistance was studied. All samples resistance increased as temperature decreased, but samples resistance of 10 DNA chains (DNA1) and 40 DNA chains (DNA2) (based on sample labels given in the original article) decreased below the superconducting transition of the electrodes. Application of magnetic field decreased resistance at temperatures close to superconducting transition, which is observed for proximity-induced superconductivity. Although inconclusive, results showed that proximity-induced superconductivity can be realized in DNA and thermal hopping is an unlikely mechanism

of charge transport in λ-DNA as resistance does not increase directly with a decrease in temperature.

While the effect of ionic contamination to the DNA conductivity is well studied, other factors do influence the conductivity of DNA molecule. Lee et al. (2002) revealed that trapped oxygen has been found to dope poly(G)-poly(C) DNA with holes and increased the conductivity. When poly(G)-poly(C) DNA was exposed to pure oxygen gas instead of air, the conductance of the DNA increased by more than 100 times. Alternatively, when poly(T)-poly(A) DNA was placed in similar conditions, conductance of the DNA decreased. This result supports the initial findings that G-C basepair is a p-type semiconductor and A-T basepair is an n-type semiconductor.

2.5.3 DNA Charge Transport Mechanisms

Over the past several years, many charge transport mechanisms have been proposed. Nevertheless, three main possible mechanisms for charge transport were suggested, which are thermal hopping, sequential tunneling and coherent tunneling. The schematic of the processes is illustrated in Figure 2.14.

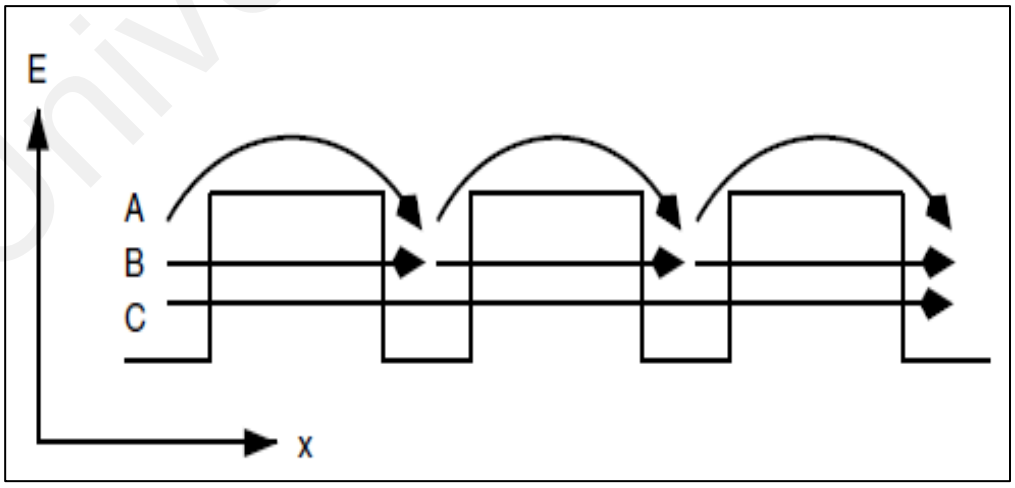

Figure 2.14: Schematic of three possible mechanisms of charge transfer in DNA, A: charges thermally hop from base to base, B: Charges tunnel from one site to another, C: charges can tunnel through the whole length of a DNA (Di Ventra & Zwolak, 2004).

Thermal hopping refers to the process where charges thermally hop from base to base as labeled as A in Figure 2.14. However, the thermal energy required for this process is quite large. Charges could also tunnel from one site to another, as demonstrated in Figure 2.14 (B). After each tunneling process, the coherence of the charge wavefunction is lost through dephasing processes such as scattering. Alternatively, charges can tunnel through the whole length of a DNA as it is shown in Figure 2.14 (C). However, this mechanism depends heavily on the distance or the length of the DNA molecule.

As the charge transport over large distances by a single tunneling step is unlikely and the high thermal energy required for thermal hopping, most researchers argue that sequential tunneling is the most likely mechanism of charge transport in DNA. In this mechanism, holes have been studied as the charge carrier. Of the four bases, the G base is the most favorable site for hole location due to the order of ionization potential.

2.5.4 DNA-Schottky Diodes

Schottky diodes, also known as hot carrier diodes, were named after the German physicist Walter H. Schottky. It is made up of a metal-semiconductor junction which creates the Schottky barrier (Mishra & Singh, 2007). Common metals are used in conventional Schottky diodes whereas the semiconductor would normally be n-type Si. In contrast, DNA-Schottky diodes are made up of DNA as the semiconductor, and common metals used in prior researches include Al and gold (Al-Ta'ii, Amin, & Periasamy, 2015; Al-Ta'ii, Periasamy, & Amin, 2015; Al-Ta'ii, Periasamy, & Amin, 2016).

There are some organic materials such as DNA that show semiconducting behavior followed by unusual magnetic, electric and optic properties. These enable the materials to attract much attention from physicist, biologist and chemist to employ them in the fabrication of molecular electronic devices (Aydoğan et al., 2005) mainly due to their low

cost and ease of processing. DNA has been demonstrated to be a good organic material with semiconducting behavior in nano-dimensions to be used in fabricating devices (Hwang et al., 2003). Biologically, the basic function of DNA is to code for functional proteins that are the expressed form of hereditary genetic information. However, in the last decades, discovering the conductivity property of DNA besides its special features, makes it one the most promising materials to be used in other interesting fields compared to its current usage in biophysics (Bhalla et al., 2003).

There were previous studies that made different device structures from DNA molecules based on theoretical aspects related with the DNA structure itself. DNA has phosphate bridges acting as tunnel junctions in the Coulomb blockade regime, and hydrogen bonds have capacitive properties (Ben-Jacob et al., 1999). The experimental measurements indicated that DNA transports electrical current as a proper semiconductor and so it is a good choice for electronic devices. Using DNA bases to form organic-inorganic Schottky structures and organic field effect transistors (OFET) has become one of the most important issues for scientists in the last few years.

The study on DNA-Schottky diodes is a relatively new area. Nonetheless, there has been previous researches on the study of DNA-Schottky diodes with varying setups and its vast applications such as sensors in various fields including thermal, optical, radiation and magnetic are well documented (Al-Ta'ii, Periasamy, & Amin, 2015; Al-Ta'ii, Periasamy, & Amin, 2016; Güllü & Türüt, 2011; Al-Ta'ii, Periasamy, & Amin, 2016; Gupta, Yakuphanoglu, Hasar, & Al-Khedhairy, 2011; Khatir et al., 2012; Zang & Grote, 2007; Al-Ta'ii, Periasamy, & Amin, 2016; Al-Ta'ii, Amin, & Periasamy, 2015; Al-Ta'ii, Periasamy, & Amin, 2015) contributing to the understanding of DNA-Schottky diodes.

Güllü and his team are one of the pioneers in the subject of DNA-Schottky diodes with works as early as 2008. In one of the researches published, an Al/DNA/p-Si Schottky

device was fabricated using the self-drying method of the DNA solvent (Güllü et al., 2008a). Electrical measurements of the Schottky device demonstrated rectifying effects and DNA has properties of semiconductor-like material with a wide band gap of 4.12 eV and resistivity of 1.6 x 10^{10} V cm representing p-type conductivity.

Research by Güllü and his co-workers were published in the subsequent years with varying device setups and research outcomes. These includes an Al/DNA/p-InP type device which had a remarkable ideality factor of 1.26 (Güllü et al., 2008c) and later using a similar junction architecture obtained improved ideality factor value of 1.087 (Güllü, Pakma, & Türüt, 2012). Changes in the electronic properties of Al/DNA/p-Si sandwich devices in regard to the temperature was also studied (Güllü & Türüt, 2011). Results indicated that ideality factor and the barrier heights varied with a change of temperature from -73°C to 26°C (200 to 300 K), suggesting the suitability of the DNA-Schottky diodes as a temperature sensor.

Güllü et al. (2008b) studied the fabrication of DNA-based organic-on-inorganic (OI) Schottky device (Güllü et al., 2008b). DNA was used as an interlayer on conventional metal/semiconductor structure in order to study the suitability and possibility of using organic material on inorganic semiconductor contact barrier diode to be used in modification of the barrier of metal-semiconductor (MS) junction. Al, DNA and indium phosphide semiconductor (InP) were used in the experiment to form the required structure. The results of the *I-V* measurement of the experiment demonstrated that this DNA-based structure shows an excellent rectifying behavior, and that the DNA film increases the effective barrier height by influencing the space charge region of InP. However, here the DNA layer was reported to be an insulator on the InP semiconductor to form hybrid layer to modify the Schottky barrier height.

There are some other researches (Güllü & Türüt, 2011; Güllü & Türüt, 2015; Al-Ta'ii et al., 2015) that used DNA in fabricating MS devices with rectifying behavior besides calculating the electronic parameters to indicate close characteristics as with the conventional Schottky diodes but with more advantages related to the special properties of DNA. One of the works carried out in our research group involved the electrical measurement of Schottky diode structure in the form of Au/DNA/ITO showed a strong rectification (Al-Ta'ii et al., 2016) and an improved rectification phenomenon of self-assembled DNA films in the presence of electric field (Chan et al., 2015). The experiment involved conducting *I-V* characterizations for ITO-DNA-Al structure aligned using electric field and repeated without alignment. Results showed higher rectification for the aligned sample compared to the non-aligned, suggesting that the orientation of DNA strands affects their conductivity. Figure 2.15 below shows the *I-V* profile for the ITO-DNA-Al structure before and after alignment.

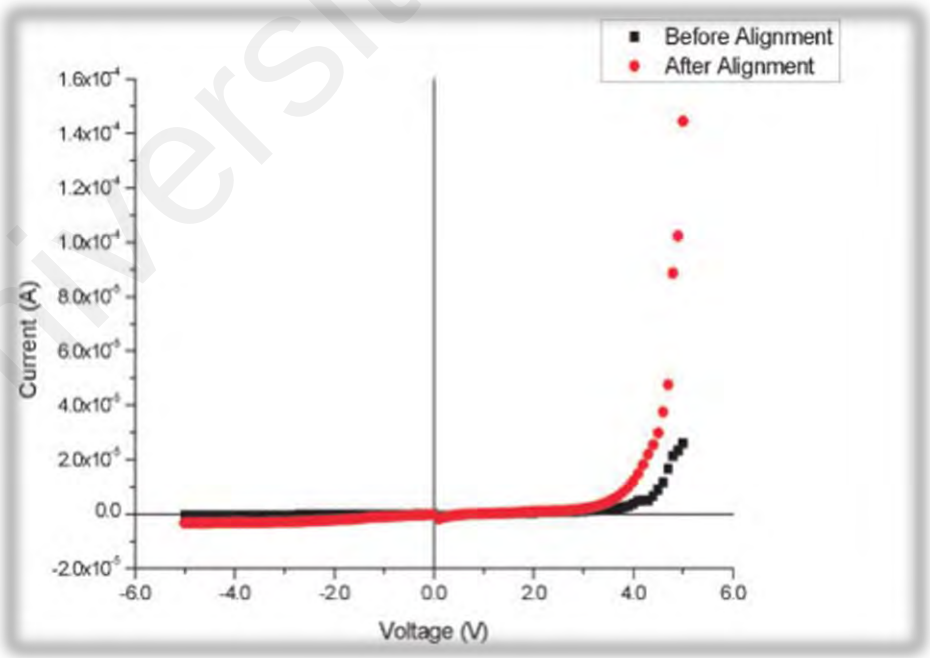

Figure 2.15: *I-V* profile for ITO/DNA/Al device before and after alignment with electric field (Chan et al., 2015).

Electrical characterization of DNA-Schottky diodes were carried out by various groups throughout the years utilizing different set-ups. All the researches indicated rectifying

behavior of the device. In one such research, Au/DNA/n-Si/Au junction fabricated had a typical ideality factor of 1.22 (Sönmezoğlu et al., 2010). Another study discussed the effect of thickness and coverage of DNA film on the electrical characterization and interface properties of Au/DNA/n-Si Schottky diodes (Okur, Yakuphanoglu, Ozsoz, & Kadayifcilar, 2009). The thickness and coverage rate of the DNA layer significantly affects the electrical properties of the Au/DNA/n-Si organic-on-inorganic structures. Al-Ghamdi's research group meanwhile developed DNA-based sensor and compared the electronic performance of DNA/Si junction with SiO_2/Si junction (Al-Ghamdi et al., 2012). The ideality factor for the DNA/Si junction is lower at 1.82 as compared to 3.31 for the latter junction.

Aside from the application of DNA-Schottky diodes as a temperature sensor, researchers had demonstrated that an Ag/DNA/p-Si/Al diode can be used as an optical sensor (Gupta et al., 2011). The photoresponse of the diode was measured with varying frequencies. At lower frequencies, the capacitance of the diodes was found to increase as an effect of the change in interfacial states. It was also observed that the series resistance of the diode is decreased with increasing light intensity and increased with decreasing frequency under constant light intensity.

DNA-Schottky diodes have also demonstrated its ability to behave as magnetic and radiation sensors. The effects of magnetic field on Au/DNA/Au Schottky diodes were demonstrated where results indicated a decrease in conductivity with increase of magnetic field strength, suggesting a potential application as a magnetic sensor (Khatir et al., 2012). More recently, studies on the effect of alpha particle radiation on an Au/DNA/ITO device was carried out (Al-Ta'ii et al., 2016). Barrier heights from *I-V* measurements were calculated from 0.7284 eV for the non-radiated samples which increased to 0.7883 eV when exposed to 0.036 Gy of alpha radiation. Based on the results, the authors suggested

that the Au/DNA/ITO Schottky junction sensor may be utilized as a sensitive alpha particle detector.

The properties of the DNA-metal Schottky junction were utilized to respond variably in a highly characteristic manner in both the positive and negative bias regions towards different base sequences. This known aspect of DNA's semiconductive behavior as a Schottky junction is the basis for the current research reported in this thesis in terms of DNA characterization and detection using the electronic signatures. Based on these electronic data, analysis of the solid-state behavior of the respective DNA-Schottky structures consisting of various quantitative solid-state parameters can then be calculated to quantify the observations numerically. Closely related DNA can be characterized, associated and distinguished, thus providing an avenue for creating a database of DNA Schottky profiles. The database of DNA Schottky profiles or electronic database can then be used to identify and profile unknown DNAs.

2.6 Effect of Ionic Liquid on the Long-Term Stability of DNA

2.6.1 Overview

Due to the large effect of electrostatic interactions, DNA duplex stability can be influenced by the surrounding environments (McFail-Isom, Sines, & Williams, 1999). Different buffer conditions, small molecule concentrations, higher salt concentrations or even different solvents can all affect the stability of DNA (Bonner & Klibanov, 2000; Lerman, 1964). Binding of the DNA to a substrate can affect the secondary structure, which also changes the stability (Macquet & Butour, 1978). This is a key component in the design of biosensors or the use of DNA for targeted applications.

DNA has been widely studied in a variety of solvents. The majority of these solvents consist of either aqueous or organic components. The presence of ions or salts in these solvents can further alter the DNA properties by changing the melting point or helical

structure. The size, charge and concentration of these additional components can all affect the behaviour of DNA. A new class of solvents known as ionic liquids (ILs) have recently gained popularity. ILs are comprised of entirely of ions and can be liquid at RT. Due to the low volatility and ability to dissolve both polar and non-polar substances, they are generating high levels of interest as 'green solvents' (Zhang, 2006). Although the interaction between DNA and ILs has been characterized, the potentials of this interaction is still being studied.

2.6.2 Ionic Liquids

ILs, also known as organic salts, are liquids that are comprised entirely of ions. Unlike molecular solvents, every molecular unit of IL has an ionic charge. Even more interesting is the fact that many of these are liquids at RT. The presence of the ionic species results in vastly different thermodynamic properties, making them highly interesting. Additionally, ILs have no identifiable vapour pressure, resulting in no detectible emission of volatile organic compounds, allowing ionic solvents to be perfect for 'green' methods (Seddon, 1997; Rogers & Seddon, 2003; Plechkova & Seddon, 2008; Earle & Seddon, 2000; Brennecke & Maginn, 2001; Holbrey & Seddon, 1999; Blanchard, Hancu, Beckman, & Brennecke, 1999). A large source of environmental pollution is the volatile organic compounds that are the by-product of traditional industrial solvents. Using ILs would reduce this emission intensity (Rogers & Seddon, 2003).

Since ionic solvents able to dissolve both polar and non-polar substances and remain in a liquid state for a much larger range of temperatures as compared to molecular solvents (Brennecke & Maginn, 2001). Many ionic solvents are immiscible in other molecular solvents, allowing for phase separation as a means of extraction or the fabrication of multiple phase systems (Welton, 2011). Depending on the eventual goal and use, ILs can be tailored to fit the desired objective. For example, ILs can be prepared to be either

hydrophobic or hydrophilic simply by changing the anion. Hydrophilic anions, such as iodide and chloride, result in ILs that are miscible in water. If hydrophilic anions such as Hexafluorophosphate (PF_6^-) are used, the resulting IL is hydrophobic and immiscible in aqueous mediums. Increasing the chain length of the cation has also been found to increase the hydrophobicity (Huddleston et al., 2001).

2.6.3 Applications in DNA Chemistry

Although interest in ILs has surged recently, there are only several cases in which ILs have been utilized in conjunction with DNA. Many of these examples deal with electrochemistry, where DNA is stabilized within an IL solvent. The ILs present a good environment for electrochemical applications due to their high conductivity and good solubility (Leone et al., 2001; Guo et al., 2007; Nishimura et al., 2005; Qin & Li, 2003; Sun et al., 2008). ILs have also been used to create DNA films with high conductivity (Nishimura & Ohno, 2002; Ohno & Nishimura, 2001).

One application of electrochemistry is the ability to detect hybridization of double-stranded DNA without the use of a label or dye. The value of impedance changes upon hybridization. If the DNA strand probe is first immobilized onto an electrode, the hybridization can be detected through the increase in electron transfer resistance. Although this is possible without the use of ILs, their presence could largely enhance the sensitivity (Zhang et al., 2009).

ILs can also be used to enhance the detection of specific bases. Both adenine and guanine show characteristic oxidation peaks. This allows for a comparison of the ratio between the peaks, such that a single strand of DNA can be measured for both A or G content (Sun, Li, Duan, & Jiao, 2008). It was found that the presence of IL in these sensors

can greatly enhance the peak, essentially increasing the sensitivity of the probe (Sun et al., 2008).

Although ILs are said to be inert, this does not infer that there is no interaction between DNA and the IL. A detailed study was carried out to determine the interaction characteristics between DNA and 1-butyl-3-methylimidazolium tetrafluroborate. It was found that the IL could interact with DNA through electrostatic interactions, even going so far as to be able to replace some molecules that had already bound to the DNA (Xie et al., 2008). A schematic of this interaction is shown in Figure 2.16. Another research showed that the addition of IL with the DNA dye conjugate could cause a decrease in fluorescence. It was hypothesized that this IL bound competitively with the DNA, eventually being able to displace the EB completely (Ding, Zhang, Xie, & Guo, 2010).

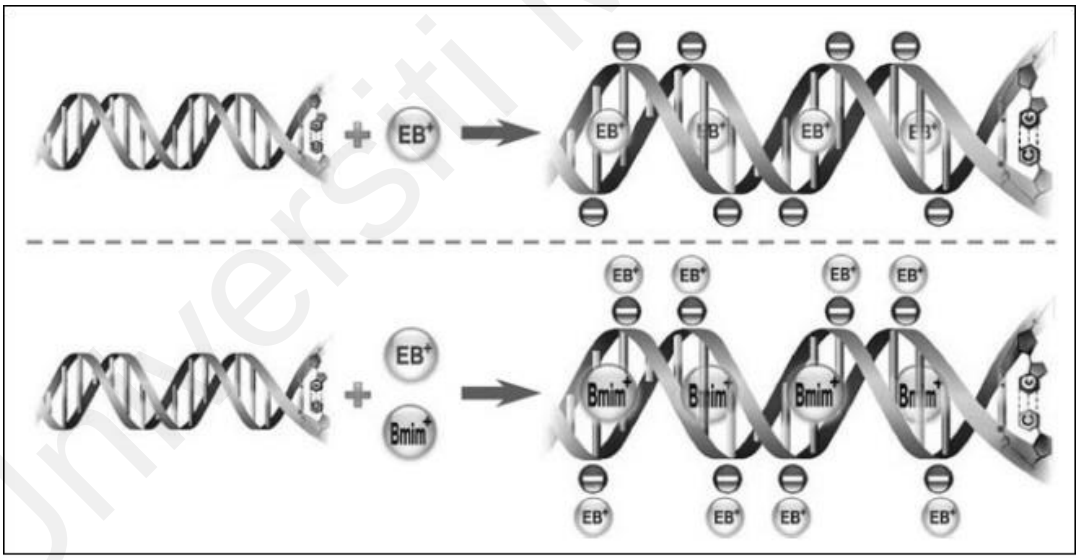

Figure 2.16: Interaction between ethidium bromide (EB), IL and DNA (Cheng et al., 2007).

With respect to the DNA itself, some ILs such as choline dihydrogenphosphate have been found to significantly increase DNA stability. Generally, DNA is stored under refrigeration, as the double helix structure could be disrupted in a month of storage at RT (Fujita et al., 2005). However, if stored in ILs, this structure remains uncompromised, even if left at RT for up to six months (Fujita et al., 2006). Additionally, it has been

reported that ILs improves temperature stability of the duplex by preventing denaturation at higher temperatures as compared to an aqueous medium (Tateishi-Karimata & Sugimoto, 2014).

In some hydrated ILs, DNA can be stabilized up to a temperature of 100°C, which is significantly higher than in a fully aqueous medium (Vijayaraghavan et al., 2010). Other ILs, such as the hydrophobic propylammonium nitrate (PN) has been found to destabilize the DNA duplex by lowering the melting point. As low as 1% concentration was enough to change the melting point by 8°C. Higher concentrations can bring the melting point to below RT (Menhaj et al., 2012).

2.7 Ultraviolet-Visible Spectroscopy

UV-Vis spectroscopy is an analysis technique which uses visible (400 to 700 nm) and ultraviolet (190 to 400 nm) regions of the electromagnetic spectrum to obtain information about organic molecules (Tissue, 2002). It can also be performed to determine the impurities in a sample. Additional peaks other than the specimen substance's peak indicate the presence of impurities. It gives information about structural elucidation of the specimen. Combination and location of peaks helps us to analyse whether saturation, unsaturation and hetero atoms exist in the specimen or not. Quantitative analysis of compounds which absorb UV or visible radiation can be performed using Beer-lambert law (Mäntele & Deniz, 2017).

Qualitative analysis can then be performed to determine the type of compounds present in the specimen. The spectrum obtained by UV-Vis spectrophotometer is compared to the spectra of known compounds. Qualitative analysis of functional groups can also be determined as presence of a band at certain wavelength determines the presence of a particular group.

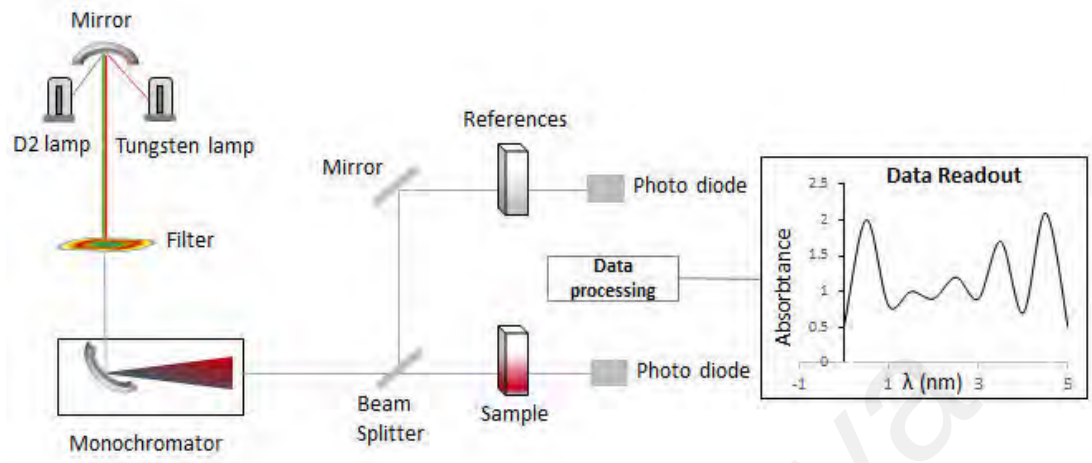

Figure 2.17: Schematic diagram of a UV-Vis spectrophotometer (Source: Shakir, 2017).

The schematic diagram of a UV-vis spectrophotometer is shown in Figure 2.17. When the molecules that possess non-bonding or π electrons are irradiated by the UV-Vis light, the electrons get excited to higher anti-bonding orbitals. Lesser the energy gap between HOMO and LUMO of a material, easier is the excitation of electrons by longer wavelength radiations. When a molecule with energy gap between HOMO-LUMO equal to ΔE (change in energy) is exposed to radiation with wavelength corresponding to ΔE, electron jumps from HOMO to LUMO. This is referred to as σ-σ^* transition. The plot between wavelength on *x*-axis and absorbance on *y*-axis is obtained and analysed (Lott, 1968).

2.8 Significance of This Study

DNA electronics gave birth to the idea and the possibility of nucleic acid assisted production of small-scale electronic devices and denser circuits. This study utilised new device production methods due to the difficulties and limitations of conventional technologies when it comes to nanoscale processing (Porath et al., 2006). In this research, the DNA molecules were utilized to create a DNA-metal (semiconductor-metal) device

and study the effect of electric current conduction across it. By sandwiching the DNA with a metal, a Schottky diode is created which generates a rectifying *I–V* profile specific to the type of DNA used. This DNA-specific Schottky diode may have potential applications ranging from biosensors (Hu, 2009; Al-Ta'ii et al., 2015; Zang & Grote, 2007; Al-Ta'ii et al., 2016; Al-Ta'ii et al., 2016; Al-Ta'ii et al., 2015; Al-Ta'ii et al., 2015) to DNA detection and identification as will be demonstrated in Chapter 4.

Molecular diagnostic techniques alone are not enough for species identification. However, these tools are often not readily available for rapid diagnosis. The cost of equipment and technical expertise necessary for these techniques is usually high. On the other hand, the morphology characteristics is the basis to identify the species but in some cases, morphology alone can bring incorrect identification. The major drawbacks of these techniques are time consuming. PCR technology requires technical expertise, special equipment and specific primer design and also not user-friendly.

The current method reported in this thesis however, consists of acquiring characteristic electronic signals from semiconducting DNA molecules, which could be a simpler, rapid and cost-effective, compared to the molecular techniques.

CHAPTER 3: MATERIALS AND METHODS

3.1 DNA Materials Preparation and Qualification

3.1.1 DNA Isolation

Fresh fruiting bodies of six different species of mushrooms *Pleurotus eryngii* (KLU-M 1380), *P. floridanus* (KLU-M 1382), *P. pulmonarius* (KLU-M 1384), *P. giganteus* (KLU-M 1227, KLU-M 1385), *P. cystidiosus* (KLU-M 1388) (Figure 3.1), and two control species *Lentinula edodes* (KLU-M 1386) and *Flammulina velutipes* (KLU-M 1387) were used in this study (Table 3.1). A small piece of dried tissue about 6 milligrams (dried in a food dehydrator for 24 hours) was cut and placed in a 2 ml micro centrifuge tube. Total genomic DNA was extracted using Forensic DNA Extraction Kit (Omega Bio-tek) according to the manufacture's protocol with modification.

Initially, 100 μl STL buffer was added and samples were grinded for 2 min. Then another 100 μl STL buffer was added and incubated for 15 min at 55°C. After brief centrifugation, 25 μl OB protease solutions was added to the samples and mixed by vortexing and incubated for 45 min at 60°C with occasional mixing. The samples were centrifuged to remove any droplets from the lids. Then 225 μl BL buffer was added to the tubes and incubated for 10 min at 60°C. The tubes were briefly centrifuged and 225 μl absolute ethanol was added to the samples and mixed thoroughly by vortexing. After centrifugation, the aqueous phase was removed. Meanwhile, HiBind DNA columns were inserted into the collection tube.

Equilibrium buffer (100 μl) was added into the columns and left for 4 min at RT. It was then spun at 13000×g for 30 s by using microcentrifuge (Eppendorf MiniSpin plus centrifuge). The entire sample including precipitation that formed was transferred from the microcentrifuge tubes to the earlier prepared HiBind DNA columns. HiBind DNA column containing samples were spun at 8000×g for 1 min to bind the DNA to the matrix

of columns. The collection tubes and flow through liquid were discarded and columns were placed into new collection tubes. HB buffer (500 μl) was pipetted into columns and were centrifuged at 8000×g for 1 min. The flow through liquid was discarded while collection tubes were reused. DNA were washed by pipetting 750 μl of wash buffer into column and centrifuged at 8000×g for 1 min.

Figure 3.1: The eight different species of mushrooms; (a) *Pleurotus cystidiosus* (KLU-M 1388), (b) *Pleurotus floridanus* (KLU-M 1382), (c) *Pleurotus eryngii* (KLU-M 1380), (d) *Pleurotus giganteus* (KLU-M 1385), (e) *Pleurotus giganteus* (KLU-M 1227), (f) *Lentinula edodes* (KLU-M 1386), (g) *Flammulina velutipes* (KLU-M 1387) and (h) *Pleurotus pulmonarius* (KLU-M 1384). Bar scale = 1.0 cm.

Table 3.1: Details of the six types of *Pleurotus* species and two control species from different genus.

Common Name	Species Name	Specimen Code	Sources
King Oyster	*Pleurotus eryngii*	KLU-M 1380	Imported from China
White Oyster	*Pleurotus floridanus*	KLU-M 1382	Locally grown (Damansara Sdn Bhd)
Gray Oyster	*Pleurotus pulmonarius*	KLU-M 1384	Locally grown (Damansara Sdn Bhd)
Seri Pagi	*Pleurotus giganteus*	KLU-M 1227	Origin from China
Wild *P. giganteus*	*Pleurotus giganteus*	KLU-M 1385	Collected from local forest
Abalone	*Pleurotus cystidiosus*	KLU-M 1388	Locally grown (Gano farm)
Shiitake	*Lentinula edodes*	KLU-M 1386	Origin from China
Enoki	*Flammulina velutipes*	KLU-M 1387	Korea

Both flow through liquid and collection tubes were discarded. New collection tubes were used, and DNA washed for second time by pipetting 750 μl of wash buffer into column and centrifuged at 8000×g for 1 min. The flow through liquid was discarded while collection tubes were stored. The columns were centrifuged at 13000×g for 2 min to dry the columns. All columns were transferred to new 1.5 ml Eppendorf tubes.

Preheated elution buffer (50 μl) at 70°C was added to columns and left for 3 min at RT. Columns were then centrifuged at 8000×g for 1 min for elution. Second elution was done by adding another 50 μl of preheated elution buffer (70°C) to columns and left for 3 min at RT. Columns were then centrifuged at 8000×g for 1 min for elution. DNA samples contained in Eppendorf tubes were then stored at -20°C freezer for future use. The DNA qualitfication was measured using NanoDrop spectrophotometer and ultraviolet-visible spectroscopy.

3.1.2 DNA Qualification Using NanoDrop and Ultraviolet-Visible Spectroscopic Measurement

The DNA quality was determined by using a NanoDrop spectrophotometer (Figure 3.2). The ratios of absorbance (A) at 260 to 280 nm and 260 to 230 nm were provided to assess DNA purity; A260/280 nm for protein contamination, and A260/230 nm for salt and phenol contamination. Pure DNA is known to absorb light at 260 nm and the A260/280 and A260/230 ratio is observed to be 1.8 to 2.0 and 2.0 to 2.2, respectively (Wilfinger, Mackey, & Chomczynski, 1997). This experiment has been repeated three more times for different samples that obtained from the experiments in the following sections: 3.1.4, 3.1.5 and 3.1.6.

Figure 3.2: The NanoDrop spectrophotometer used in this research (Institute of Biological Sciences, Faculty of Science, University of Malaya).

UV-Vis Spectroscopy is a method of characterization where a beam of varying wavelength ranging from the UV to the visible light spectrum passes through a sample solution and the absorbance of the sample across the wavelength is measured. The UV-

Vis spectroscopy works on the principle of Beer-Lambert law (Spectronic, 2012), which states that;

$$A = \log_{10} \frac{I_o}{I} = \varepsilon cL$$

where A is the measured absorbance, I_o is the intensity of the incident light, I is the transmitted intensity, ε is the molar absorptivity constant, c is the concentration of the sample and L is the path length through the sample. In this study, all UV-Vis analysis was obtained using a Shimadzu UV–visible spectrometer (UV-2600, Japan) to emphasize on the existence of DNA film on the substrate and to confirm DNA functionality. DNA monolayer film deposited on quartz slides was left to dry for 2 min prior to the UV-Vis measurement. Scanning wavelength was chosen from 240 to 300 nm representing the visible region of the electromagnetic spectrum normalized against a clean quartz slide used as reference for the measurement.

3.1.3 DNA Concentration Adjustment

In this research, the same amount of fruit bodies of each species was extracted to obtain almost the same concentration of DNA for the DNA extraction process. After which, the DNA concentration was measured using NanoDrop spectrophotometer. For the same sample, measurement is taken three times and the average calculated. The nearest concentrations were chosen.

To evaluate the effect of different concentration on the electronic properties of DNA, six species of mushrooms *Pleurotus eryngii* (KLU-M 1380), *P. floridanus* (KLU-M 1382), *P. pulmonarius* (KLU-M 1384), *P. giganteus* (KLU-M 1227, KLU-M 1385) and *P. cystidiosus* (KLU-M 1388) were chosen. The concentrations of the DNA solutions were then adjusted to about 100 ng/μl to 5 ng/ μl with the addition of the elution buffer. The experiment with the same species was the repeated with different concentrations. *I-*

V experiments were conducted to assess the influence of the differences in concentration of the extracted DNA to the electronic properties of the DNA-Al diodes.

3.1.4 pH Adjustment Using HCl and NaOH Aqueous Solutions

Six species of mushrooms *Pleurotus eryngii* (KLU-M 1380), *P. floridanus* (KLU-M 1382), *P. pulmonarius* (KLU-M 1384), *P. giganteus* (KLU-M 1227, KLU-M 1385) and *P. cystidiosus* (KLU-M 1388) were chosen, to evaluate the effect of different pHs on the electronic properties of DNA. The result for *Pleurotus eryngii* (KLU-M 1380) is presented in Chapter 4 (Results and Discussion). Profiles for other five DNA samples, which are following the same trends are shown as Supplementary profiles in Appendix A (Figure S1-S10) to avoid repetition.

pH of the extracted DNAs used initially was at around pH 8. The pH values of DNA solutions were then adjusted to 7.0 to 14.0 and 7.0 to 1.0 with the addition of 1 M NaOH and 1 M HCl, respectively. DNA quality was further assessed using NanoDrop spectrophotometer after adjusting the pH for all DNA solutions.

3.1.5 Dissolution of DNA in Ionic Liquid and Storage

Six species of mushrooms *Pleurotus eryngii* (KLU-M 1380), *P. floridanus* (KLU-M 1382), *P. pulmonarius* (KLU-M 1384), *P. giganteus* (KLU-M 1227, KLU-M 1385) and *P. cystidiosus* (KLU-M 1388) were chosen, to evaluate effect of IL on the long-term structural and chemical stability of genomic DNAs. The results for *Pleurotus eryngii (KLU-M 1380), P. floridanus (KLU-M 1382)* and *P. pulmonarius (KLU-M 1384),* are presented in Chapter 4 (Results and Discussion). Profiles for other three genomic DNA samples are shown as supplementary in Appendix B (Figure S1-S3) as the results are followed the same trends.

The extracted genomic DNAs in elution buffer (DNA aqueous solution, aq/DNA) was used for *I-V* characterization before proceeding with storage at different temperatures and time intervals. Briefly, 20 μl of the aq/DNA was added into the vials containing 40 μl of [BMIM][Ace] which stored at different temperatures and time intervals. The DNA samples was stored in the following conditions; aq/DNA stored for 1 week at 4°C, aq/DNA stored for 1 week at RT (28± 2°C), aq/DNA stored for 1 month at 4°C, aq/DNA stored for 1 month at RT, aq/DNA stored for 2 months at RT, aq/DNA stored for 3 months at RT, DNA dissolved in [BMIM][Ace] (IL/DNA) stored for 1 day at RT, IL/DNA stored for 1 week at RT, IL/DNA stored for 1 month at RT, IL/DNA stored for 2 months at RT and IL/DNA stored for 3 months at RT. Meanwhile, IL was used as a control. The IL ([BMIM][Ace]) was obtained from Sigma Aldrich (Missouri, United States) and dried under vacuum prior to use to remove any water content.

3.1.6 Polymerase Chain Reaction (PCR)

PCR was used to amplify the desired ribosomal DNA of the following regions which are internal transcribed spacer (ITS), large subunit ribosomal DNA (LSU) and second largest subunit of RNA polymerase II (RPB2). There are generally three stages in PCR which include denaturation, annealing and extension. A total of 50 µl PCR mixture contain 5.0 µl of 10X $MgCl_2$ free buffer, 2.0 µl of 10 mM dNTP mixture, 1.0 µl of 1 U/ml i-Taq DNA Polymerase, 2.0 µl DNA template (with concentration of 53 to 54 ng/µL), 2.5 µl of 10 µM forward primer, 2.5 µl of 10 µM reverse primer and 35 µl of sterile distilled water. The primer pairs used for ITS region were ITS1 (5'-TCCGTAGGTGAACCTGCGG -3') (White et al, 1990) and ITS4 (5'-TCCTCCGCTTATTGATATGC-3') (White et al, 1990); primer pairs used for LSU region were forward primer LR0R (5'-ACCCGCTGAACTTAAGC-3') and reverse primer LR5 (5'-ATCCTGAGGGAAACTTC-3') (Vilgalys & Hester, 1990) and primer pairs used for LSU region were RPB2 fRPB2-5F forward primer

(GAYGAYMGWGATCAYTTYGG) (Liu et al., 1999) and bRPB2-7.1R reverse primer (CCCATRGCYTGYTTMCCCATDGC) (Matheny, 2005) primers. The reaction mixtures were mixed by suspension using micropipette, then were spun for about 4 s using Eppendorf MiniSpin plus centrifuge prior transferred to thermocycler (BioRad Mycycler TM Thermal Cycler).

PCR protocol was set to initial denaturation at 95°C for 4 min, followed by 35 cycles of denaturation at 94°C for 30 s, annealing between the range of 55°C to 60°C for 1 min for all three different regions, extension at 72°C for 1 min. Final extension of the protocol was set at 72°C for 5 min. DNA quality was further assessed using NanoDrop spectrophotometer. The amplified DNA in PCR mixture [DNA aqueous solution (aq/DNA)] was used for the *I-V* characterization before proceeding with storage at different temperatures and time intervals.

3.1.6.1 Purification of amplified-PCR products

PCR amplification products were purified using MEGAquick-spin^{TM} PCR & Agarose Gel DNA Extraction System Kit (iNtRON Biotechnology, Inc.) following manufacturer protocol with modification. Five volumes of BNL buffer was added to the PCR products and the mixture was resuspended using micropipette. Columns were placed into collection tubes. The suspended mixtures were transferred to columns and spun at 13000 rpm for 1 min. The flow through liquid was discarded. Washing buffer (700 µl) was added and spun at 13000 rpm for 1 min. The flow through liquid was discarded. Next, 500 µl of washing buffer was added and spun at 13000 rpm for 1 min for second washing. The flow through liquid was discarded. Columns were dried by centrifuged at 13000 rpm for 1 min.

Collection tubes were discarded, and columns were transferred to 1.5 ml Eppendorf tubes. Elution buffer (20 µl) was added to the columns and left for 1 min at RT. Elution was carried out by centrifugation at 13000 rpm for 1 min. The elution was repeated by

adding 20 µl of elution buffer and left for 1 min. Next, columns were centrifuged again at 13000 rpm for 1 min. The columns were discarded, and purified PCR products were stored at -20°C. Purified PCR products were subjected to gel electrophoresis for examination.

3.1.7 Gel Electrophoresis Analysis

PCR products were examined using gel electrophoresis. Agarose gel was prepared by mixing agarose powder with 1×Tris-Borate EDTA (TBE) buffer. Mixture was heated using microwave to allow the agarose to melt. After the mixture form a clear solution indicating agarose fully melted, the solution was cooled using running tap water and RedSafe TM nucleic acid staining solution (20000×) was added and mixed with the solution. The solution was then poured onto a mould, comb was placed, and the gel was left for about 30 min for cooling and solidifying.

PCR products (5.0 µl) was mixed with 1.2 µl of iNtRON loading dye before loaded into the well and 1×BE buffer was used as running buffer. The gel separation was carried out for 60 min at 100 V. After electrophoresis, the gel was viewed under autoradiograph machine (AlphaDigiDoc UV transilluminator). The same procedure using same amount and same concentration were used for gel electrophoresis analysis of genomic DNA. The purified PCR products were sent to NextGene laboratory for outsourcing DNA sequencing services.

3.1.8 Dissolution of PCR-Amplified DNA in Ionic Liquid and Storage

Briefly, 20 μl of the PCR-amplified DNA of the same species that were mentioned in section 3.1.6 was added gradually into the vials containing 40 μl of [BMIM][Ace] which stored at different temperatures and time intervals. The PCR-amplified DNA samples was stored in the following conditions; aq/DNA stored for 1 week at 4°C, aq/DNA stored for 1 week at RT (28±2°C), aq/DNA stored for 1 month at 4°C, aq/DNA stored for 1 month

at RT, aq/DNA stored for 2 months at RT, aq/DNA stored for 3 months at RT, IL/DNA stored for 1 day at RT, IL/DNA stored for 1 week at RT, IL/DNA stored for 1 month at RT, IL/DNA stored for 2 months at RT and IL/DNA stored for 3 months at RT. In order to determine the degradation in molecular weight of DNA samples during storage, gel electrophoresis studies were carried out. The electrophoresis results for *Pleurotus eryngii (KLU-M 1380), P. floridanus (KLU-M 1382)* and *P. pulmonarius (KLU-M 1384)* using ITS region, are presented in Chapter 4 (Results and Discussion) and the rest of the results are presented as Supplementary profiles to avoid repetition in Appendix B (Figure S4-S6).

3.2 Phylogenetic Analysis

Sequencing results for sample included in studies were in the forms of both ChromasPro and FASTA format. Forward and reverse sequences which are reverse complementary were assembled into contigs and electropherogram were compared to combine both forward and reverse sequencing results using ChromasPro. Ambiguous nucleotide matches were substituted by codes according to Johnson, (2010). Ending part of both forward and reverse sequences were trimmed (5-15 bp) due to low convincing level of the sequences.

Consensus sequences were subjected to BLAST search (Altschul et al., 1990) for comparing to sequences within GenBank nucleotide database and getting a preliminary understanding of the identity of the sequences. Relevant sequences were download from GenBank nucleotide database. ClustalX (Larkin et al., 2007) was used for multiple sequence alignment of the sequences from samples included in this study and also relevant sequences downloaded from GenBank. Bioedit version 7.1.11 (Hall, 1999) was used to examine and remove ambiguous nucleotide characters through truncation of sequence terminal. Then a phylogenetic tree is produced using MEGA-X software. The

evolutionary history was inferred by using the Maximum Likelihood method and Tamura-Nei model (Tamura & Nei, 1993). Initial tree(s) for the heuristic search were obtained automatically by applying Neighbor-Join and BioNJ algorithms to a matrix of pairwise distances estimated using the Maximum Composite Likelihood (MCL) approach, and then selecting the topology with superior log likelihood value.

The phylogenetic analysis included 24 reference ITS sequences (Table 3.2), 24 reference LSU sequences (Table 3.3.) and 16 RPB2 reference sequences (Table 3.4) were downloaded from Genbank. Eight ITS, LSU and six RPB2 sequences were generated in this study (Table 3.1). Because of the unsuccessful sequencing for RPB2 region, *P. giganteu*s (KLU-M 1385) and *Lentinula edodes* (KLU-M 1386) are not included in the phylogenetic analysis. There were not enough RPB2 region reference sequences of *P. giganteus* and *P. cystidiosus* in GenBank; therefore, they are not included in the Table 3.4. While three species from different Genus *Flammulina, Lentinula* and *Hohenbuehelia* were used as outgroup. *Lentinula* belongs to the family of Omphalotaceae and *Flammulina* belongs to Physalacriaceae family and were used for the *I-V* characterization. Therefore, they were included in the phylogenetic analysis for comparison. *Hohenbuehelia* is closely related taxa to *Pleurotus* which is a member of Pleurotaceae family.

Table 3.2: List of species, geographical origin and GenBank accession number of ITS sequences.

Species	GenBank Accession Number	Geographical origin
Pleurotus cystidiosus	KR149589	Pakistan
Pleurotus cystidiosus	KP164598	China
Pleurotus cystidiosus	KX787089	China
Pleurotus eryngii	FJ904770	Italy
Pleurotus eryngii	FJ904769	Italy
Pleurotus eryngii	FJ904757	Italy
Pleurotus floridanus	MG819742	India
Pleurotus floridanus	MG819737	India
Pleurotus floridanus	MG324371	India
Pleurotus pulmonarius	JN942347	USA
Pleurotus pulmonarius	KF724533	China
Pleurotus pulmonarius	KX688468	China
Pleurotus giganteus	MN244447	China
Pleurotus giganteus	MK855519	India
Pleurotus giganteus	KY800375	China
Flammulina velutipes	JQ713571	China
Flammulina velutipes	EF015573	India
Flammulina velutipes	MK634571	USA
Lentinula edodes	AY636052	India
Lentinula edodes	AY636053	India
Lentinula edodes	JN790683	India
Hohenbuehelia sp. R-113	KR135368	Mexico
Hohenbuehelia atrocoerulea	KX349906	Finland
Hohenbuehelia mastrucata	KX349907	Finland

Table 3.3: List of species, geographical origin and GenBank accession number of LSU sequences.

Species	Genbank Accession No.	Geographical origin
Pleurotus cystidiosus	KX787098	China
Pleurotus cystidiosus	NG_057793	China
Pleurotus cystidiosus	EU365639	China
Pleurotus eryngii	EU365653	China
Pleurotus eryngii	EU365652	China
Pleurotus eryngii	KX787100	China
Pleurotus floridanus	EU365656	China
Pleurotus floridanus	MG282510	China
Pleurotus floridanus	MG282544	China
Pleurotus pulmonarius	MH447275	Taiwan
Pleurotus pulmonarius	MH395999	New Zealand
Pleurotus pulmonarius	MH396003	New Zealand
Pleurotus giganteus	KX809689	China

Table 3.3, continued

Species	Genbank Accession No.	Geographical origin
Pleurotus giganteus	KX809688	China
Pleurotus giganteus	KX809687	China
Flammulina velutipes	NG027630	USA
Flammulina velutipes	AY207200	Germany
Flammulina velutipes	MH867626	Netherlands
Lentinula edodes	MH868347	Netherlands
Lentinula edodes	MH868346	Netherlands
Lentinula edodes	MK278257	Hungary
Hohenbuehelia thornii	KU355400	Italy
Hohenbuehelia atrocoerulea	MK278144	Hungary
Hohenbuehelia josserandii	KU355404	Italy

Table 3.4: List of species, geographical origin and GenBank accession number of RPB2 sequences.

Species	Genbank Accession No.	Geographical origin
Pleurotus cystidiosus	GU186819	USA
Pleurotus eryngii	KX870370	China
Pleurotus eryngii	KX870367	China
Pleurotus eryngii	KX870365	China
Pleurotus floridanus	KX870341	China
Pleurotus floridanus	KX870336	China
Pleurotus floridanus	KX870338	China
Pleurotus pulmonarius	KY865580	China
Pleurotus pulmonarius	JQ513872	China
Pleurotus pulmonarius	KU613033	China
Flammulina velutipes	AY786055	USA
Flammulina velutipes	KY201340	China
Flammulina velutipes	KY201378	China
Hohenbuehelia petaloides	KU214437	Austria
Hohenbuehelia cyphelliformis	KU214447	Austria
Hohenbuehelia thornii	KU355426	Italy

3.3 Fabrication of the Al/DNA Schottky Junction Diode

ITO slides (KINTEC, Hong Kong) of width 1.1 mm, had a layer thickness of 100 nm with a dimension of 2 cm × 2 cm and 377.0 Ω/sq and about 10^4 S/cm of sheet resistance and conductivity, respectively. The thickness of the Al wire electrodes used was (0.50 ± 0.05) mm and purity 99.999% (Sigma Aldrich, USA). Prior to diode fabrication, the ITO

substrates were thoroughly cleaned by rinsing with soap in an ultrasonic bath for 10 to 15 min. The slides were washed using deionized water and immersed in acetone and isopropanol for 5 min each, followed by a final rinse using deionized water. Finally, the slides were dried using nitrogen gas to remove any water and other residues. A droplet of 10 µl of DNA/PCR-amplified DNA solution was then applied onto the cleaned ITO glass substrate using the simple and economical method of self-assembly. The entire preparation and fabrication process were undertaken in a 1K clean room to make sure the same environmental conditions (temperature at about 21°C and 70 to 80% relative humidity (RH)) were maintained.

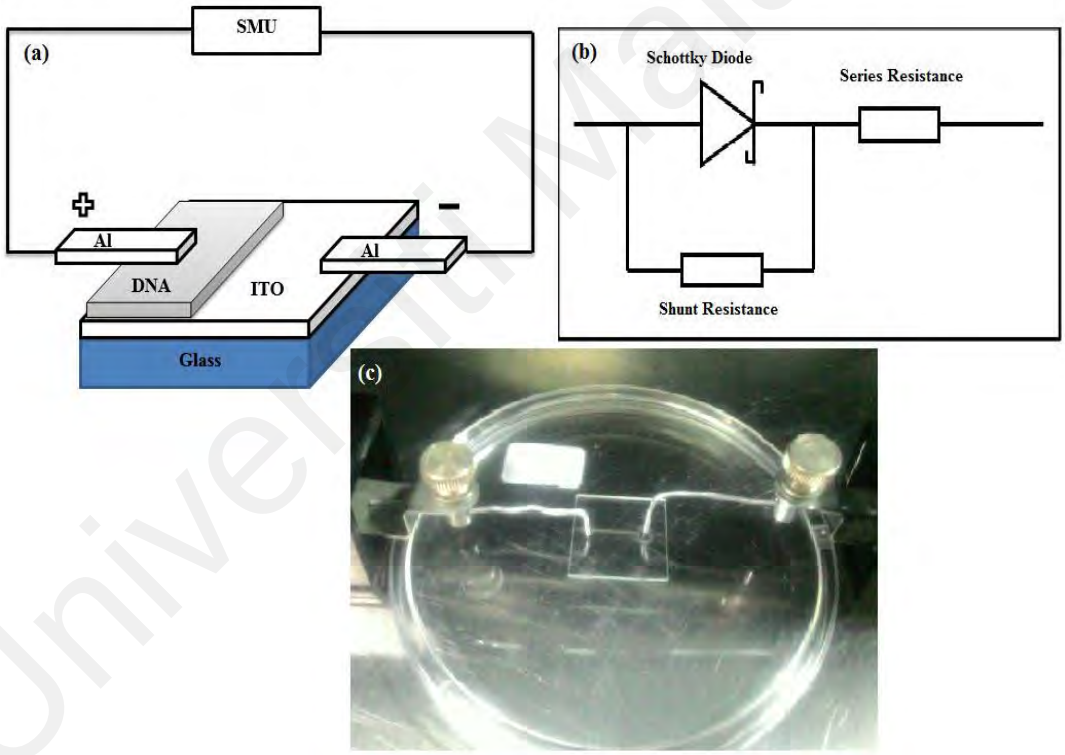

Figure 3.3: (a) The schematic diagram of the DNA-specific Schottky diode fabricated for the study while (b) represents the equivalent electrical circuit and (c) the actual photograph.

Figure 3.3 demonstrates the schematic diagram and picture of the fabricated sensor for the measurement of the *I-V* characteristics (Keithley Electrometer, SMU 236). *I-V* characteristic of the forward and reverse bias regions was used to obtain various quantitative solid-state parameters such as ideality factor, barrier height, shunt resistance,

series resistance, turn-on voltage, knee-voltage, breakdown voltage and breakdown current. Each data obtained from the DNA samples were generally averaged over six replicate measurements to allow for a higher statistical significance.

CHAPTER 4: RESULTS AND DISCUSSION

4.1 DNA Characterizations Studies

4.1.1 DNA Qualification for Both Genomic and PCR-Amplified DNA Using NanoDrop Spectrophotometer and UV-Vis Spectroscopy analysis

Sample quality was assessed by using absorbance measurements at 260 nm and 280 nm as shown in Figures 4.1 and 4.2, respectively. DNA concentration and absorbance ratio using a NanoDrop spectrophotometer were shown in Table 4.1 and Table 4.2. As shown in tables, the DNA concentrations were almost similar. It is understood that the exact concentrations of DNA cannot be attained as Nanodrop method will always show small variations in the reading.

The absorbance ratio of 260 nm to 280 nm was used to assess the DNA purity. Pure DNA has a A260/280 ratio of 1.8 to 2.0, and the expected A260/230 value should be in the range of 2.0 to 2.2. The lower A260/230 values of samples indicate the contamination of chaotropic salts and carbohydrates. Meanwhile, the higher A260/230 ratio may be the result of dirty pedestal for blank measurement and blank measurement with an inappropriate solution. The abnormal A260/280 ratios usually indicate contamination with protein or reagent such as phenol, salts and other contaminants (Wilfinger et al., 1997). However, in this experiment both values of ratios fall within the suggested values for pure DNA, demonstrating the high purity of the isolated DNA used for this study.

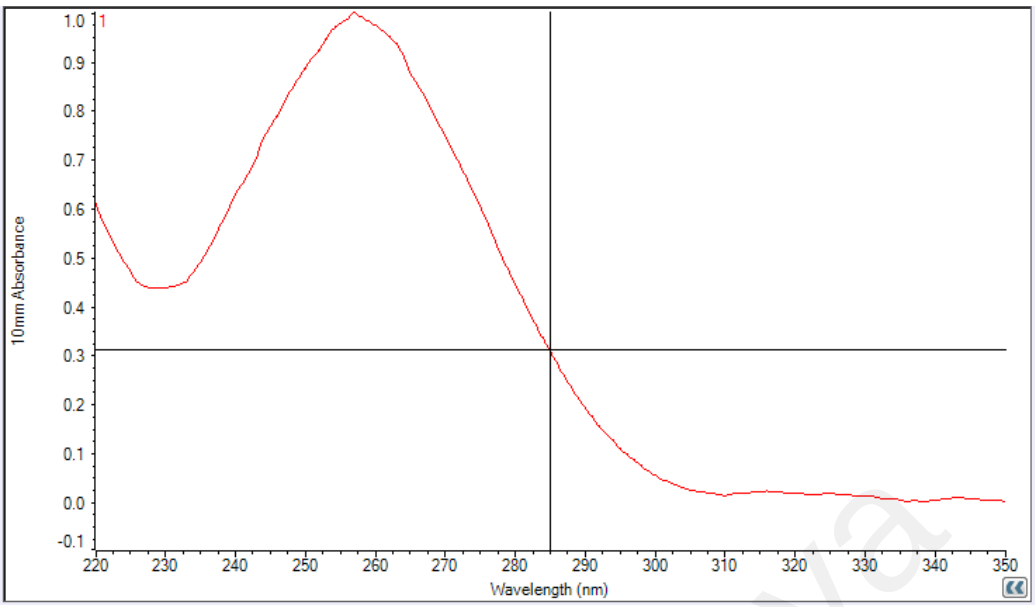

Figure 4.1: Absorption spectra of genomic DNA sample (KLU-M 1380).

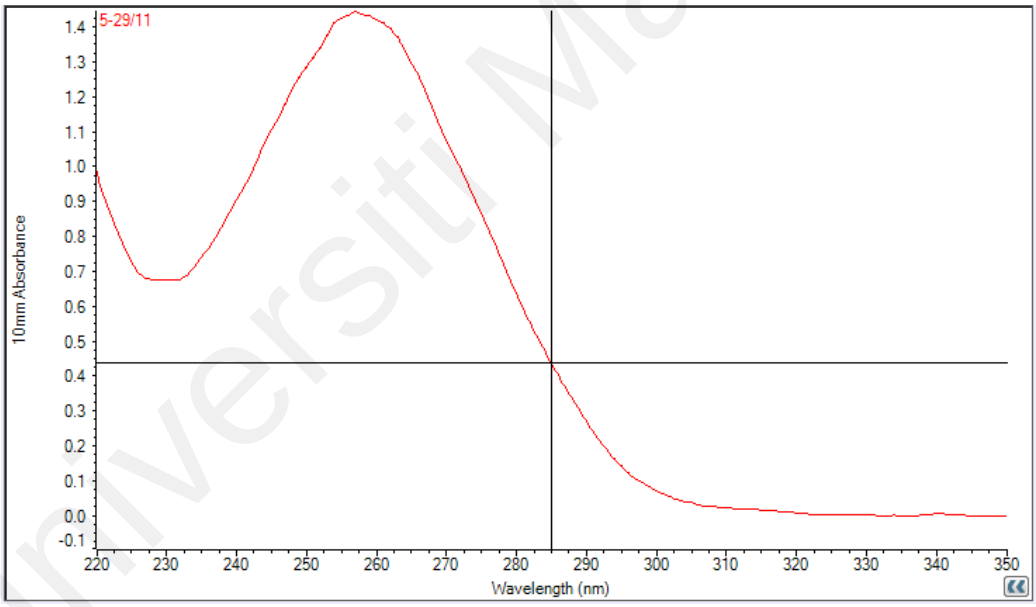

Figure 4.2: Absorption spectra of PCR-amplified DNA sample (KLU-M 1380).

Table 4.1: NanoDrop results of the genomic DNA of the eight *Pleutorus* species investigated in this study.

Sample	*P. floridanus (KLU-M 1382)*	*P. pulmonarius (KLU-M 1384)*	*P. eryngii (KLU-M 1380)*	*P. giganteus (KLU-M 1227)*	*P. giganteus (KLU-M 1385)*	*P. cystidiosus (KLU-M 1388)*	*F. velutipes (KLU-M 1387)*	*L. edodes (KLU-M 1386)*
Nucleic Acid Concentration ng/µL	53.9	53.1	54.8	53.7	54.2	53.1	54.4	53.3
A260/A280	1.95	1.85	1.98	1.80	1.85	1.83	1.86	1.81
A260/A230	2.15	2.19	2.00	2.21	2.18	2.20	2.10	2.04

Table 4.2：NanoDrop results of the PCR-amplified DNA of the eight *Pleurotus* species investigated in this study.

ITS region								
Sample	***P. floridanus (KLU-M 1382)***	***P.pulmonarius (KLU-M 1384)***	***P. eryngii (KLU-M 1380)***	***P. giganteus (KLU-M 1227)***	***P. giganteus (KLU-M 1385)***	***P. cystidiosus (KLU-M 1388)***	***F. velutipes (KLU-M 1387)***	***L. edodes (KLU-M 1386)***
Nucleic Acid Concentration ng/µL	197.7	195.2	197.0	196.1	189.9	199.2	193.5	196.7
A260/A280	1.79	1.81	1.92	1.85	1.86	1.99	1.98	1.88
A260/A230	2.21	2.12	2.18	2.20	2.09	2.19	2.08	2.11

Table 4.2, continued.

RPB2 region								
Sample	***P. floridanus (KLU-M 1382)***	***P.pulmonaris (KLU-M 1384)***	***P. eryngii (KLU-M 1380)***	***P. giganteus (KLU-M 1227)***	***P. giganteus (KLU-M 1385)***	***P. cystidiosus (KLU-M 1388)***	***F. velutipes (KLU-M 1387)***	***L. edodes (KLU-M 1386)***
Nucleic Acid Concentration ng/µL	196.8	196.1	199.3	194.9	201.1	198.6	188.2	192.6
A260/A280	2.01	1.80	1.91	1.89	1.94	1.86	1.89	1.97
A260/A230	2.03	2.20	2.09	2.11	2.18	2.06	2.13	2.01
LSU region								
Sample	***P. floridanus (KLU-M 1382)***	***P.pulmonaris (KLU-M 1384)***	***P. eryngii (KLU-M 1380)***	***P. giganteus (KLU-M 1227)***	***P. giganteus (KLU-M 1385)***	***P. cystidiosus (KLU-M 1388)***	***F. velutipes (KLU-M 1387***	***L. edodes (KLU-M 1386)***
Nucleic Acid Concentration ng/µL	188.4	201.3	200.8	194.6	199.9	189.3	203.7	179.2
A260/A280	1.82	1.96	1.87	1.93	1.85	2.02	1.90	1.85
A260/A230	2.22	2.18	2.11	2.05	2.20	2.14	2.07	2.16

Pure DNA is known to have an absorption peak at 260 nm within the ultraviolet region where photon at this wavelength has the sufficient energy to release electrons in DNA molecules corresponding to the p-p* electrons transition of C=C DNA bases bonds (Zang & Grote, 2007; Tataurov et al., 2008). The UV-Vis analysis on the sample showed a maximum absorbance at 260 nm as seen in Figures 4.3 and 4.4. This observation is indicative of the successful transfer of DNA molecules from the surface of the buffer subphase to the solid substrate while maintaining the integrity and purity of the molecules.

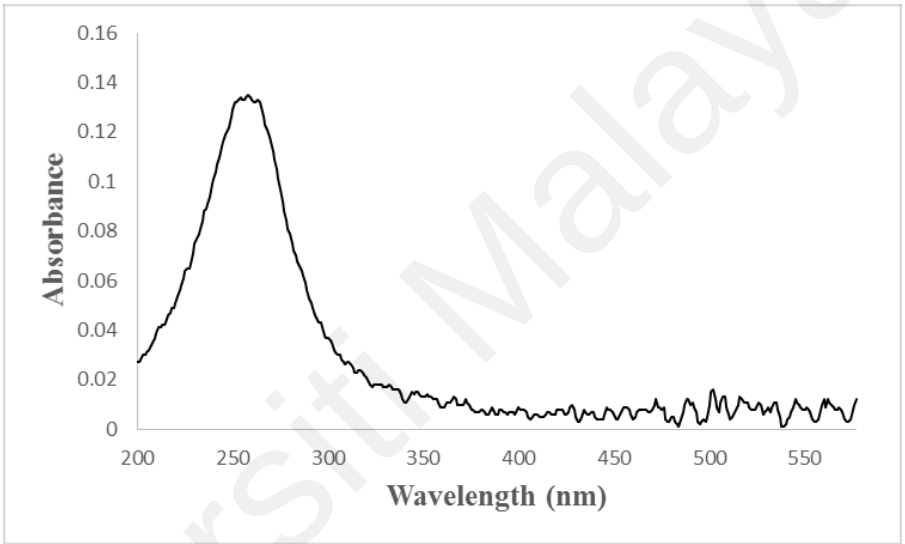

Figure 4.3: UV-Vis analysis of genomic DNA sample (KLU-M 1380).

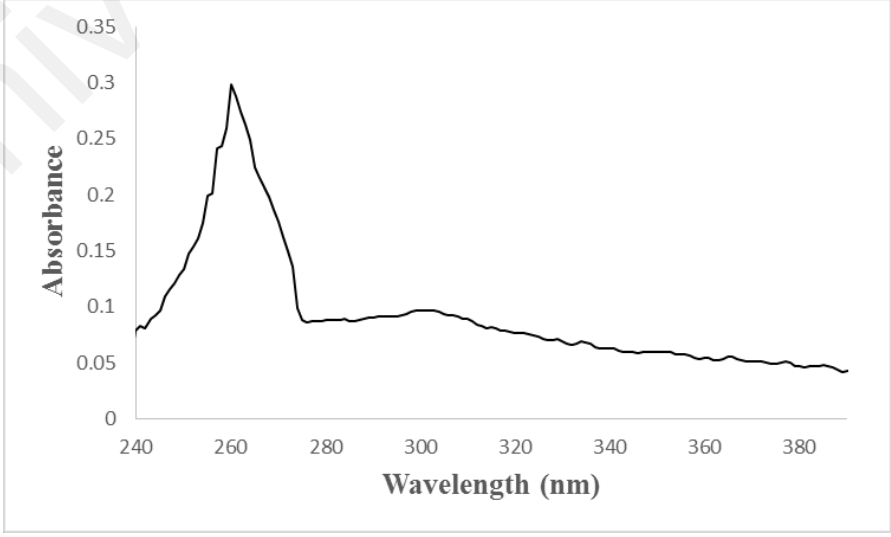

Figure 4.4: UV-Vis analysis of PCR-amplified DNA sample (KLU-M 1380).

4.2 Genetic Marker (ITS, LSU, RPB) Amplification and Sequencing

The ITS, LSU and RPB DNA had been successfully amplified for 24 samples (eight samples for each region) confirmed by the presence of the bands in the gel electrophoresis. For DNA sequencing, eight out of eight samples for ITS and LSU and six out of eight samples for RPB were successfully amplified. Unsuccessful sequencing for *P. giganteus* (KLU-M 1385) and *Lentinula edodes* (KLU-M 1386) using RPB may be attributed to the contamination during the DNA extraction process.

4.2.1 Gel Electrophoresis Analysis

Gel electrophoresis is one of the major techniques used in molecular biology for the analysis of DNA. This method involves the migration of fragments of DNA through a gel where they are separated based on their size. DNA samples are loaded into the gel, and an electric current is applied to pull them through the gel.

DNA fragments are negatively charged, so they move towards the positive electrode. Because all DNA fragments have the same amount of charge per mass, small fragments move through the gel faster than the larger ones. When a gel is stained with a DNA-binding dye, the DNA fragments can be seen as bands, each representing a group of same-sized DNA fragments. However, for long molecules of DNA, it is quite difficult to avoid breakage, which leads to breaking it into smaller fragments generating smears of DNA on the gel. This smear contains many different sizes of DNA that cannot be easily distinguished. Figure 4.5 shows the result of gel electrophoresis of genomic DNA isolated from the eight different species of *Pleurotus*. As it is shown, sizes of molecules in genomic DNA are manifested as smears.

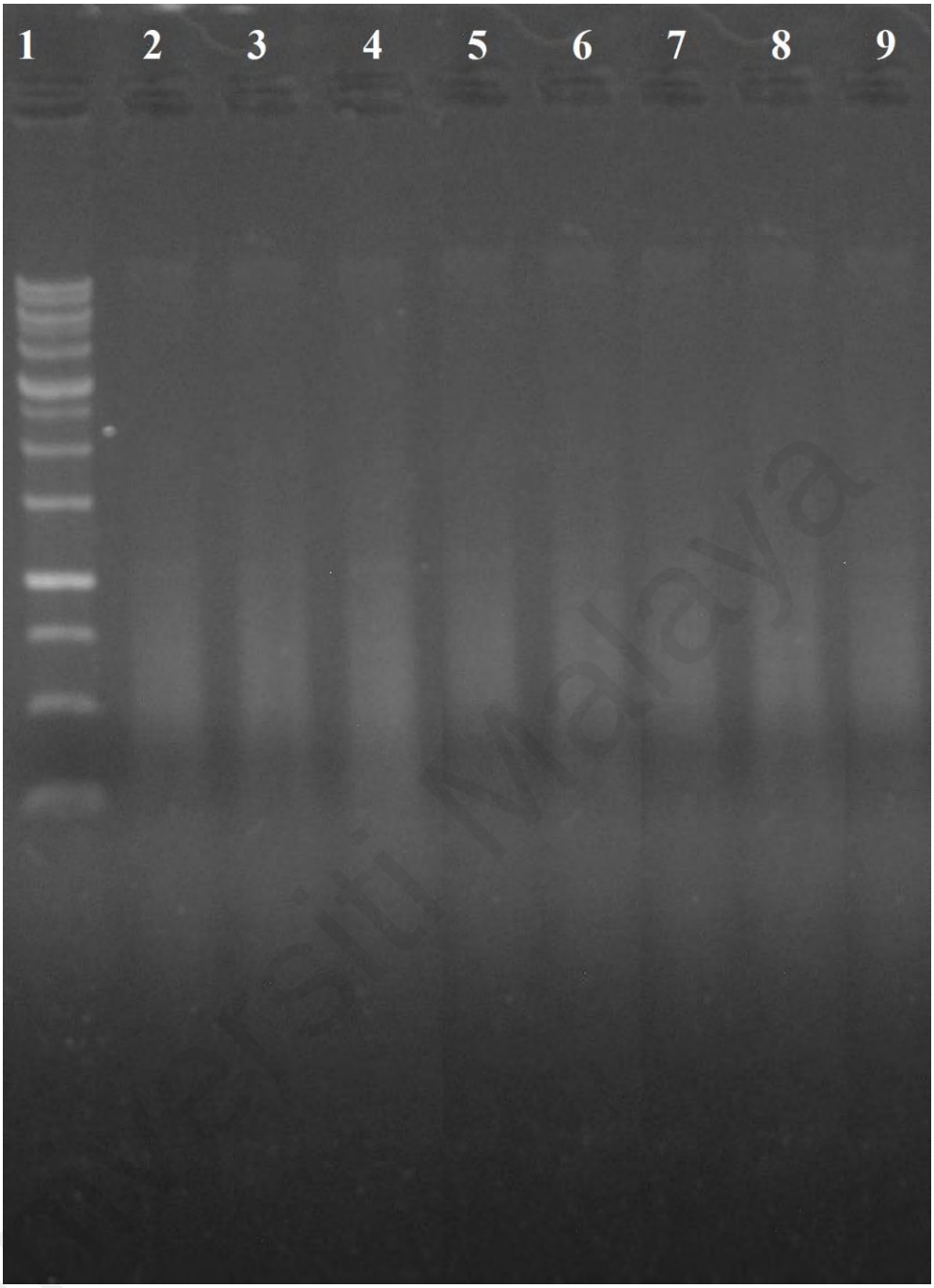

Figure 4.5: Electrophoresis of genomic DNA isolated from eight different species of *Pleurotus*; DNA samples were separated on a 0.8% agarose gel in 1×TBE buffer. Lane 1: 1 kb DNA ladder; Lane 2: genomic DNAs of *Pleurotus cystidiosus* (KLU-M 1388), lane 3: *Pleurotus floridanus* (KLU-M 1382), lane4: *Pleurotus eryngii* (KLU-M 1380), lane5: *Pleurotus giganteus* (KLU-M 1385), lane 6: *Pleurotus giganteus* (KLU-M 1227), lane 7: *Pleurotus pulmonarius* (KLU-M 1384), lane 8: *Lentinula edodes* (KLU-M 1386) and lane 9: *Flammulina velutipes* (KLU-M 1387), respectively.

The PCR-amplified DNA in the ITS region were visualized as a single band in agarose gel. The size of the PCR fragments was between 700 to 800 bp. The size of PCR amplification products in the LSU region produced visible amplicons between 900 to

1000 bp, while in the RPB2 region it produced single visible band in size of 1100 to 1200 bp. No amplification products were found for the negative controls (Figure 4.6).

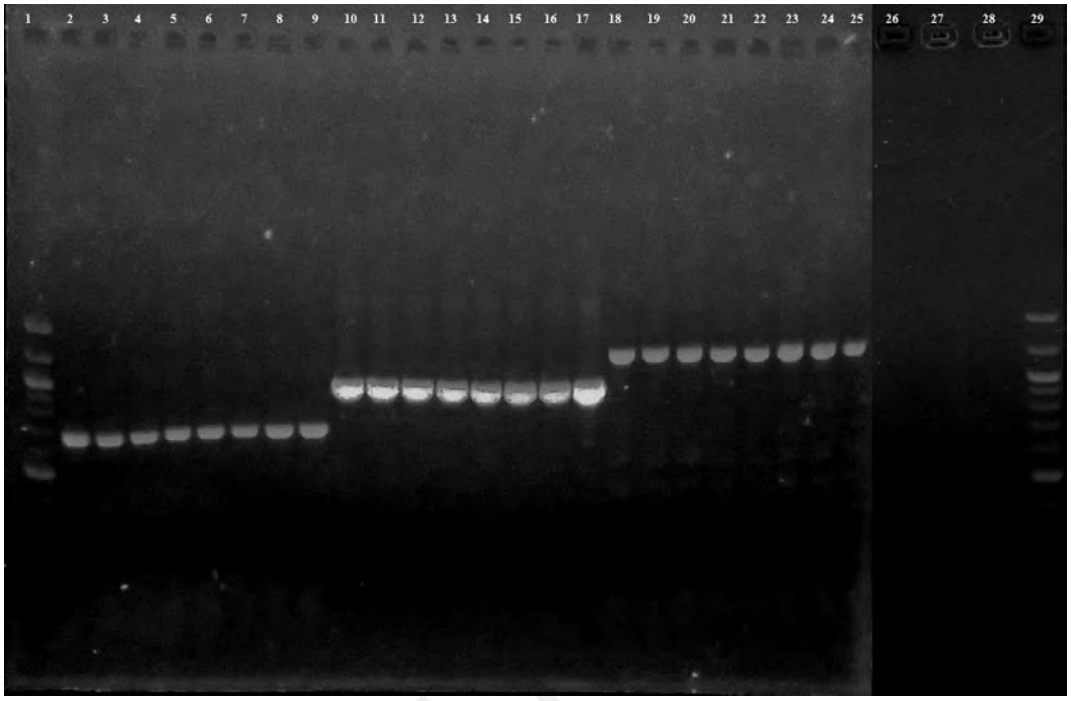

Figure 4.6: Gel electrophoresis of PCR amplification products obtained from eight different species of *Pleurotus* with ITS1/ITS4 (lane 2-9), LSU: LR0R/LR5 (lane 10-17) and RPB2: fRPB2-5F/bRPB2-7.1R (lane 18-25) primers set. Lane 1: 1 kb DNA ladder; lane 2: ITS amplicons of *Pleurotus cystidiosus* (KLU-M 1388), lane 3: *Pleurotus floridanus* (KLU-M 1382), lane 4: *Pleurotus eryngii* (KLU-M 1380), lane 5: *Pleurotus giganteus* (KLU-M 1385), lane 6: *Pleurotus giganteus* (KLU-M 1227), lane 7: *Pleurotus pulmonarius* (KLU-M 1384), lane 8: *Lentinula edodes* (KLU-M 1386) and lane 9: *Flammulina velutipes* (KLU-M 1387), respectively; lane 10: LSU amplicons of *Pleurotus cystidiosus* (KLU-M 1388), lane 11: *Pleurotus floridanus* (KLU-M 1382), lane 12: *Pleurotus eryngii* (KLU-M 1380), lane 13: *Pleurotus giganteus* (KLU-M 1385), lane 14: *Pleurotus giganteus* (KLU-M 1227), lane 15: *Pleurotus pulmonarius* (KLU-M 1384), lane 16: *Lentinula edodes* (KLU-M 1386) and lane 17: *Flammulina velutipes* (KLU-M 1387), respectively; lane 18: RPB2 amplicons of *Pleurotus cystidiosus* (KLU-M 1388), lane 19: *Pleurotus floridanus* (KLU-M 1382), lane 20: *Pleurotus eryngii* (KLU-M 1380), lane 21: *Pleurotus giganteus* (KLU-M 1385), lane 22: *Pleurotus giganteus* (KLU-M 1227), lane 23: *Pleurotus pulmonarius* (KLU-M 1384), lane 24: *Lentinula edodes* (KLU-M 1386) and lane 25: *Flammulina velutipes* (KLU-M 1387), respectively; lane 26: negative control for ITS region, lane 27: negative control for LSU region, and lane 28: negative control for RPB2 region; line 29: 1 kb DNA ladder.

4.2.2 Phylogenetic Analysis

The trimmed alignment contained 590 base-pairs amplified from ITS region were used for phylogenetic analysis. Figure 4.7 compiles a comprehensive phylogenetic relation within the *Pleurotus* species and outgroup using ITS region. The differentiation of the species into separate clade was identified based on reliability criteria by generation of bootstrap values via 500 replicates. The tree was divided into several main clades. Clade A consists of *P. eryngii* supported by a bootstrap value of 99%. Clade B includes *P. floridanus* which has low bootstarp value support of 73%. Clade C consists of *P. pulmonarius* supported by bootstrap value of 99%. Clade D includes *P. cystidiosus* supported by bootstrap value of 100% while Clade E consists of *P. giganteus* supported by bootstrap value of 100%. Genus *Hohenbuehelia* (outgroup) is closely related taxa of *Pleurotus* which both belong to the same family Pleurotaceae.

In general, all of the species used in this study are monophyletic clade which includes a single ancestor and all of its descendents. All *Pleurotus* species in the tree are sister group and fall under the same categories, having similar sequences and sharing same ancestor. Based on the result presented here, this region can be used as a genetic marker for identification into species level.

Overall, the performed phylogenetic analysis generally supports the results of previously published studies (Avin et al., 2017; Shnyreva & Shnyreva, 2014; Pánek et al., 2019; Li et al., 2017; Schoch et al., 2012a; Avin et al., 2012; Begerow et al., 2010; Schoch et al., 2012b; Seifert, 2009). Internal transcribed spacer region is known as a highly variable region between the conserved sequences of the small subunit, 5.8S, and large subunit rRNA genes, has been adopted as standard barcode region to delimit the species of *Pleurotus* (Avin et al., 2017; Pánek et al., 2019; Li et al., 2017; Begerow et al., 2010;

Schoch et al., 2012b), although studies have shown that this gene region often fails to distinguish closely related mushroom species (Schoch et al., 2012b).

The ITS sequences from different species of *Pleurotus* contained indels, variation that often exists among conspecific individuals that can complicate sequence alignment and subsequent data analysis. Schoch et al. (2012b) however concluded ITS have fewer problems with PCR amplification. The difficulties in generating a reliable alignment are an important drawback to the use of ITS as a DNA barcode marker (Dentinger et al., 2011; Seifert et al., 2007). Furthermore, sequence variation among paralogues can result in uncertain base calls. Additional markers beyond ITS are needed for mushroom barcoding, but finding suitable loci that can be easily amplified across the diversity of mushrooms remains a challenge (Robert et al., 2011; Stielow et al., 2015). Despite these caveats, the availability of ITS sequences from a large number of mushroom species in GenBank is a major advantage that often outweighs the complications introduced by alignment problems. In this study, most of the samples had high homology with the NCBI Genbank sequences.

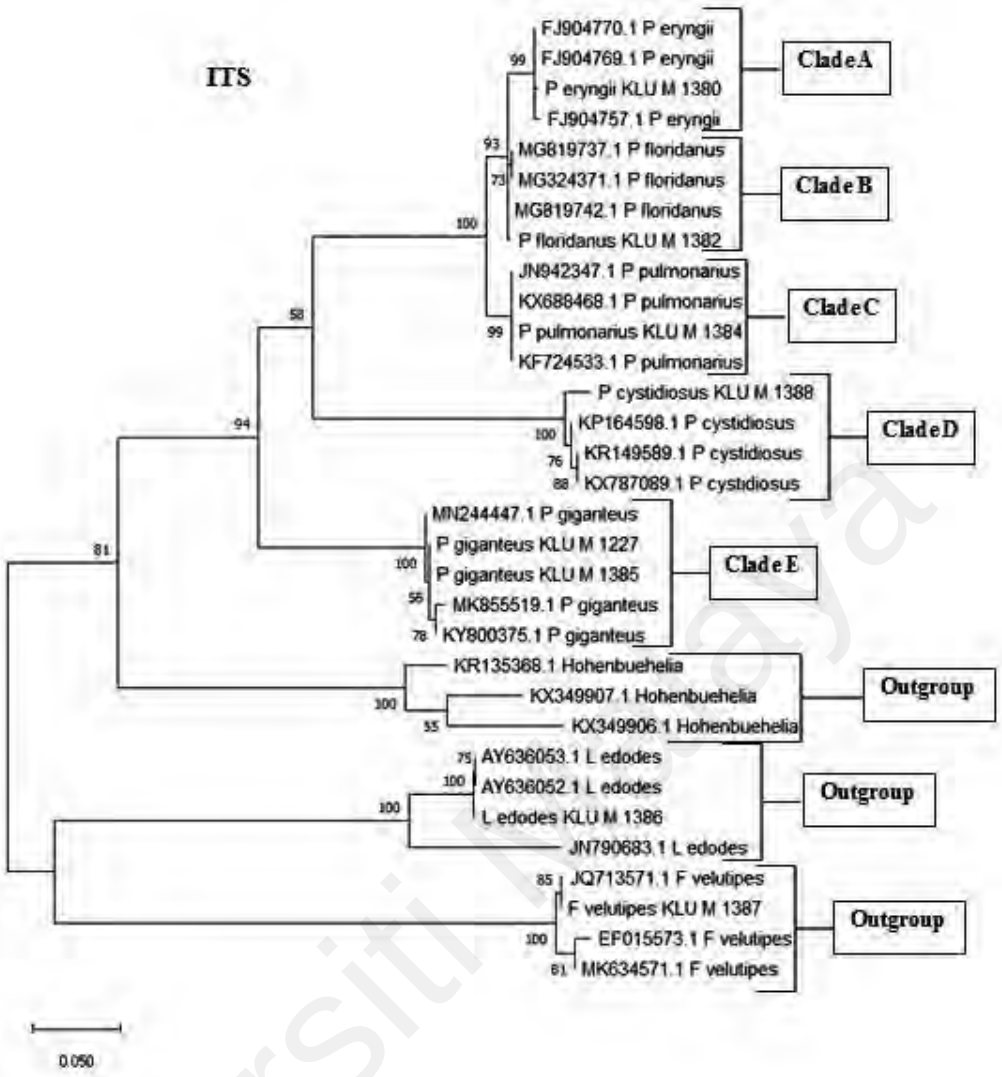

Figure 4.7: Phylogenetic tree of similarity of *Pleurotus* species based on ITS sequences and constructed with the Maximum Likelihood method. Numbers on branches indicate bootstrap values (in %).

The trimmed alignment contained 595 base-pairs amplified from LSU region were used for phylogenetic analysis. The phylogenetic analysis resolved to seven clades including three outgroups as presented in Figure 4.8. Clade A consists of *P. pulmonarius* and *P. floridanus* is not fully resolved into species delimitation supported with low bootstrap value of 51%. It might be due to the conserved region or the high similarity (67% conserved region) in the base pair sequences. This clade is polyphyletic since there is more than one ancestor in the clade and some of the species do not share the most common recent ancestor. Clade B consists of *P. eryngii* (bootstrap value of 76%). Clade

C includes *P. cystidiosus* supported with high bootstrap value of 95%. This clade is defined as polyphyletic for high precision phylogenetic studies.

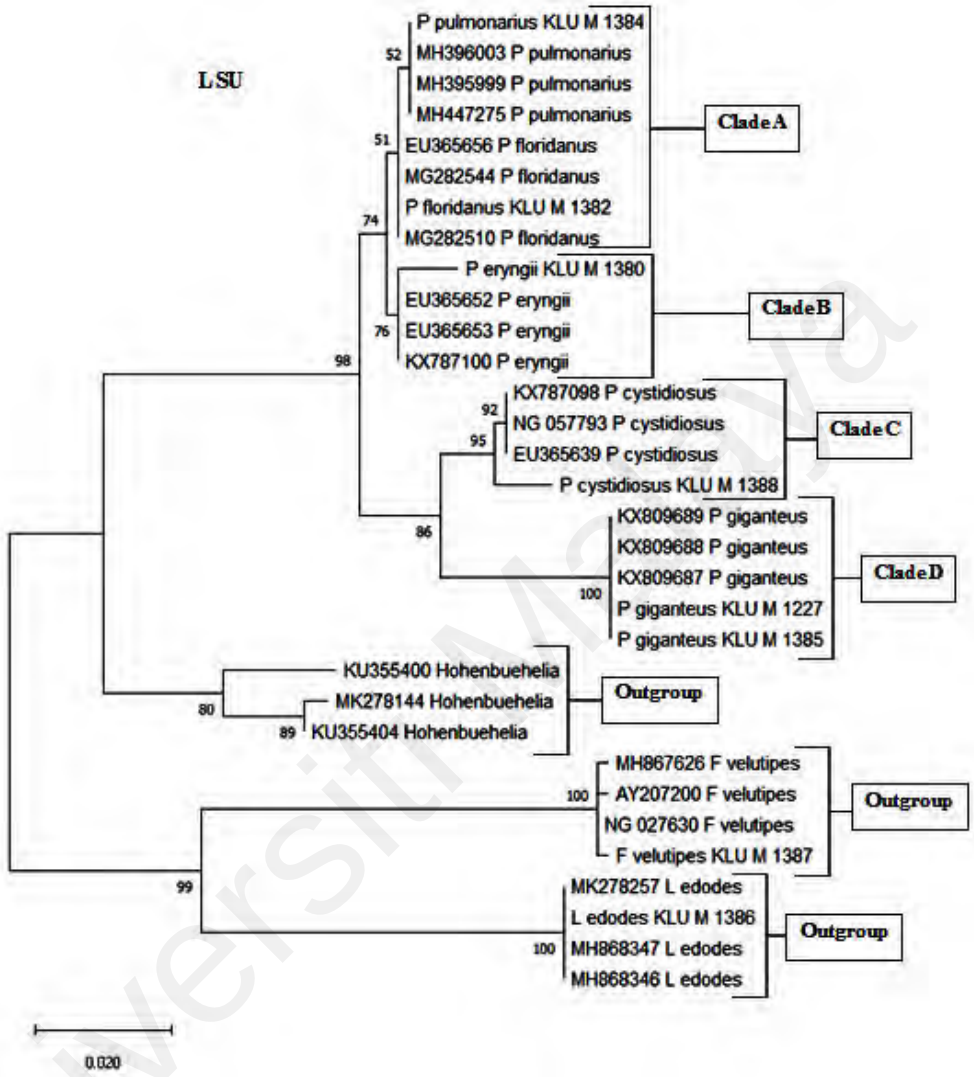

Figure 4.8: Phylogenetic tree of similarity of *Pleurotus* species based on LSU sequences and constructed with the Maximum Likelihood method and Tamura-Nei model (MEGA-X). Numbers on branches indicate bootstrap values (in %).

The trimmed alignment containing 744 base-pairs of RPB2 region were used for phylogenetic analysis. The RPB2 tree (Figure 4.9) was generated to elucidate relationships of mushroom species. It contains six out of eight *Pleurotus* species from this study including *P. cystidiosus* (KLU-M 1388), *P. floridanus* (KLU-M 1382), *P. pulmonarius* (KLU-M 1384), *P. eryngii* (KLU-M 1380), *P. giganteus* (KLU-M 1227) and one outgroup *F. velutipes* (KLU-M 1387). Because of unsuccessful sequencing for *P.*

giganteus (KLU-M 1385) and *Lentinula edodes* (KLU-M 1386), these species are not included in the phylogenetic analysis. Based on this analysis and due to lack of sequence database for *P. giganteus* and *P. cystidiosus* in GenBank, RPB2 region might not be able to serve as genetic marker to delimit *Pleurotus* into species level. Five clades were presented in this phylogenetic tree which two of them served as outgroup. Clade A consists of *P. floridanus* and *P. pulmonarius*, which is polyphyletic and all the species fall under the same categories, having similar sequences (73% conserved region), almost identical morphology, sharing same ancestor and supported by low bootstrap value of 50%. Clade B consists of *P. eryngii* supported with bootstrap value of 81%. Clade C includes *P. cystidiosus* and *P. giganteus* and is supported by high bootstrap value of 91%. All *Pleurotus* in the tree are defined as sister group. Based on the result, further morphology studies, combination of three markers (ITS, LSU and RPB2) and more variable molecular markers (IGS1 and ITS) are needed for the identification of species in genus *Pleurotus*.

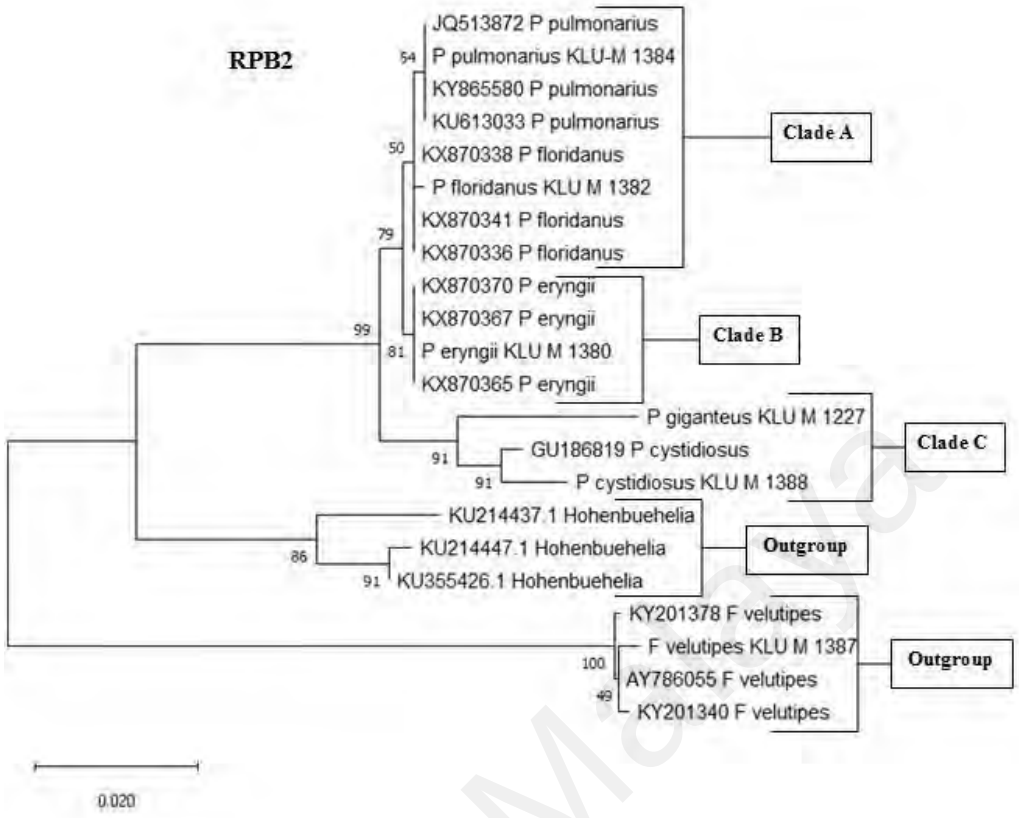

Figure 4.9：Phylogenetic tree of similarity between strains of *Pleurotus* species and other species from different genus based on RPB sequences and constructed with the Maximum Likelihood method and Tamura-Nei model (MEGA-X). Numbers on branches indicate bootstrap values (in %).

DNA barcoding is a very useful method to reduce ambiguity of species identification and determine its boundaries correctly. However, determining the most suitable region and utilized as a barcode for a specific taxon is very complex and ongoing process for researchers. The other major problem in DNA barcoding and DNA taxonomy is the lack of a taxonomical standard DNA analysis and a reliable database. An analysis should comprise great number of sample taxa, large-scale sequencing of representative samples, and a suitable algorithmic procedure to define species limits. A comprehensive database provides a reference sequence for correct identification within millions of species in seconds. The other problem is the presence of cryptic species. Unexpected intraspecific genetic diversity among samples may indicate a broad range of cryptic species for many organisms. The discovery of cryptic species over the last decade is largely a result of molecular phylogenetic studies of taxa. At this point, selecting the most suitable region

for a specific taxon seems as the challenging step for phylogeny and DNA barcode studies. Therefore, the electronic methods can be a suitable alternative method for identification of different species.

4.3 *I-V* Characterization and Calculation of Electronic Parameters

4.3.1 *I-V* Characterization and Calculation of Electronic parameters for Mushroom Genomic DNA

Figures 4.10 and 4.11 show the *I-V* profiles for the DNAs obtained from different mushroom species for the forward and reverse bias. A significant difference was observed when generating *I-V* profiles for each type of mushroom in the positive (Figure 4.10) and negative (Figure 4.11) regions. In the positive region, a clear rectifying profile can be observed for each mushroom. Figure 4.10 shows the comparison between different species of the same genus as well as two control species from different genus. It can be clearly seen from the profiles that the difference between the control species was much more significant compared to the ones generated by the different species of the same genus.

A band of close yet distinguishable profiles was meanwhile observed for the mushroom specimens of the same genus in both the positive and negative regions. This demonstrates the potential to utilize the *I-V* profiles to fingerprint and characterize the different species and genus. Both the figures also allow for measurement of various solid-state parameters for in-depth characterization of each type of DNA based on its base pair sequence electronics. Profiles generated from the positive bias region further enables the measurement of turn-on voltage, series resistance, shunt resistance, ideality factor and barrier height (Tables 4.3 and 4.4). When the DNA-specific Schottky diodes were negatively biased, the characteristic profiles generated as shown in Figure 4.11 can then

be utilized to measure its knee-voltage, breakdown voltage and breakdown current (Table 4.5).

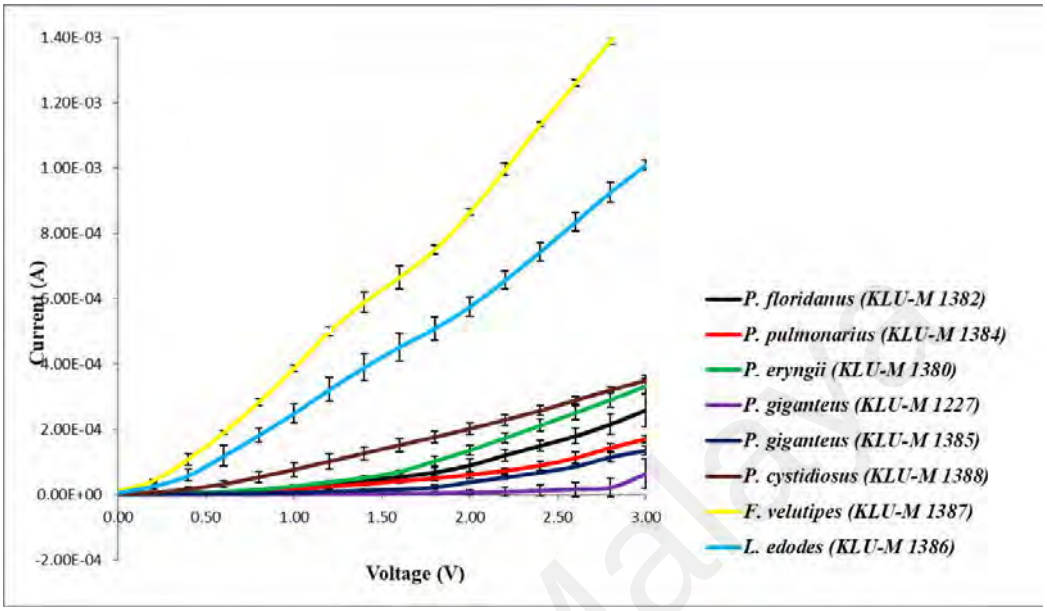

Figure 4.10: Positive biased *I-V* profiles for different mushroom species. Each profile was averaged over six mushroom specimens for improving statistical significance.

Table 4.3: Selected electronic parameters calculated for mushroom genomic DNA.

Sample		*P. floridanus (KLU-M 1382)*	*p. pulmonarius (KLU-M 1384)*	*P. eryngii (KLU-M 1380)*	*P. giganteus (KLU-M 1227)*	*P. giganteus (KLU-M 1385)*	*P. cystidiosus (KLU-M 1388)*	*F. velutipes (KLU-M 1387)*	*L. edodes (KLU-M 1386)*
Method 1	***n***	22.7	30.7	22.2	34.4	25.5	37.3	53.8	57.6
	Ø	0.89	0.87	0.88	0.93	0.90	0.84	0.78	0.79
	R_s	-	-	-	-	-	-	-	
Method 2	***n***	14.25	11.40	15.16	23.51	24.32	10.24	20.56	17.77
	Ø	0.88	0.89	0.87	0.94	0.88	0.84	0.77	0.79
	R_s	4999	6694	3451	8307	2184	6058	1170	1870

Table 4.4: Electronic parameters (turn-on voltage (V), series resistance (R_s), shunt resistance (R_{sh})) calculated for mushroom genomic DNA.

Sample	*P. floridanus (KLU-M 1382)*	*p. pulmonarius (KLU-M 1384)*	*P. eryngii (KLU-M 1380)*	*P. giganteus (KLU-M 1227)*	*P. giganteus (KLU-M 1385)*	*P. cystidiosus (KLU-M 1388)*	*F. velutipes (KLU-M 1387)*	*L. edodes (KLU-M 1386)*
Shunt Resistance (kΩ)	189.73	105.98	73.36	552.18	162.13	31.52	4.62	7.56
Series Resistance (kΩ)	11.58	17.54	9.00	46.43	22.25	8.56	1.97	2.97
Turn-on Voltage (V)	0.95	0.90	0.80	1.10	1.00	0.45	0.35	0.30

Table 4.3 and Table 4.4 list the parameters calculated from the positive bias region. The results indicate characteristic values depending on the type of DNA used within the Schottky structure. Turn-on voltage observed in Figure 4.10 is defined as a certain amount of positive voltage to be applied across diode to operate and conduct current. Each different sample shows its respective and different turn-on voltage.

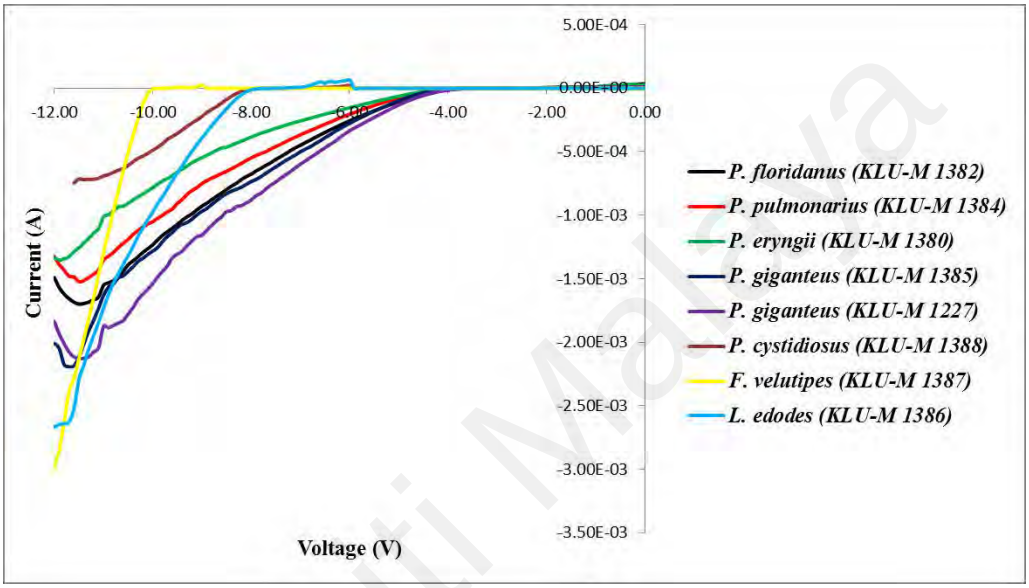

Figure 4.11: The negative biased (0 to -12V) *I-V* profiles for the eight types of mushroom species.

The DNA-specific negative biased profiles generated allows for discriminating knee-voltages, breakdown voltages and breakdown current that could also be applied as possible parameters for identifying different mushroom species (Figure 4.11). Similar values in the measured knee-voltage values may indicate the different species within the same genus or how closely related they are, while significantly higher values for the controls (-10.9 and -8.40) indicate different genus. Similar to a Zener diode, which operates in the reverse bias region in voltage regulating and switching applications, larger negative voltages or knee voltages are required to induce current amplifications. It was observed that similar breakdown voltages generated resulted in very different values of the breakdown current. There are many origins and sources of electrical breakdown, and the "breakdown phenomenon" itself may not yet be a deterministic phenomenon.

Statistical viewpoints may provide some discussions regarding the nature of the process. However, it should be noted that the electrical breakdown voltage is not an “injection” parameter. Still, these negative region parameters clearly demonstrate the possibility of utilizing them as a tool to identify different DNA species (Table 4.5).

Table 4.5: Values of knee voltage, breakdown voltage and breakdown current for the negative region.

Sample	*P. floridanus (KLU-M 1382)*	*p. pulmonarius (KLU-M 1384)*	*P. eryngii (KLU-M 1380)*	*P. giganteus (KLU-M 1227)*	*P. giganteus (KLU-M 1385)*	*P. cystidiosus (KLU-M 1388)*	*F. velutipes (KLU-M 1387)*	*L. edodes (KLU-M 1386)*
Knee-voltage (V)	-4.00	-4.20	-4.30	-4.10	-4.00	-8.10	-10.90	-8.40
Breakdown voltage (V)	-11.40	-11.50	-11.90	-11.30	-11.70	-11.25	Not within the voltage range investigated	-11.80
Breakdown current x 10^{-3} (A)	-1.700	-1.523	-1.352	-2.115	-2.192	-0.716	Not within the voltage range investigated	-2.642

Note: *F. velutipes* does not show the breakdown voltage within this region and were not measured since the range of investigation was only until -12V.

Values of series resistance, R_S as shown in Figure 4.12 were calculated from the junction resistance formula $R_S=\partial V/\partial I$ as measured from the *I-V* profiles of the DNA diode. The figure generally demonstrates the series resistance values for regions 0 to 1 V, which can be utilized for identifying the DNA. Here, the maximum peak values were observed to occur characteristic to the type of mushroom. Maximum value of series resistance belongs to *P. giganteus* (KLU-M 1227), while the lowest is for *F. velutipes* (KLU-M 1387). Region 1 to 3 V meanwhile demonstrates a decreasing trend in the series resistance complementing with the significant rectification of current beyond the turn-on voltage, which also show a predictable region.

It was observed that the control samples (*L. edodes* and *F. velutipes*) registered lower values of series resistance. These may be contributed in some ways to the evolving intrinsic dynamics of base-pair sequencing when introduced in the current environmental condition. In the study, similar trend was observed despite the different series resistance values between the two methods employed (Tables 4.3 and 4.4). Shunt resistance meanwhile was determined from the maximum resistance shown in Figure 4.12 and its characteristic behavior can easily be deduced especially for the controls, which demonstrated the lowest values. The highest shunt resistance was observed for the *P. giganteus* (KLU-M 1227), while the lowest is for *F. velutipes* (KLU-M 1387). Unlike the other species, *P. giganteus* (KLU-M 1227) however can be observed to generate two distinct maximums or shunt resistances, which may represent the characteristic charge transfer mechanism within its specific base pair sequence.

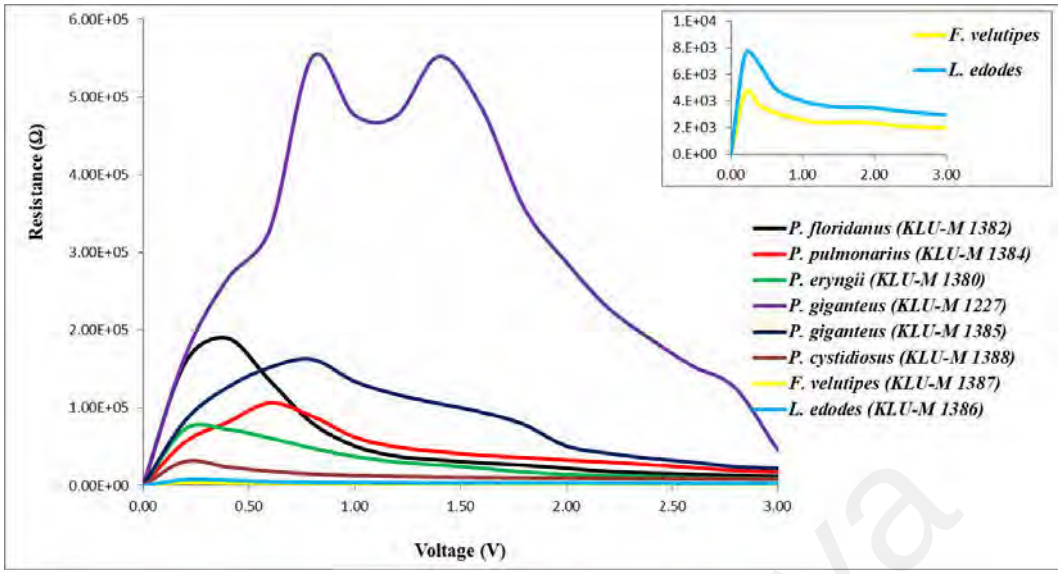

Figure 4.12: Resistance profile against bias voltage for all the mushroom samples. The insert illustrates the enlarged resistance profile against bias voltage for *F. velutipes* (KLU-M 1387) and *L. edodes* (KLU-M 1386) DNA.

Values of the barrier height of the DNA based Schottky diode meanwhile were calculated from the *y*-axis intercepts of the semi log-forward bias *I-V* plots (Figure 4.13) using Equation (3). The barrier height is the connection potential barrier existing at the interface between the inorganic and organic layers, which in this case is the DNA/Al interface. Figure 4.13 shows the experimental *I-V* characteristics of Schottky diode. The low forward bias of *I-V* measure was used to extract the diode parameter since the current is mostly affected by series resistance and deviates from linearity.

The ideality factor, barrier height and series resistance of all samples are shown in Table 4.3. Both methods show higher values for the ideality factor, indicating the possible presence of interfacial thin film, barrier inhomogeneity and/or other phenomena. These could lead to some level of uncertainty in the *I-V* characteristics measured which shows deviation from ideal Schottky diode in which the values are much higher than 1 (Reddy et al., 2011; Gupta & Yakuphanoglu, 2012; Sze & Ng, 2006). The ideality factor determined using Eq. (4) and Eq. (6) in Method 1, was relatively larger compared to the values obtained in Method 2 using Cheung and Cheung's approach with Eq. (7). This

variation could be due to the effects of series resistance which was ignored in Method 1 which decreases the ideality factor significantly when the effects of series resistance were considered using Method 2. As for the barrier height calculated with Method 1 using Eq. (4) and Eq. (5) shows similar results with Method 2 calculated using Eq. (8) and Eq. (9), which shows that it was not affected much by the series resistance. Furthermore, the values for series resistance obtained from Cheung and Cheung's method using *dV/dlnI* versus *I* and *H(I)* versus *I* plots were in good argument with the values obtained from the resistance profile against bias voltage plot. Therefore, Cheung and Cheung's method was suggested to be the most reliable method to extract diode parameters in this case.

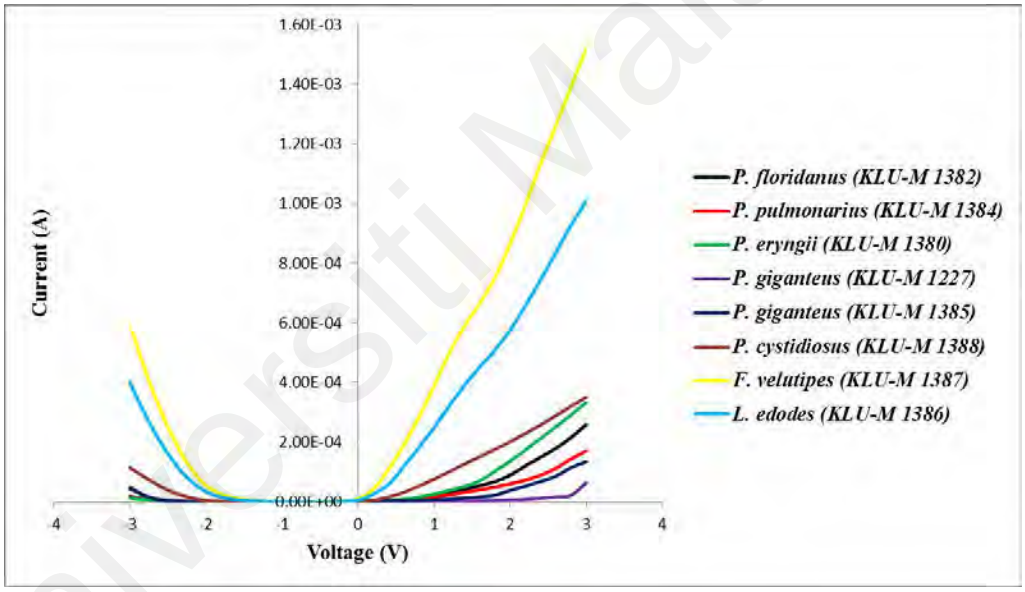

Figure 4.13: Semi-log *I* versus voltage profiles for the eight types of mushrooms.

Figures 4.14 and 4.15 shows the profiles plotted for the barrier height and ideality factor for the mushrooms based on the data listed in Table 4.3. The characteristic maximum obtained for the ideality factor for each mushroom therefore could be used as the identification method. Significantly similar values of the barrier height may indicate how close the mushroom species relates to each other, demonstrating that it may be classified within the same genus. Values obtained in this research vary from 0.77 to 0.94, which corresponds between the values generated by Al/p-Si and Al/n-Si Schottky

junctions, respectively. These values may correspond to the choice of metal contact used. The closer the barrier height values are to zero, the more Ohmic the contacts are, indicating the importance of the choice of the metal contact (Herbert, 1977).

In this research, Al was utilized due to its easy availability and cheaper option. However, the significant difference observed in these values may be utilized as one of the characteristic properties to identify different DNA sequence. Therefore, each parameter corresponds to specific features related to the charge transfer mechanism within a base sequence, which may provide an electronic database or profiles for each species that may be relevant to a better understanding of the in-depth fundamentals studies of any DNA species.

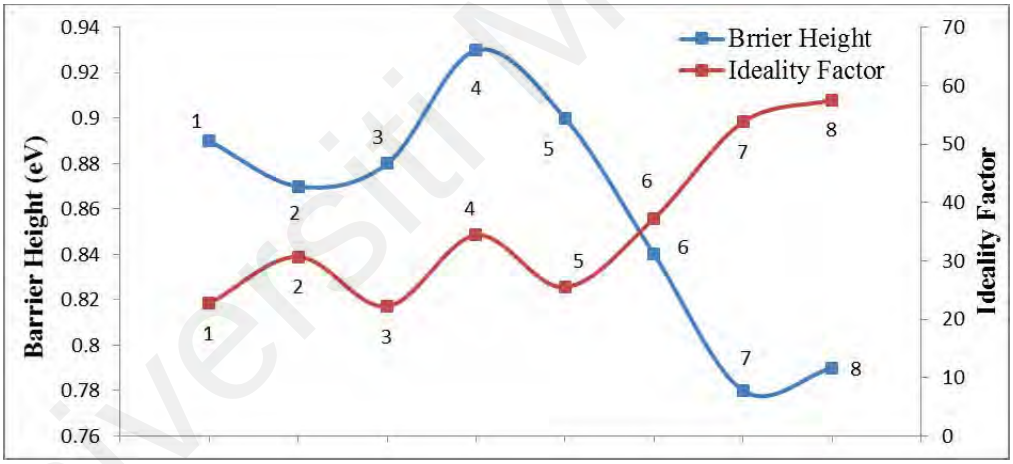

Figure 4.14: Ideality factor and barrier height profiles for all eight mushrooms; 1: *P. floridanus* (KLU-M 1382), 2: *P. pulmonarius* (KLU-M 1384), 3: *P. eryngii* (KLU-M 1380), 4: *P. giganteus* (KLU-M 1227), 5: *P. giganteus* (KLU-M 1385), 6: *P. cystidiosus* (KLU-M 1388), 7: *F. velutipes* (KLU-M 1387) and 8: *L. edodes* (KLU-M 1386) obtained from Table 4.3 (Method 1).

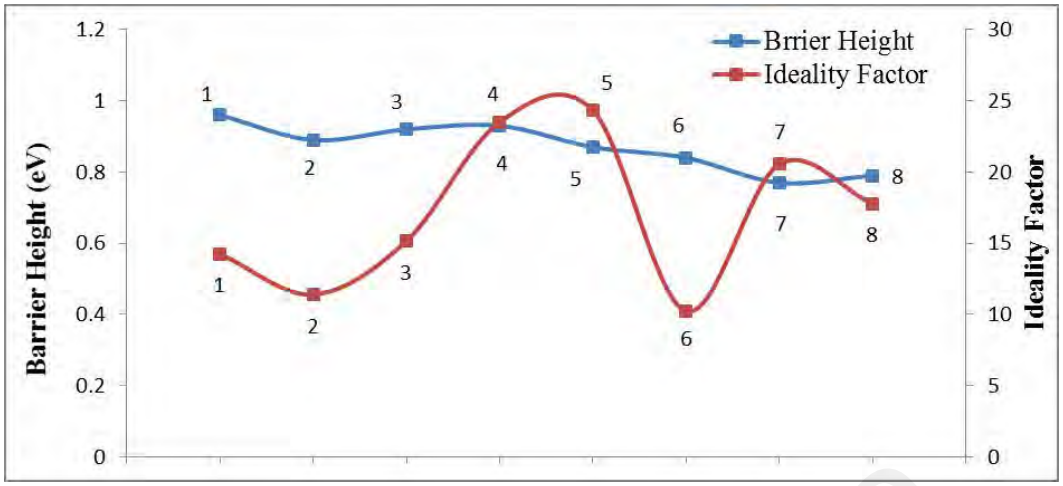

Figure 4.15: Ideality factor and barrier height profiles for all eight mushrooms; 1: *P. floridanus* (KLU-M 1382), 2: *P. pulmonarius* (KLU-M 1384), 3: *P. eryngii* (KLU-M 1380), 4: *P. giganteus* (KLU-M 1227), 5: *P. giganteus* (KLU-M 1385), 6: *P. cystidiosus* (KLU-M 1388), 7: *F. velutipes* (KLU-M 1387) and 8: *L. edodes* (KLU-M 1386) obtained from Table 4.3 (Method 2).

Ideality factor representing the dominant charge transfer process in conventional diodes show a non-ideal condition in DNA-based Schottky structures. Significant differences observed in these values may provide a detection or identification method, as sensitive ideality factor values are acceptably significant based on the profile shown in Figures 4.14 and 4.15. However, some closer similarities are to be clearly observed within certain DNA sequences.

Each parameter represents certain properties pertaining to the dynamics of charge transfer within each respective base sequence, which may represent common features pertaining to the respective species investigated. As such, further interrogation on the genetics of these mushroom species may provide some key answers. The behavior remains constant and repetitions among the same batch samples generate highly reproducible patterns. The significant difference observed in these values may generally point towards the varying fundamentals including charge transfers and mobility underlying each DNA type according to its specific base sequences. Therefore, identification of various species of mushrooms could be achieved based on these parameters which can be utilized as an accurate and efficient method. It will provide an

electronic database or profiles for each species which may be applied to understand the essential information for in-depth studies of any DNA species in future.

4.3.2 *I-V* Characterization and Calculation of Electronic Parameters for PCR-Amplified Genomic DNA

4.3.2.1 *I-V* Profiles and Calculation of Electronic Parameters for PCR-Amplified Genomic DNA of Internal Transcribed Spacer Region

Figures 4.16 and 4.18 show the *I-V* profiles for each type of mushroom DNA for forward and reverse bias, respectively. This measurement shows that each profile has differences in both positive and negative bias region demonstrating a rectifying effect for all the different types of DNA samples. A band of distinguishable profiles was observed between the control species and different species of *Pleurotus* genus in the positive region. This pattern demonstrates the potential to utilize the *I-V* profile as a fingerprint for at least genus- and/or family-level identification. As it is shown in Figure 4.16, some regions of different species overlap with each other. It might be due to the high similarity in the base pair sequences.

Based on the literature, this is the first of its kind in this field and it is in the light of this that it was aimed at investigating the variability of some mushroom DNAs using ITS regions. DNA identification using biosensor is an essential diagnostic tool for unraveling the rich biodiversity of mushrooms.

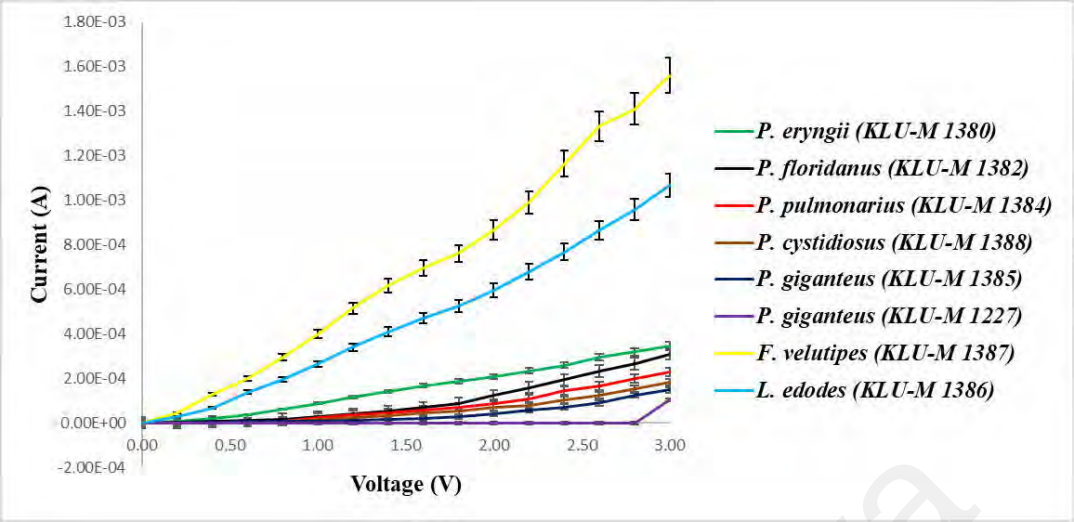

Figure 4.16: Positive biased *I-V* profiles for the six *Pleurotus* species and two control species from different genus (*F. velutipes* and *L. edodes*) on PCR-amplified DNA of ITS region.

The data obtained from *I-V* profile can also be used to calculate other solid-state parameters from the positive bias region (Tables 4.6 and 4.7) and the negative bias region (Table 4.8) for a more in-depth characterization of each type of DNA based on its base pair sequence electronics. Turn-on voltage observed in Figure 4.16 is defined as a certain amount of positive voltage to be applied across diode to operate and conduct current. Each different sample was observed to demonstrate its unique turn-on voltage.

Table 4.6: Selected electronic parameters calculated for the PCR-amplified DNA of ITS region.

Sample		*P. floridanus (KLU-M 1382)*	*p. pulmonarius (KLU-M 1384)*	*P. eryngii (KLU-M 1380)*	*P. giganteus (KLU-M 1227)*	*P. giganteus (KLU-M 1385)*	*P. cystidiosus (KLU-M 1388)*	*F. velutipes (KLU-M 1387)*	*L. edodes (KLU-M 1386)*
Method 1	***n***	27.1	26.3	31.9	31.5	26.7	25.0	54.4	58.1
	Ø	0.87	0.88	0.84	0.94	0.90	0.89	0.78	0.79
	R_S	-	-	-	-	-	-	-	
Method 2	***n***	10.02	16.78	7.78	23.7	23.83	25.03	20.83	24.91
	Ø	0.87	0.88	0.84	0.94	0.90	0.87	0.78	0.78
	R_S	9047	3387	6956	7024	2290	3933	1506	1459

Table 4.7: Electronic parameters (turn-on voltage (V), series resistance (R_s), shunt resistance (R_{sh})) calculated for the PCR-amplified DNA of ITS region.

Sample	*P. floridanus (KLU-M 1382)*	*p. pulmonarius (KLU-M 1384)*	*P. eryngii (KLU-M 1380)*	*P. giganteus (KLU-M 1227)*	*P. giganteus (KLU-M 1385)*	*P. cystidiosus (KLU-M 1388)*	*F. velutipes (KLU-M 1387)*	*L. edodes (KLU-M 1386)*
Shunt Resistance (kΩ)	60.68	366.79	25.84	843.88	130.11	156.09	4.36	6.69
Series Resistance (kΩ)	9.69	13.15	8.68	163.73	20.39	16.29	1.92	2.80
Turn-on Voltage (V)	0.60	0.80	0.50	1.00	0.90	0.85	0.40	0.35

The ideality factor, barrier height and series resistance of all samples were calculated using the two different methods and the values are shown in Table 4.6. In Method 1, the effects of series resistance were ignored at lower region of the forward bias voltage. The ideality factor measured for mushroom species clearly shows deviation from ideal Schottky diode in which the values are larger than 1. These values decrease significantly when the effects of series resistance were considered using Method 2. It can be seen that ignoring the series resistance may cause errors in calculating the electrical parameters of the Schottky diode especially for ideality factor.

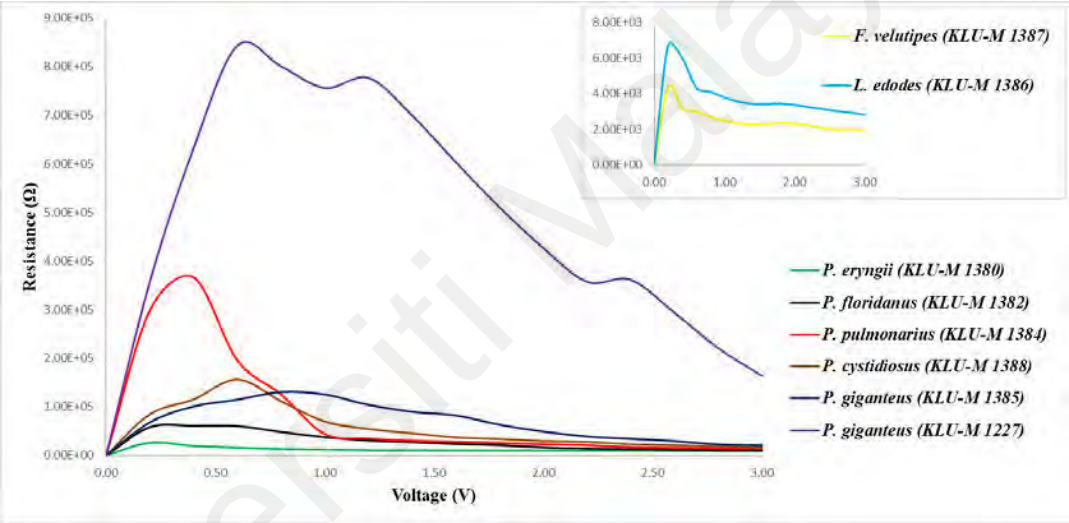

Figure 4.17: Resistance profile against bias voltage for all the PCR-amplified DNA of ITS region. The insert illustrates the enlarged resistance profile against bias voltage for *F. velutipes* (KLU-M 1387) and *L. edodes* (KLU-M 1386) PCR-amplified DNA.

Shunt and series resistance values extracted from the *I-V* profiles are as shown in Table 4.7. Shunt resistance normally occur when there are high conductivity paths within the diode while series resistance represents the performance of Schottky-based devices. Figure 4.17 illustrates the resistance profile against bias voltage for all PCR-amplified DNA mushroom samples involved in this experiment targeted on ITS region. Based on the *I-V* characteristics in forward region, the values of shunt and series resistance could be clearly distinguished and applied in the identification of the mushroom species.

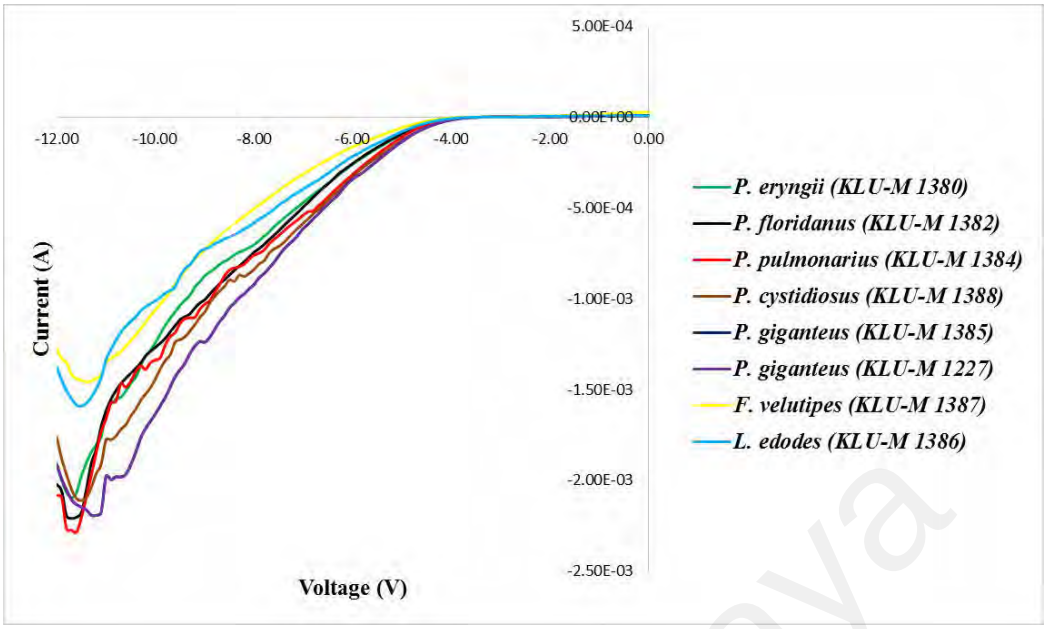

Figure 4.18: Negative biased *I-V* profiles for the six *Pleurotus* species and two control species from different genus (*F. velutipes* and *L. edodes*) of the PCR-amplified DNA of ITS region.

In reverse biased region (Figure 4.18), it was observed that Al/DNA Schottky sensors exhibited significantly defined *I-V* profiles with breakdown currents occurring at a voltage region between -11.2 V to about -11.7 V. Properties attributed to the mechanisms of current flow in negative region allows acquisition of electronic parameters such as knee voltage, breakdown voltage and breakdown current (Table 4.8). These values also depend on the type of the species of mushroom DNA used and may suggest a possible DNA identification and detection technique following an in-depth study on the mechanism behind such observation.

Table 4.8: Values of knee voltage, breakdown voltage and breakdown current for the negative region for the PCR-amplified DNA of ITS region.

Sample	*P. floridanus (KLU-M 1382)*	*p. pulmonarius (KLU-M 1384)*	*P. eryngii (KLU-M 1380)*	*P. giganteus (KLU-M 1227)*	*P. giganteus (KLU-M 1385)*	*P. cystidiosus (KLU-M 1388)*	*F. velutipes (KLU-M 1387)*	*L. edodes (KLU-M 1386)*
Knee-voltage (V)	-4.50	-4.40	-4.60	-4.30	-4.25	-4.20	-5.00	-4.90
Breakdown voltage (V)	-11.60	-11.70	-11.60	-11.20	-11.30	-11.50	-11.40	-11.50
Breakdown current x 10^{-3} (A)	-2.2002	-2.284	-2.095	-2.192	-2.190	-2.110	-1.456	-1.591

4.3.2.2 *I-V* Profiles and Calculation of Electronic Parameters for PCR-Amplified Genomic DNA of Ribosomal Polymerase II Region

In forward biased region (Figure 4.19), it is clearly shown that each species exhibited a specific rectifying profile with a small overlap among some species such as *P. giganteus* (KLU-M 1385), *P. floridanus* (KLU-M 1382) and *P. pulmonarius* (KLU-M 1384). It might be due to the conserved region in the base pair sequences (73% conserved region). However, the values obtained from the solid-state parameters show significant differences for different species. The *I-V* profiles in Figure 4.19 shows features similar to a typical semiconducting junction, consisting of an insulating region followed by a highly conducting region. It is well known that semiconducting materials have a small band gap between valance and conduction bands, which the electrons in the valance band must be able to overcome by obtaining sufficient energy to jump to the conduction band.

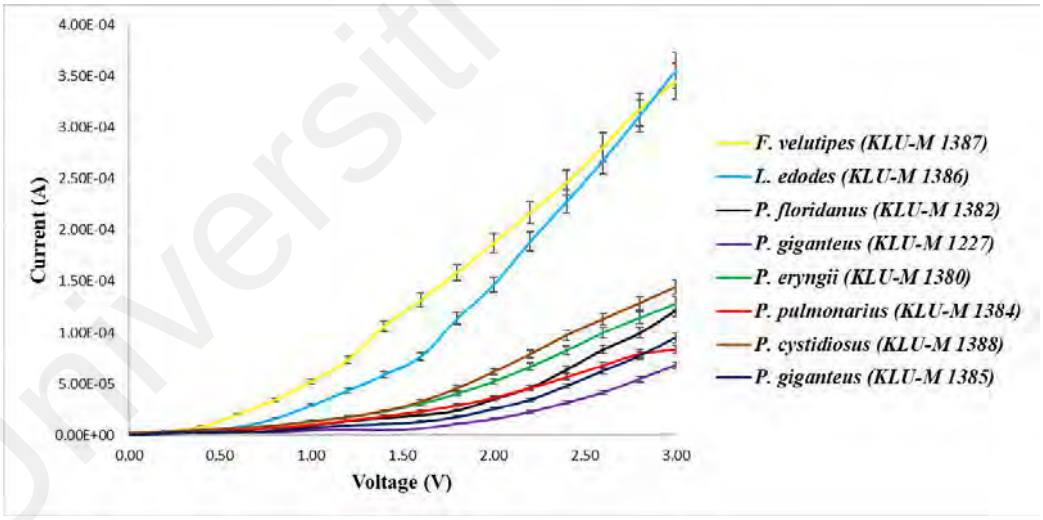

Figure 4.19: Positive biased *I-V* profiles for the six *Pleurotus* species and two control species from different genus (*F. velutipes* and *L. edodes*) of the PCR-amplified DNA of RPB2 region.

The energy band gap for semiconductors is in the order of 1 eV, which represents the insulating region in the *I-V* profile. High current conduction is achieved beyond the threshold or turn-on voltage defined as the voltage required to create current flow through the junction. In Schottky junction, the turn-on voltage is smaller than in conventional p-

n diodes since metallic junctions are more conductive and as such allows easier flow of electrons. Turn-on voltages extracted from Figure 4.19 for each species demonstrate its unique and characteristic values.

To calculate other electronic solid-state parameters (barrier height, shunt resistance, series resistance and ideality factor) for the DNA-Schottky junction, the Conventional and graphical methods of calculation was used according to the thermionic emission theory of diode as explained before. From the junction resistance graph, $R=\partial V/\partial I$ versus bias voltage V, shunt and series resistance were calculated. Figure 4.20 indicates the resistance profile against bias voltage for all mushroom samples used in this experiment. The values of both series resistance and shunt resistance could be clearly distinguished from the *I-V* profiles in forward region which can be used in the identification of the *Pleurotus* species.

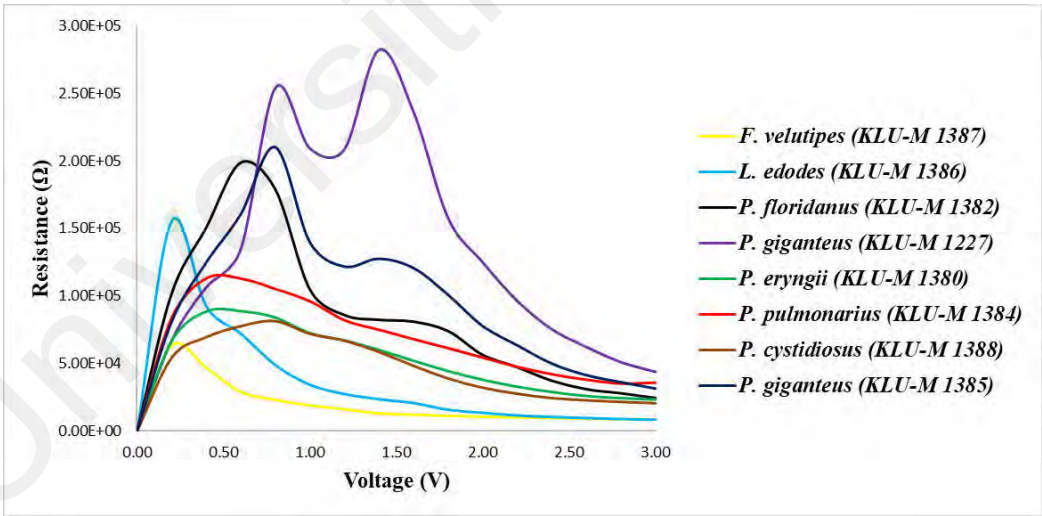

Figure 4.20: Resistance profile against bias voltage for all the PCR-amplified DNA of RPB2 region.

The value of ideality factor, barrier height and series resistance of all samples were calculated using the two different methods and the values are shown in Table 4.9. All these parameters correspond to specific characteristics linked to the charge transfer

mechanism within a base sequence. Closer relationship between species shows closer similarities between values.

Table 4.9: Electronic parameters (series resistance (R_S), barrier height ($Ø$), ideality factor (n)) calculated for all PCR-amplified samples of RNA polymerase II gene region.

Sample		*P. floridanus (KLU-M 1382)*	*p. pulmonarius (KLU-M 1384)*	*P. eryngii (KLU-M 1380)*	*P. giganteus (KLU-M 1227)*	*P. giganteus (KLU-M 1385)*	*P. cystidiosus (KLU-M 1388)*	*F. velutipes (KLU-M 1387)*	*L. edodes (KLU-M 1386)*
Method 1	***n***	29.9	36.5	33.4	26.2	29.6	31.4	43.1	30.8
	Ø	0.89	0.88	0.87	0.92	0.89	0.87	0.83	0.85
	R_S	-	-	-	-	-	-	-	
Method 2	***n***	26.70	9.05	19.08	16.09	8.85	19.75	21.02	12.61
	Ø	0.88	0.88	0.87	0.94	0.89	0.87	0.82	0.86
	R_S	2179	2370	8173	8382	5683	6877	5673	3692

Table 4.10: Electronic parameters (turn-on voltage (V), series resistance (R_s), shunt resistance (R_{sh})) calculated for all PCR-amplified samples of RNA polymerase II gene region.

Sample	*P. floridanus (KLU-M 1382)*	*p. pulmonarius (KLU-M 1384)*	*P. eryngii (KLU-M 1380)*	*P. giganteus (KLU-M 1227)*	*P. giganteus (KLU-M 1385)*	*P. cystidiosus (KLU-M 1388)*	*F. velutipes (KLU-M 1387)*	*L. edodes (KLU-M 1386)*
Shunt Resistance (kΩ)	198.58	113.30	88.51	282.08	209.89	81.62	63.31	155.29
Series Resistance (kΩ)	24.58	36.00	23.35	43.92	31.52	20.75	8.69	8.43
Turn-on Voltage (V)	0.80	0.60	0.50	0.95	0.90	0.70	0.50	0.60

Solid-state parameters were calculated from the positive region as listed in Table 4.10. Significant changes in the values calculated for series and shunt resistances, and turn-on voltage could be observed. The *I-V* behavior of the Schottky junction is affected by parasitic resistance such as series resistance and shunt resistance. At sufficiently high forward bias, the junction resistance approaches a constant value (Tuğluoğlu & Karadeniz, 2012), which is the series resistance.

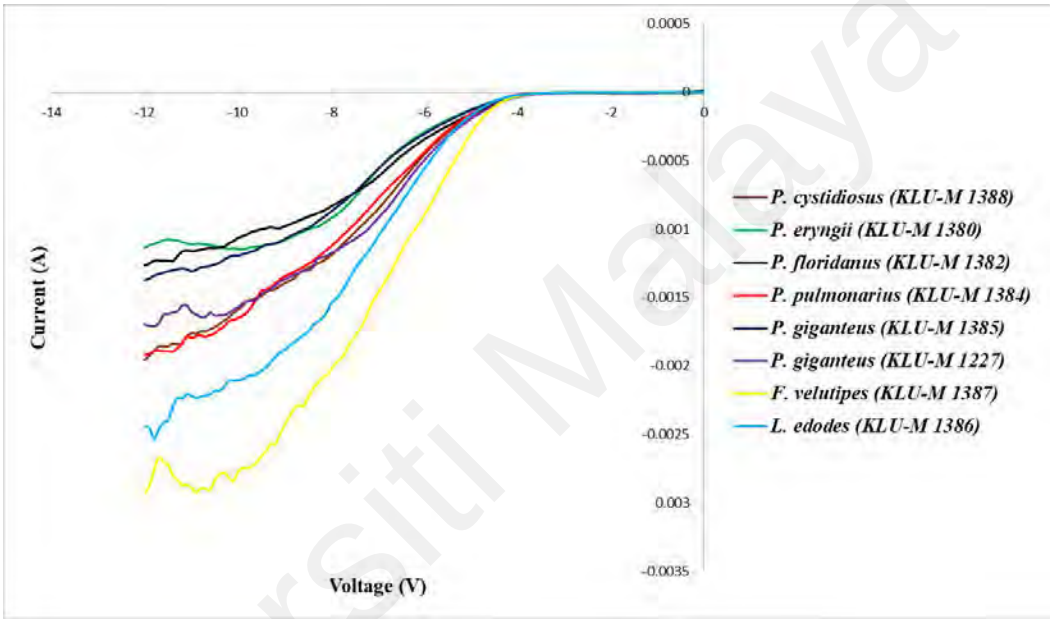

Figure 4.21: Negative biased *I-V* profiles for the six *Pleurotus* species and two control species from different genus (*F. velutipes* and *L. edodes*) the PCR-amplified DNA of RPB2 region.

Shunt resistance meanwhile might be one of the reasons of non-linear *I-V* characteristics at low bias for Schottky junction, causing a variation of diode ideality factor. In Figure 4.20, shunt resistance is indicated at low bias with a sharp rise in the values of resistance. Among the mushroom species, *P. giganteus* (KLU-M 1227) demonstrated the highest value of shunt resistance, which is 282.08 kΩ, while the lowest is for *F. velutipes* (KLU-M 1387) with the value of 63.31 kΩ. Series resistance meanwhile can be determined from the lowest saturating trend in the resistance against bias voltage graph. *Lentinula edodes* (KLU-M 1386) seems to demonstrate a lower value of series

resistance with 8.43 kΩ of resistance, while the maximum value of series resistance is for *P. giganteus* (KLU-M 1227) with 43.92 kΩ.

The data obtained from the *I-V* profiles in Figure 4.21 was also used to calculate other solid-state parameters such as knee-voltage, breakdown voltage and breakdown current from the negative bias region. This measurement shows that each profile has significant differences in the negative bias region (Table 4.11). These values may provide important information regarding the species which allow for a better characterization of each type of DNA based on its base pair sequence electronics.

Table 4.11: Values of knee voltage, breakdown voltage and breakdown current for the negative region of all the PCR-amplified samples of RNA polymerase II gene region.

Sample	*P. floridanus (KLU-M 1382)*	*p. pulmonarius (KLU-M 1384)*	*P. eryngii (KLU-M 1380)*	*P. giganteus (KLU-M 1227)*	*P. giganteus (KLU-M 1385)*	*P. cystidiosus (KLU-M 1388)*	*F. velutipes (KLU-M 1387)*	*L. edodes (KLU-M 1386)*
Knee-voltage (V)	-4.20	-4.50	-4.40	-4.30	-4.20	-4.60	-4.50	-4.70
Breakdown voltage (V)	-11.40	-11.50	-10.00	-10.50	Not within the voltage range investigated	Not within the voltage range investigated	-10.70	-11.80
Breakdown current x 10^{-3} (A)	-1.226	-1.896	-1.140	-1.642	Not within the voltage range investigated	Not within the voltage range investigated	-2.894	-2.463

Note: *P. cystidiosus* (KLU-M 1388) and *P. giganteus* (KLU-M 1385) did not show the breakdown voltage within this region and were not measured since the range of investigation was only until -12 V.

4.3.2.3 *I-V* Profiles and Calculation of Electronic parameters for PCR-Amplified DNA of Large Subunit Ribosomal DNA Region

I-V characteristic of the forward bias region are shown in Figure 4.22 and summarized in Tables 4.12 and 4.13. The comparison between different species of the same genus and two control species (*F. velutipes*, *L. edodes*) is clear from the profile. However, the difference between the control species was much more considerable compared to the different species of the same genus. The close but still distinguishable profiles were meanwhile observed for different species of the same genus. It might be due to the conserved region or the high similarity in the base pair sequences (67% conserved region).

Electronic parameters (forward biased region) used for comprehensive study in identification of different mushroom species are summarized in Tables 4.12 and 4.13. It can be deduced from the results that these parameters can provide more information about the species and its possible applications in terms of identification. The electronic parameters (series resistance (R_S), barrier height ($\varnothing$), ideality factor (n)) of the samples were calculated and the results show significantly discernable values (Table 4.12).

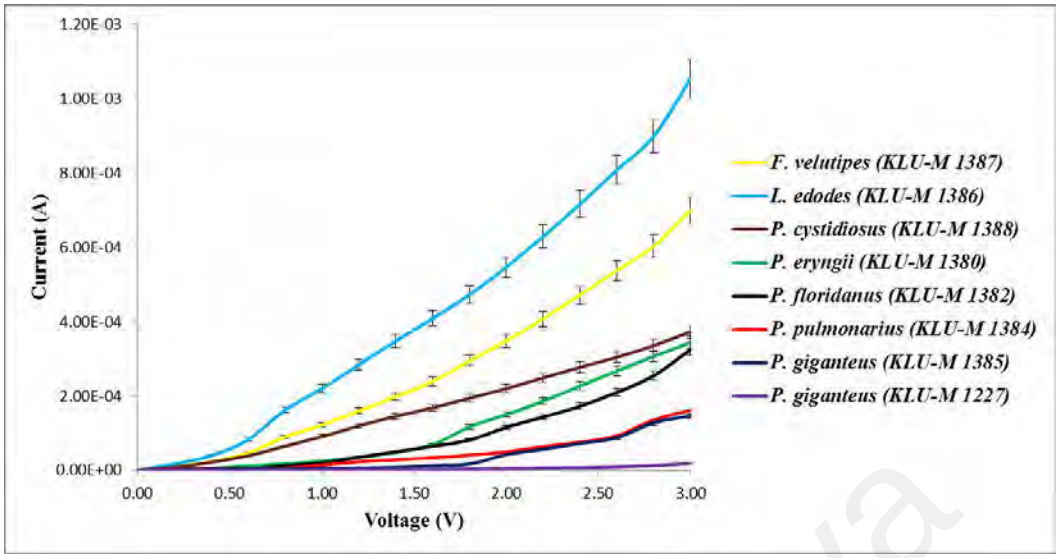

Figure 4.22: Positive biased *I-V* profiles for the six *Pleurotus* species and two control species from different genus (*F. velutipes* and *L. edodes*) of PCR-amplified DNA of LSU region.

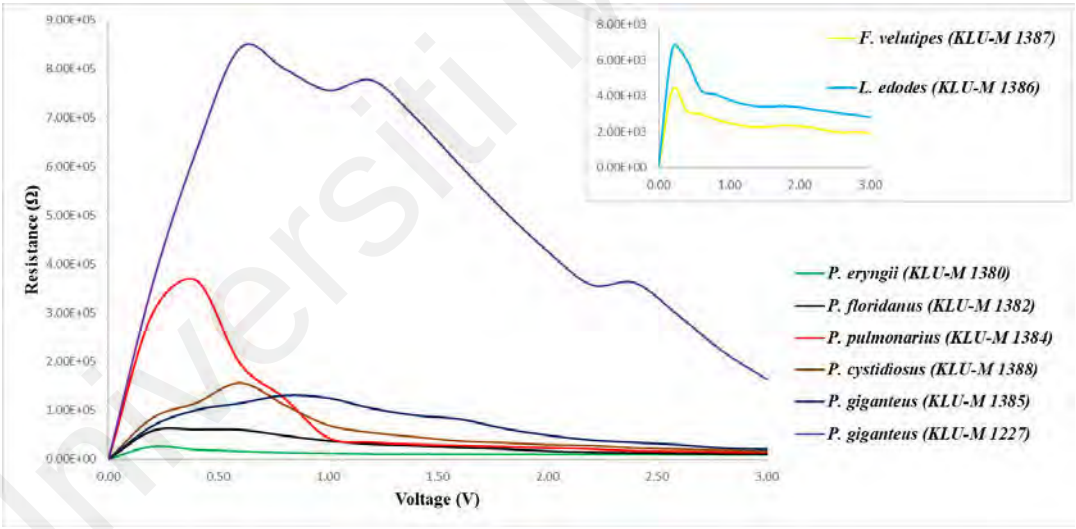

Figure 4.23: Resistance profile against bias voltage for all of PCR-amplified DNA of LSU region. The insert illustrates the enlarged resistance profile against bias voltage for *F. velutipes* (KLU-M 1387) and *L. edodes* (KLU-M 1386) PCR-amplified DNA.

Values shown in Table 4.13 were obtained from Figures 4.22 and 4.23. As such, the values shown in the tables were only for a summarized understanding from the original curves. For instance, the turn-on voltage was derived from Figure 4.22. The semiconducting behavior of the DNA can be generally deduced based on the existence of turn-on voltage, beyond which a significantly conducting region could be observed.

Table 4.12: Electronic parameters (series resistance (R_s), barrier height ($Ø$), ideality factor (n)) calculated for all PCR-amplified DNA of LSU region.

Sample		*P. floridanus (KLU-M 1382)*	*p. pulmonarius (KLU-M 1384)*	*P. eryngii (KLU-M 1380)*	*P. giganteus (KLU-M 1227)*	*P. giganteus (KLU-M 1385)*	*P. cystidiosus (KLU-M 1388)*	*F. velutipes (KLU-M 1387)*	*L. edodes (KLU-M 1386)*
Method 1	***n***	29.6	34.1	28.4	29.9	20.6	58.0	45.4	51.9
	Ø	0.86	0.87	0.86	0.94	0.92	0.81	0.81	0.79
	R_S	-	-	-	-	-	-	-	
Method 2	***n***	21.00	28.92	13.42	7.17	20.55	6.27	15.73	27.35
	Ø	0.86	0.87	0.86	0.94	0.91	0.83	0.82	0.78
	R_S	2855	3973	3577	7181	5741	6764	2335	1231

Table 4.13: Electronic parameters (turn-on voltage (V), series resistance (R_s), shunt resistance (R_p)) calculated for all of PCR-amplified DNA of LSU region.

Sample	*P. floridanus (KLU-M 1382)*	*p. pulmonarius (KLU-M 1384)*	*P. eryngii (KLU-M 1380)*	*P. giganteus (KLU-M 1227)*	*P. giganteus (KLU-M 1385)*	*P. cystidiosus (KLU-M 1388)*	*F. velutipes (KLU-M 1387)*	*L. edodes (KLU-M 1386)*
Shunt Resistance (kΩ)	217.73	136.58	70.57	830.02	202.44	24.29	19.62	11.87
Series Resistance (kΩ)	9.22	18.51	8.71	152.91	20.50	8.04	4.29	2.85
Turn-on Voltage (V)	0.60	0.80	0.50	1.00	0.90	0.45	0.50	0.40

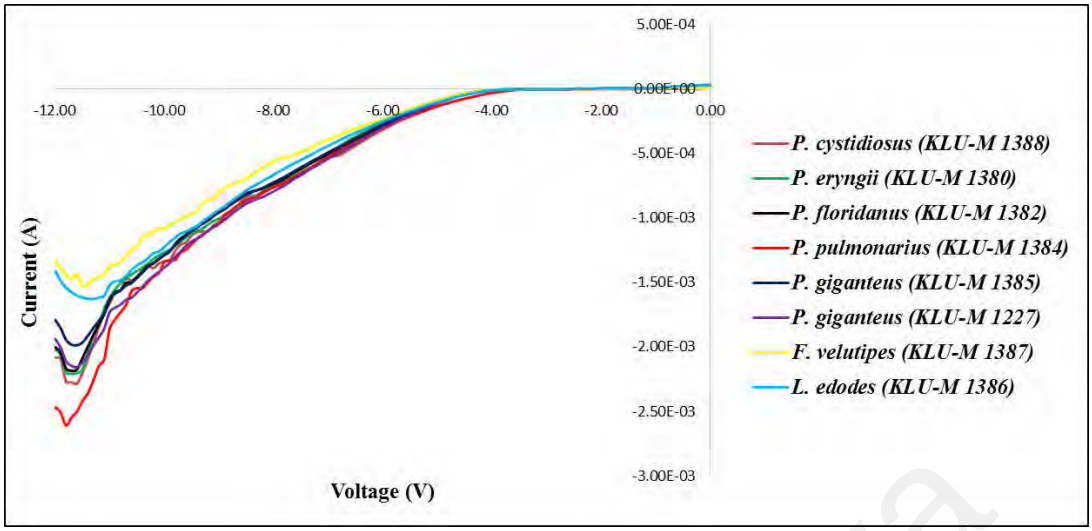

Figure 4.24: Negative biased *I-V* profiles for the six *Pleurotus* species and two control species from different genus (*F. velutipes* and *L. edodes*) of PCR-amplified DNA target on LSU region.

Values shown in Table 4.14 were obtained from Figure 4.24, which are the negative biased I-V curve profiles that can be utilized to differentiate the types of mushroom. A significant difference in quantitative measurements such as knee voltage, breakdown voltage and breakdown current were observed.

Table 4.14: Values of knee voltage, breakdown voltage and breakdown current for the negative region using LSU primer.

Sample	*P. floridanus (KLU-M 1382)*	*p. pulmonarius (KLU-M 1384)*	*P. eryngii (KLU-M 1380)*	*P. giganteus (KLU-M 1227)*	*P. giganteus (KLU-M 1385)*	*P. cystidiosus (KLU-M 1388)*	*F. velutipes (KLU-M 1387)*	*L. edodes (KLU-M 1386)*
Knee-voltage (V)	-4.50	-4.40	-4.60	-4.70	-4.80	-4.70	-4.90	-4.80
Breakdown voltage (V)	-11.60	-11.80	-11.60	-11.50	-11.70	-11.60	-11.40	-11.30
Breakdown current x 10^{-3} (A)	-2.172	-2.614	-2.207	-2.125	-1.988	-2.284	-1.514	-1.628

I-V profile results for PCR-amplified DNA were compared with the genomic DNA. However, the use of this technique for identification of genomic DNA is easier but it can also be used to detect PCR-amplified DNA. Moreover, this new technique provides the potential to achieve sensitive and high-throughput species identifications.

Based on the results, potential DNA markers vary from species to species. However, ITS has showed better results with less overlapping profiles for most of DNA samples due to high degree of interspecific variability, conserved primer sites and multiple copy nature in the genome. Other regions such as LSU and RPB2 genes may be accepted as secondary choice for mushroom DNA samples for electrochemical method. Therefore, *I-V* profiles and electronic parameters of DNA samples using ITS region may be effective for finer-scale species-level identification of specific mushrooms.

Internal transcribed spacer is a highly variable region between the conserved sequences of the small subunit, 5.8S, and large subunit rRNA genes, has been adopted as the primary DNA barcode marker for mushrooms. Despite its routine usage, the region is not a universal barcode for mushrooms. In addition to its advantages, the region has also few disadvantages. For instance, this region may not be useful especially for some genera with high variability in the sequence of ITS region. This results in the poor identification to the species level. The presence of polymorphism among sequences of different taxonomic groups causes complications and difficulties in the identification studies. Only half of the ITS sequences deposited in databases are annotated to species level. Moreover, misidentified and/or low-quality sequences are encountered in database and more than 10% of identified mushrooms species based on ITS sequences are incorrectly annotated at the species level.

The ideal DNA barcode region is easy to amplify and variable enough to discriminate between species, a condition that is best met when variation within species is low and

divergence between species is high, i.e. intra- and interspecific distances creating a "barcode gap". The barcoding gap value is also important to explore the utility of a region as a DNA barcode.

Secondary DNA markers for the mushroom kingdom have been suggested to overcome the limitations of the ITS region. LSU may be useful to further supplement information for taxa when ITS and protein coding gene regions are insufficient. It is the most conservative and insufficient marker to distinguish species reliably. Moreover, variable length, low-quality LSU sequences and lack of an accurate and validated sequence database are limitations of using this region as a DNA marker.

RPB2 region could be excellent secondary markers for the vast majority of mushrooms. Even though RPB2 have high species resolving power, but PCR, sequencing and alignment failings as well as having slow rate of sequence divergence limit their potential. This makes them useful only for higher-level phylogenetic studies. However, the results obtained from *I-V* profiles could provide different distinguishable data which can be used for identification of mushrooms from the kingdom to species level.

4.4 Effect of Concentration on the Electronic Properties of DNA-Al Diodes

In this technique different concentrations of DNA strands were prepared to investigate the sensitivity of the sensor operation. Extensive experiments were carried out to obtain data from different concentrations of DNAs (high to lowest levels) to proof the sensitivity of this electronic sensor. Figure 4.25 shows the positive biased *I-V* profiles for different concentrations of genomic DNAs (from 5 ng/ul to 100 ng/ul). The following steps were undertaken to demonstrate the reproducibility and sensitivity of the electronic sensor, which requires only low amount and concentration of biological material for sensor preparation.

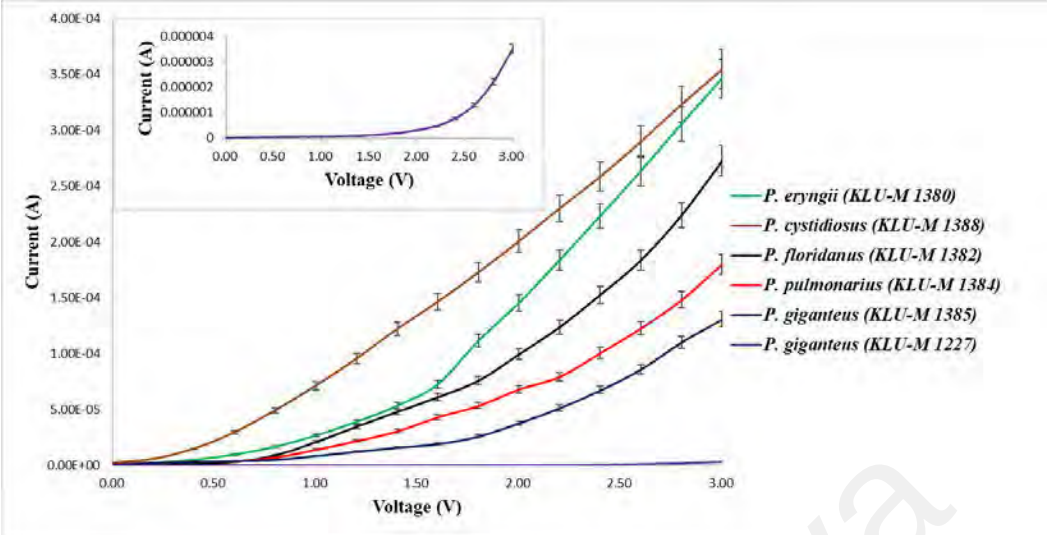

Figure 4.25: Positive biased *I-V* profiles for different concentrations of the genomic DNA of the six types of mushroom sub-species (from about 5 ng/ul to 100 ng/ul). The insert illustrates the enlarged rectifying behavior of *P. giganteus* (KLU-M 1227) DNA.

The measurements clearly show that the variations in concentrations does not significantly alter and influence the electronic properties of the DNA-Al diodes. As such, the bulk variation in the electronic data may be largely due to the different DNA base pair sequence in the various samples investigated rather than due to the different DNA concentrations.

4.5 Effect of pH on the Conductivity of mushroom DNAs

4.5.1 DNA Qualification Using NanoDrop Spectrophotometer

The concentration and absorbance ratio for *Pleurotus eryngii* (KLU-M 1380) DNA measured using NanoDrop spectrophotometer at 260 nm to 280 nm is shown in Table 4.15. Both values of the ratios were found to fall within the suggested values for pure DNA, which indicated the high purity of the DNA isolated in this research.

Table 4.15: DNA concentration and purity.

Sample	*P. eryngii* (KLU-M 1380)
Nucleic Acid Concentration ng/µL	55.2
Absorption at 260/280 ratio	1.84
Absorption at 260/230 ratio	2.05

Different pH conditions could significantly affect the A260/A280 ratio. This results in changing of the purity ratio of A260/A280 into 0.2 to 0.3 units lower or higher when DNA are in acidic solutions and basic solutions, respectively (Vesty et al., 2017; Dilhari et al., 2017; Sauer et al., 1998; Beaven et al., 1955). The results in Table 4.16 illustrate variations in A260/280 ratio by adjusting the pH in the DNA solution. These results indicate that the variations in the A260/280 ratio are primarily pH-dependent because of the degree of ionization of the bases at different pH. Table 4.16 revealed that the pH of the solutions used for NanoDrop analysis can substantially influence the qualitative determinations of DNA.

Table 4.16: The effect of pH on the A260/280 ratio of DNA.

pH	Absorption at 260/280 Ratio
1.05	0.67
1.52	0.90
2.13	1.00
2.53	1.06
3.01	1.17
3.53	1.25
4.08	1.29
4.51	1.33
5.02	1.40
5.51	1.42
6.06	1.46
6.52	1.51
6.98	1.66
7.48	1.70
8.09	1.80
8.47	1.84
8.91	1.90
9.42	1.94
9.89	2.10
10.55	2.16
11.09	2.20
11.46	2.34
11.96	2.50
12.49	2.61
12.97	2.83
13.54	2.84
14.01	2.86

4.5.2 *I-V* Profiles and Calculation of Electronic Parameters for the genomic DNA at Different pH Conditions

Figures 4.26 and 4.27 show the *I-V* profiles of the forward bias region for DNA samples under different pH conditions. The results show that the variation in pH values demonstrate the significant consequences in the DNA conductivity. It is observed that at higher and lower pH values, DNA demonstrated increased conductivity representing a shift from semiconductive to conductive by nature towards both pH extremes. The figures show strong conductive profiles in agreement to Ohm's law at basic pH 13 to 14 and acidic 1 to 2, as shown in the inset of Figures 4.26 and 4.27. Meanwhile, Figure 4.28 demonstrates increasing conductive current profiles from acidic (pH 1 to 2) to basic (pH 13 to 14) DNA solutions. Higher current may be attributed to the higher H^+ concentration (or proton) at lower or strong acidic pH conditions, resulting in the higher DNA conductivity. DNA conductivity at different pH values are summarized in Table 4.17, where conductive behavior is observed at both pH extremes.

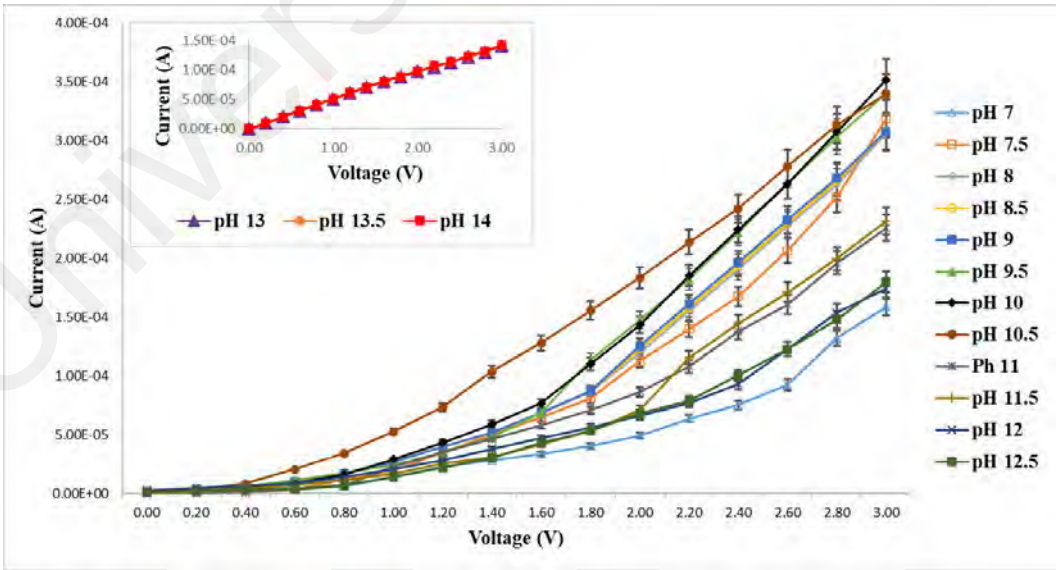

Figure 4.26: Positive biased *I-V* profiles for *Pleurotus eryngii* (KLU-M 1380) genomic DNA at different alkaline pH adjusted with NaOH. The insert illustrates the enlarged conductive profile observed from DNA solution in pH 13 to 14.

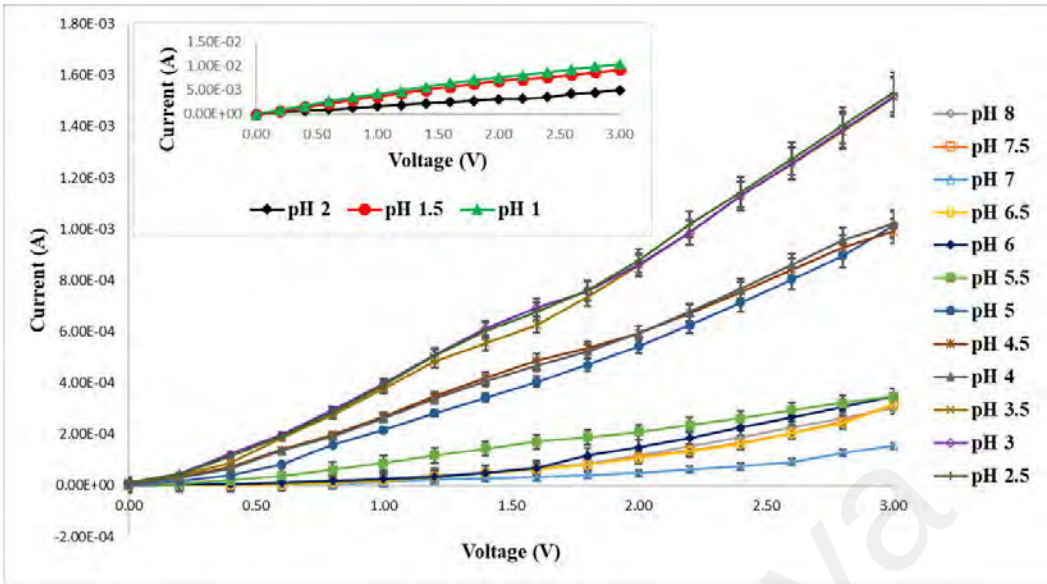

Figure 4.27: Positive biased *I-V* profiles for *Pleurotus eryngii* (KLU-M 1380) genomic DNA at different acidic pH adjusted with HCl. The insert illustrates conductive profiles of DNA in pH 1 to 2. Neutral pH condition is included as the reference.

Table 4.17: The effect of pH on conductivity of DNA.

Conductivity	pH value
conductive	1.05
conductive	1.52
conductive	2.13
semiconductive	2.53
semiconductive	3.01
semiconductive	3.53
semiconductive	4.08
semiconductive	4.51
semiconductive	5.02
semiconductive	5.51
semiconductive	6.06
semiconductive	6.52
semiconductive	6.98
semiconductive	7.48
semiconductive	8.09
semiconductive	8.47
semiconductive	8.91

Table 4.17, continued.

Conductivity	pH value
semiconductive	9.42
semiconductive	9.89
semiconductive	10.55
semiconductive	11.09
semiconductive	11.46
semiconductive	11.96
semiconductive	12.49
conductive	12.97
conductive	13.54
conductive	14.01

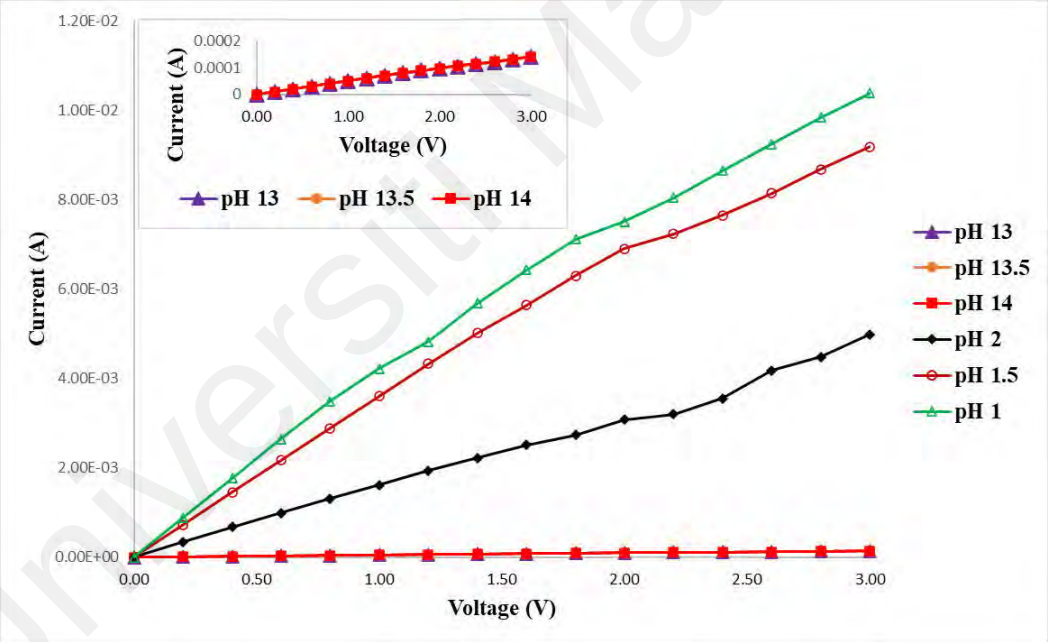

Figure 4.28: Conductive profiles observed from DNA solutions in basic (pH 13 to 14) and acidic (pH 1 to 2) conditions. As expected, highest conductivity was observed for pH 1, followed by 1.5 and 2. The inset meanwhile shows significantly lower but completely overlapping conductive current profiles in very strong alkaline conditions (pH 13 to 14), in contrast with separate profiles seen for the conductive acidic extremes.

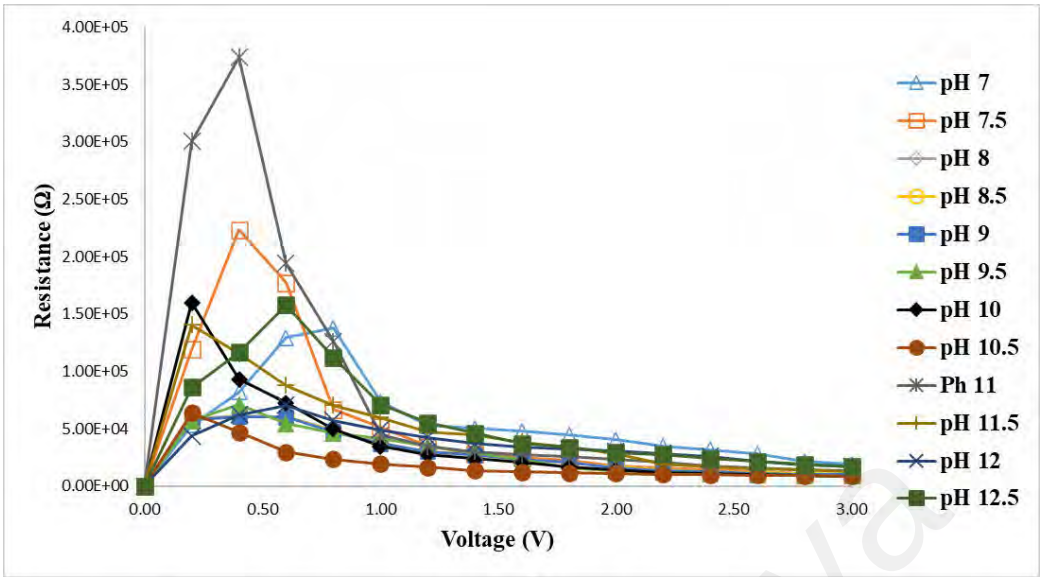

Figure 4.29: Resistance profile against bias voltage for *Pleurotus eryngii* (KLU-M 1380) DNA samples at different basic pH adjusted with NaOH. Neutral pH condition is included as the reference.

As in the previous section, data obtained from the *I-V* profile was used to calculate the solid-state parameters (Tables 4.18 to 4.21). Shunt and series resistances values obtained meanwhile are shown in Tables 4.18 and 4.19. From Figures 4.29 and 4.30, and Tables 4.18 and 4.19, the highest values for shunt and series resistance for acidic conditions are measured to be 230.65 kΩ and 19.33 kΩ, respectively. Meanwhile under alkaline conditions, these parameters correspond to 373.83 kΩ and 18.88 kΩ, for the shunt and series resistance, respectively.

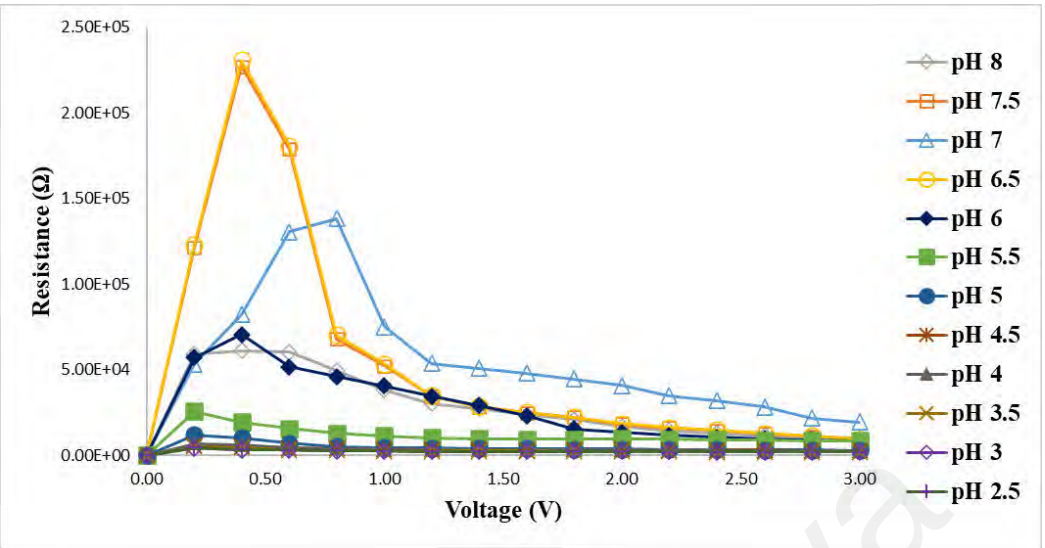

Figure 4.30: Resistance profile against bias voltage for *Pleurotus eryngii* (KLU-M 1380) DNA samples at different acidic pH adjusted with HCl. Neutral pH condition is included as the reference.

Table 4.18: Electronic parameters (turn-on voltage (V), series resistance (R_s), shunt resistance (R_p)) calculated for the DNA samples at different pH adjusted with NaOH.

pH	Shunt Resistance (kΩ)	Series Resistance (kΩ)	Turn-on Voltage (V)
pH 7.01	137.54	18.88	1.00
pH 7.49	223.36	9.40	0.85
pH 8.08	60.84	9.79	0.80
pH 8.48	60.67	9.72	0.80
pH 8.95	60.39	9.73	0.80
pH 9.44	70.94	8.80	0.75
pH 9.88	159.83	8.52	0.70
pH 10.53	63.95	8.81	0.60
pH 11.07	373.83	13.27	0.85
pH 11.47	140.37	12.93	0.90
pH 11.98	70.22	17.22	0.95
pH 12.47	157.61	16.67	0.95

Table 4.19: Electronic parameters (turn-on voltage (*V*), series resistance (R_S), shunt resistance (R_p)) calculated for the conductive DNA samples at different pH adjusted with HCl.

pH	Shunt Resistance (kΩ)	Series Resistance (kΩ)	Turn-on Voltage (V)
pH 8.07	61.11	9.88	0.80
pH 7.49	226.96	9.48	0.85
pH 7.01	138.33	19.33	1.0
pH 6.49	230.65	9.48	0.85
pH 6.02	70.69	8.63	0.75
pH 5.48	25.83	8.61	0.50
pH 4.99	12.09	2.95	0.45
pH 4.52	6.04	3.02	0.40
pH 4.05	6.74	2.93	0.40
pH 3.51	5.04	1.98	0.30
pH 3.3	4.40	1.97	0.25
pH 2.51	4.47	1.95	0.25

Interestingly stable values are observed for the pH of 8 to 9 (Gates, 2009; Wilfinger et al., 1997; Bonnet et al., 2009; Kim et al., 2011), where values for shunt resistance (60.4 to 60.8 kΩ), series resistance (9.7 to 9.8 kΩ) and turn-on voltage (0.8 eV) were similar to previous results using the same mushroom species in Section 4.3. Values of shunt resistance, series resistance and turn-on voltage reported in this previous research were 73.4 kΩ, 9.0 kΩ and 0.80 V, respectively at a pH condition of 8. According to Cheung and Cheung's method, the values of series resistance obtained using *dV/dln(I)* versus *I*

and *H(I)* versus *I* plots, meanwhile approves the calculation using the resistance against bias voltage graphs.

Values of barrier height, ideality factor and series resistance of the DNA samples at different pH values, calculated using Methods 1 and 2 are shown in Tables 4.20 and 4.21. The effects of series resistance were ignored at lower region of positive-bias voltage in Method 1. The ideality factor measured for the DNA samples was determined from the Eqs. (4) to (6). These values in general decreased when using Method 2 due to the effects of series resistance as described in Eq. (7). The barrier height calculated with Method 1 using Eqs. (4) and (5) and Method 2 using Eqs. (8) and (9) show similar values, representing the insignificant effect of series resistance. Values of barrier height were observed to be consistent between 0.83 to 0.88 eV for alkaline genomic DNA in contrast to the reduction from 0.88 to 0.77 eV with increasing acidic pH when measured using both methods due to increasing H^+ ions (Lyon & Hupp, 1999; Hamann et al., 2006; Johansson et al., 2011; Chakrapani et al., 2005).

Table 4.20: Selected electronic parameters calculated for the genomic DNA at different pH adjusted with NaOH.

pH	Ideality Factor, *n*	Barrier Height, *Ø* (eV)	Series Resistance, R_s (kΩ)
Method 1			
pH 7.01	34.0	0.8730	-
pH 7.49	29.7	0.8645	-
pH 8.08	31.6	0.8581	-
pH 8.48	31.5	0.8581	-
pH 8.95	31.5	0.8579	-
pH 9.44	28.5	0.8629	-
pH 9.88	30.9	0.8557	-
pH 10.53	43.0	0.8302	-
pH 11.07	34.9	0.8586	-

Table 4.20, continued.

pH	Ideality Factor, *n*	Barrier Height, *Ø* (eV)	Series Resistance, R_s (kΩ)
pH 11.47	28.6	0.8749	-
pH 11.98	37.5	0.8610	-
pH 12.47	31.9	0.8724	-
Method 2			
pH 7.01	33.36	0.8527	1.34
pH 7.49	14.62	0.8791	4.70
pH 8.08	16.62	0.8687	3.30
pH 8.48	16.96	0.8691	3.37
pH 8.95	16.63	0.8682	3.53
pH 9.44	15.19	0.8754	3.34
pH 9.88	15.26	0.8711	3.27
pH 10.53	9.14	0.8721	5.72
pH 11.07	18.51	0.8702	4.33
pH 11.47	19.72	0.8739	3.33

Table 4.21: Selected electronic parameters calculated for the DNA samples at different pH adjusted with HCl.

pH	Ideality factor, *n*	Barrier Height, *Ø* (eV)	Series Resistance, R_s (kΩ)
Method 1			
pH 8.07	31.6	0.8470	-
pH 7.49	29.7	0.8647	-
pH 7.01	34.1	0.8733	-
pH 6.49	29.7	0.8651	-
pH 6.02	28.4	0.8628	-
pH 5.48	59.9	0.8120	-
pH 4.99	52.0	0.7924	-
pH 4.52	62.4	0.7832	-
pH 4.05	58.7	0.7853	-
pH 3.51	56.3	0.7775	-
pH 3.3	60.2	0.7744	-

Table 4.21, continued.

pH	Ideality factor, *n*	Barrier Height, *Ø* (eV)	Series Resistance, R_s (kΩ)
pH 2.51	58.7	0.7751	-
Method 2			
pH 8.07	19.71	0.8586	2.99
pH 7.49	14.54	0.8793	4.82
pH 7.01	32.90	0.8545	1.11
pH 6.49	26.52	0.8454	1.79
pH 6.02	16.18	0.8706	3.09
pH 5.48	8.15	0.8301	6.93
pH 4.99	23.73	0.7873	1.40
pH 4.52	9.82	0.7905	2.43
pH 4.05	12.08	0.7923	2.16
pH 3.51	18.13	0.7789	1.19
pH 3.3	15.53	0.7801	1.32
pH 2.51	16.22	0.7782	1.27

Strong acidic (or strong basic) solution will have high conductivity since the pH is a measure of the concentration of the hydrogen (and the hydroxyl) ions. For an acidic solution, the lower the pH (i.e. the higher the H^+ concentration) the greater the conductivity will be. Conductivity of the solution is also influenced by the mobility of the ions. Therefore, the higher mobility of the H^+ ion which is almost twice that of OH^- ion results in higher conductivity at lower pH conditions. As such, the conductivity of a stronger acid is higher than that for a stronger base, while for weaker acid the conductivity is higher than that of a weaker base (Leveling, 2002).

Profiles for other DNA samples isolated from *P. floridanus* (KLU-M 1382), *P. pulmonarius* (KLU-M 1384), *P. giganteus* (KLU-M 1227), *P. giganteus* (KLU-M 1385) and *P. cystidiosus* (KLU-M 1388), which are following the same trends are shown as Supplementary profiles to avoid repetition in Appendix A (Figure S1-S10).

4.6 Effect of Ionic Liquid on the Long-Term Structural and Chemical Stability of genomic DNAs

4.6.1 DNA Qualification Using NanoDrop Spectrophotometer

Table 4.22 shows DNA purity and concentration using a NanoDrop spectrophotometer. Both values of ratios fall within the suggested values for pure DNA.

Table 4.22: NanoDrop result of the three mushroom species investigated in this study.

Sample	***Pleurotus eryngii* (KLU-M 1380)**	***Pleurotus floridanus* (KLU-M 1382)**	***Pleurotus pulmonarius* (KLU-M 1384)**
Nucleic acid concentration ng/µL	60.3	58.2	53.7
Absorption at 260/280 ratio	1.83	1.85	1.87
Absorption at 260/230 ratio	2.19	2.23	2.20

4.6.2 *I-V* Profiles and Calculation of Electronic Parameters for the genomic DNA Stored at Different Temperatures and Time Intervals

Figures 4.31 to 4.33 shows the *I-V* profiles of the forward bias region for different DNA samples stored at different temperatures and time intervals. Results indicate that the addition of the IL, [BMIM][Ace] to the DNA samples demonstrate significant improvement in the rectifying profiles. The current improvement was observed to be species-dependent and the extent of the resulting dissociation of ionic liquid into ions. Meanwhile, IL only sample (control) as shown in the insets of Figures 4.31 to 4.33 demonstrate only a linear conductive profile. Significant differences in the *I-V* profiles were also observed for each type of mushroom (without addition of IL) stored at different temperatures and time intervals. In general, closer spaced profiles were observed upon

the addition of IL demonstrating the practical possibility to utilize IL as a solvent for DNA without much loss of its structure and stability for long periods of use at RT. Each profile was also observed to exhibit specific rectifying behaviors strongly corresponding to the mushroom species, potentially acting as a characterization method.

Higher conductivity profile for IL/DNA was observed to remain as semiconductive due to the specific DNA identity. The IL does not appear as a conductor most probably because the presence of IL is not in solution as an independent monomer. The molecules preferably bind at the surface and groove of the DNA. It was previously reported that the stabilization of DNA in the presence of IL had been proven in similar ways (Tateishi-Karimata & Sugimoto, 2014; Zhao, 2014; Jumbri et al., 2014; Sharma et al., 2015; Singh et al., 2017; Vijayaraghavan et al., 2010). The binding of the IL on the DNA does assist the electron transfer occurring within the DNA strains.

The possible arrangement of the IL is the electrostatic interaction between the imidazolium head group with the polar region on the surface and groove of the DNA. At this position, the transferred electrons would be contained within the DNA strain isolated from the aqueous environment. Imidazolium ions behave as electron holes allowing continuous electron transfer indicated by higher conductivity of the current measurement. The alkyl group of the IL can be a good insulator separating the charge region in DNA and the aqueous environment. Hence, the binding of IL on the DNA performs as a sufficient buffering region. This binding was demonstrated by the highly consistent and repeatability of the conductive measurement. Without the ILs, electron transfer may deviate into the aqueous environment due to hydration of DNA and polarization of water molecules under the given voltage and electric potential. This would be the reason for the lower conductivity of the DNA without ILs.

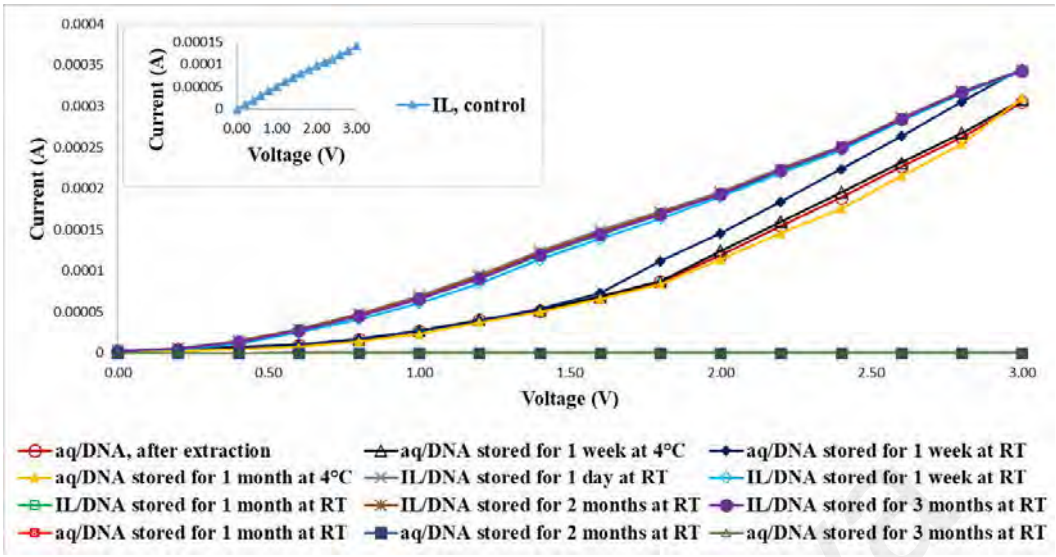

Figure 4.31: *I-V* profiles for *Pleurotus eryngii* (KLU-M 1380) genomic DNA stored at different temperatures and time intervals. The insert illustrates the conductive profile observed from IL as a control.

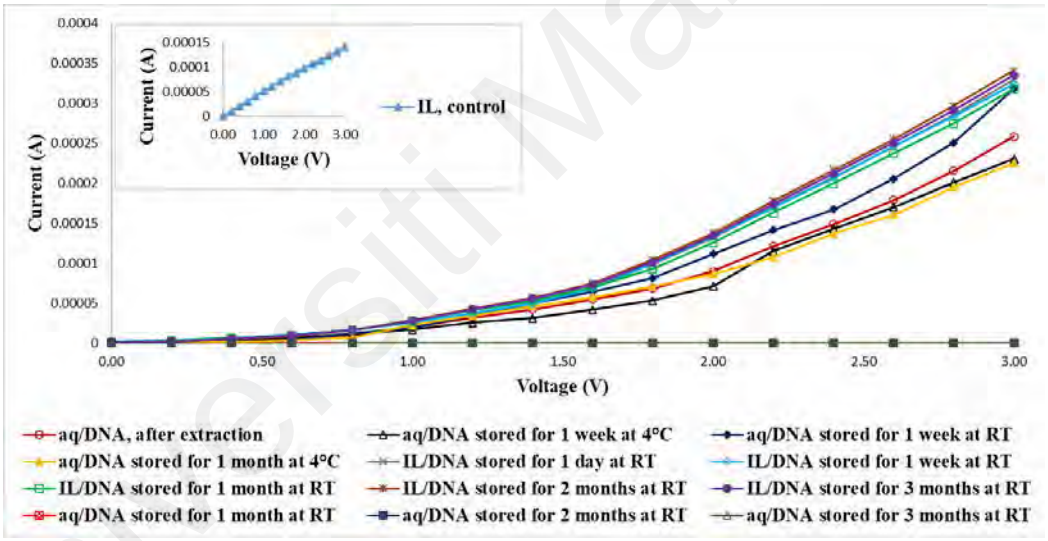

Figure 4.32: *I-V* profiles for *Pleurotus floridanus* (KLU-M 1382) genomic DNA stored at different temperatures and time intervals. The insert illustrates the conductive profile observed from IL as a control.

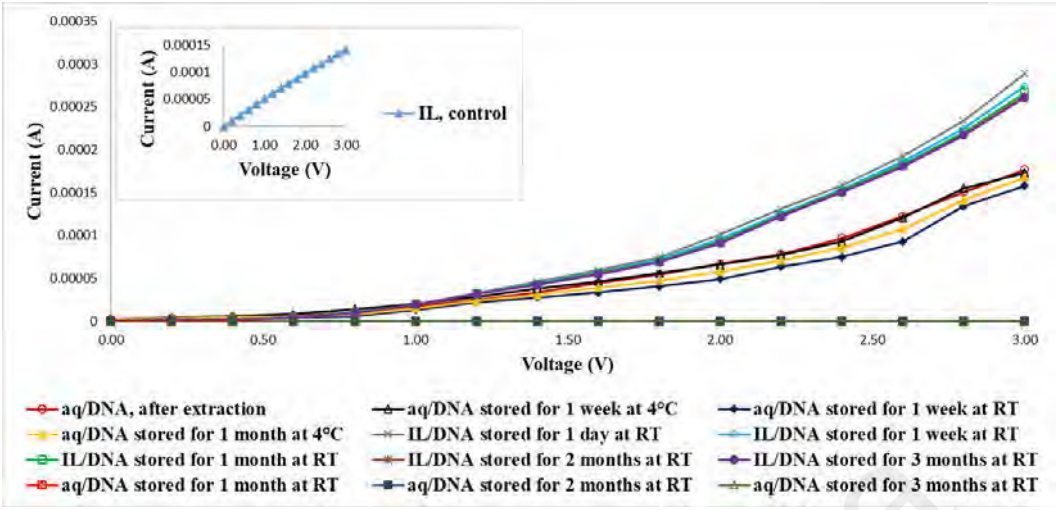

Figure 4.33: *I-V* profiles for *Pleurotus pulmonarius* (KLU-M 1384) genomic DNA stored at different temperatures and time intervals. The insert illustrates the conductive profile observed from IL as a control.

Stable values of turn-on voltage represent the key factor in the long-term stability of DNA in IL and were observed for all the IL/DNA samples as listed in Tables 4.23 to 4.25, which also shows the values of shunt and series resistances.

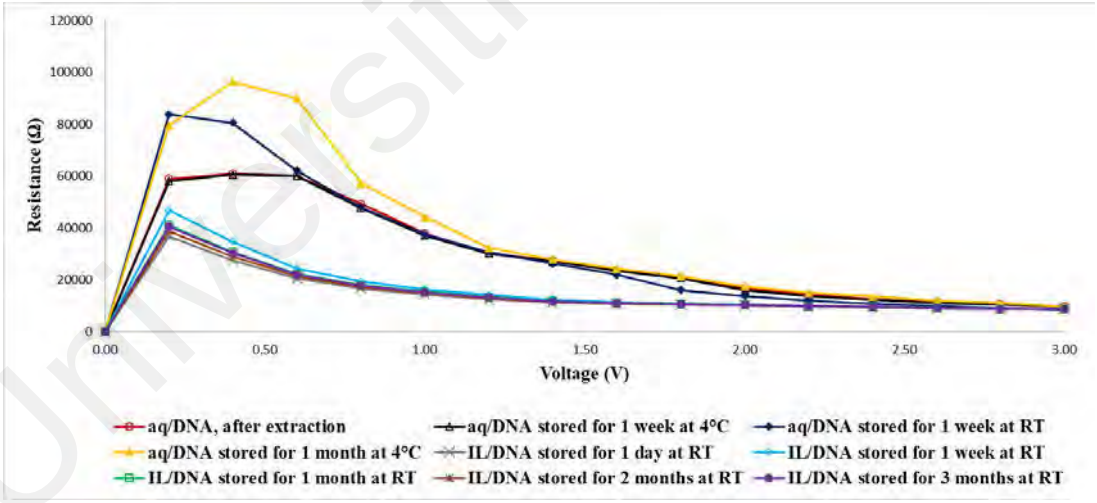

Figure 4.34: Resistance profile against bias voltage for *Pleurotus eryngii* (KLU-M 1380) DNA stored at different temperatures and time intervals.

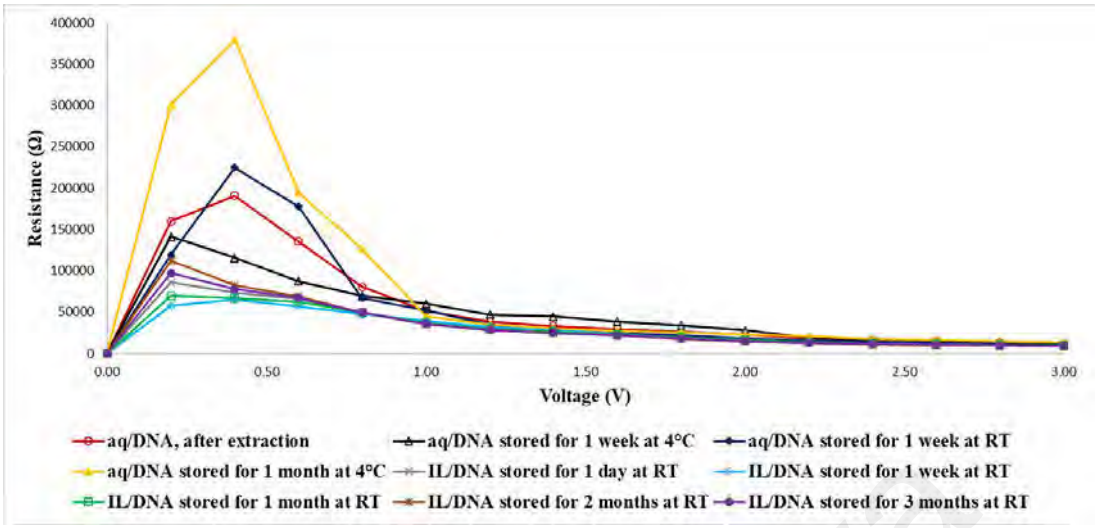

Figure 4.35: Resistance profile against bias voltage for *Pleurotus floridanus* (KLU-M 1382) genomic DNA stored at different temperatures and time intervals.

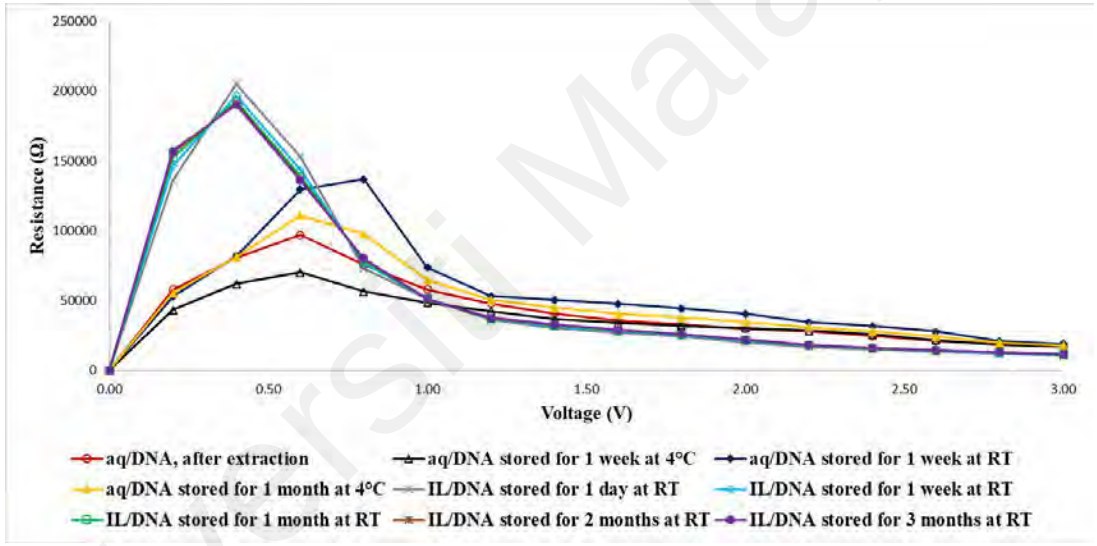

Figure 4.36: Resistance profile against bias voltage for *Pleurotus pulmonarius* (KLU-M 1384) genomic DNA stored at different temperatures and time intervals.

The highest shunt resistance was observed for the *Pleurotus floridanus* (KLU-M 1382), while the lowest is for *Pleurotus eryngii* (KLU-M 1380) (Figures 4.34 to 4.36). These parameters correspond to 379.86 kΩ and 38.80 kΩ, respectively (Tables 4.23 to 4.25).

Table 4.23: Electronic parameters (turn-on voltage (V), series resistance (R_s), shunt resistance (R_{sh})) calculated for *Pleurotus eryngii* (KLU-M 1380) genomic DNA stored at different temperatures and time intervals.

Electronic Parameters	Shunt Resistance (kΩ)	Series Resistance (kΩ)	Turn-on Voltage (V)
aq/DNA, after extraction	60.98	9.83	0.85
aq/DNA stored for 1 week at 4°C	60.53	9.73	0.85
aq/DNA stored for 1 week at RT	83.83	8.66	0.80
aq/DNA stored for 1 month at 4°C	96.29	9.67	0.90
IL/DNA stored for 1 day at RT	38.80	8.71	0.40
IL/DNA stored for 1 week at RT	42.72	8.76	0.40
IL/DNA stored for 1 month at RT	41.17	8.74	0.40
IL/DNA stored for 2 months at RT	38.86	8.72	0.40
IL/DNA stored for 3 months at RT	40.57	8.73	0.40

Table 4.24: Electronic parameters (turn-on voltage (V), series resistance (R_s) and shunt resistance (R_{sh})) calculated for *Pleurotus floridanus* (KLU-M 1382) genomic DNA stored at different temperatures and time intervals.

Electronic Parameters	Shunt Resistance (kΩ)	Series Resistance (kΩ)	Turn-on Voltage (V)
aq/DNA, after extraction	190.74	11.63	0.95
aq/DNA stored for 1 week at 4°C	141.27	13.03	0.90
aq/DNA stored for 1 week at RT	224.55	9.42	0.80
aq/DNA stored for 1 month at 4°C	379.86	13.32	0.85
IL/DNA stored for 1 day at RT	70.86	9.11	0.60
IL/DNA stored for 1 week at RT	65.50	9.27	0.60
IL/DNA stored for 1 month at RT	69.72	9.43	0.60
IL/DNA stored for 2 months at RT	75.71	8.80	0.60
IL/DNA stored for 3 months at RT	75.09	8.95	0.60

Table 4.25: Electronic parameters (turn-on voltage (V), series resistance (R_s), shunt resistance (R_{sh})) calculated for *Pleurotus pulmonarius* (KLU-M 1384) genomic DNA stored at different temperatures and time intervals.

Electronic Parameters	Shunt Resistance (kΩ)	Series Resistance (kΩ)	Turn-on Voltage (V)
aq/DNA, after extraction	97.15	16.94	0.90
aq/DNA stored for 1 week at 4°C	70.11	17.31	0.85
aq/DNA stored for 1 week at RT	137.08	19.01	0.75
aq/DNA stored for 1 month at 4°C	111.02	17.85	0.80
IL/DNA stored for 1 day at RT	205.17	10.37	0.90
IL/DNA stored for 1 week at RT	194.15	11.20	0.90
IL/DNA stored for 1 month at RT	193.37	11.25	0.90
IL/DNA stored for 2 months at RT	191.53	11.41	0.90
IL/DNA stored for 3 months at RT	190.62	11.49	0.90

Stable values are observed for the IL/DNA samples, where values for shunt resistance (38.80 to 42.72 kΩ for *Pleurotus eryngii*; 65.50 to 75.71 kΩ for *Pleurotus floridanus*; 190.62 to 205.17 kΩ for *Pleurotus pulmonarius*), series resistance (8.71 to 8.76 kΩ for *Pleurotus eryngii*; 8.80 to 9.43 kΩ for *Pleurotus floridanus*; 10.37 to 11.49 kΩ for *Pleurotus pulmonarius*), and turn-on voltage (0.4 eV for *Pleurotus eryngii*; 0.6 eV for *Pleurotus floridanus*; 0.9 eV for *Pleurotus pulmonarius*) were almost similar to each other.

In general, it was observed that values calculated for shunt resistance, series resistance and turn-on voltage are lower for all the IL/DNA samples compared to only the DNA solution. The exception however is for *Pleurotus pulmonarius* which demonstrated higher shunt resistance but similar turn-on voltage values. Again, as discussed previously, the deviation from the general trend may be contributed to enhanced characteristic current pathways specific to this particular species, the details of which remains inconclusive at the moment.

Table 4.26: Selected electronic parameters calculated for *Pleurotus eryngii* (KLU-M 1380) genomic DNA stored at different temperatures and time intervals.

Electronic Parameters	Ideality Factor, n	Barrier Height, $Ø$ (eV)	Series Resistance, R_s (kΩ)
Method 1			
aq/DNA, after extraction	31.6	0.8582	-
aq/DNA stored for 1 week at 4°C	31.5	0.8580	-
aq/DNA stored for 1 week at RT	26.7	0.8601	-
aq/DNA stored for 1 month at 4°C	29.7	0.8591	-
IL/DNA stored for 1 day at RT	51.1	0.8201	-
IL/DNA stored for 1 week at RT	50.0	0.8215	-
IL/DNA stored for 1 month at RT	50.2	0.8212	-
IL/DNA stored for 2 months at RT	50.1	0.8213	-
IL/DNA stored for 3 months at RT	50.3	0.8211	-
Method 2			
aq/DNA, after extraction	19.67	0.8586	2.98

Table 4.26, continued.

Electronic Parameters	Ideality Factor, *n*	Barrier Height, *Ø* (eV)	Series Resistance, R_s (kΩ)
aq/DNA stored for 1 week at 4°C	20.43	0.8573	2.28
aq/DNA stored for 1 week at RT	14.79	0.8753	3.36
aq/DNA stored for 1 month at 4°C	22.01	0.8538	2.55
IL/DNA stored for 1 day at RT	9.16	0.8511	6.09
IL/DNA stored for 1 week at RT	9.41	0.8589	5.93
IL/DNA stored for 1 month at RT	9.46	0.8530	6.05
IL/DNA stored for 2 months at RT	9.50	0.8501	6.12
IL/DNA stored for 3 months at RT	9.47	0.8523	6.07

Table 4.27: Selected electronic parameters calculated for *Pleurotus floridanus* (KLU-M 1382) genomic DNA stored at different temperatures and time intervals.

Electronic Parameters	Ideality Factor, *n*	Barrier Height, *Ø* (eV)	Series Resistance, R_s (kΩ)
Method 1			
aq/DNA, after extraction	30.9	0.8657	-
aq/DNA stored for 1 week at 4°C	29.7	0.8660	-
aq/DNA stored for 1 week at RT	26.6	0.8750	-
aq/DNA stored for 1 month at 4°C	34.9	0.8586	-

Table 4.27, continued.

Electronic Parameters	Ideality Factor, n	Barrier Height, $Ø$ (eV)	Series Resistance, R_s (kΩ)
IL/DNA stored for 1 day at RT	31.2	0.8569	-
IL/DNA stored for 1 week at RT	30.9	0.8585	-
IL/DNA stored for 1 month at RT	31.4	0.8575	-
IL/DNA stored for 2 months at RT	31.0	0.8563	-
IL/DNA stored for 3 months at RT	31.1	0.8566	-
Method 2			
aq/DNA, after extraction	22.12	0.8594	2.73
aq/DNA stored for 1 week at 4°C	22.47	0.8560	2.01
aq/DNA stored for 1 week at RT	28.46	0.8501	1.51
aq/DNA stored for 1 month at 4°C	33.57	0.8375	1.28
IL/DNA stored for 1 day at RT	15.66	0.8703	3.39
IL/DNA stored for 1 week at RT	15.79	0.8709	3.43
IL/DNA stored for 1 month at RT	15.86	0.8690	3.26
IL/DNA stored for 2 months at RT	15.80	0.8694	3.28
IL/DNA stored for 3 months at RT	15.99	0.8689	3.29

Table 4.28: Selected electronic parameters calculated for *Pleurotus pulmonarius* (KLU-M 1384) genomic DNA stored at different temperatures and time intervals.

Electronic Parameters	Ideality Factor, n	Barrier Height, $Ø$ (eV)	Series Resistance, R_s (kΩ)
Method 1			
aq/DNA, after extraction	34.6	0.8663	-
aq/DNA stored for 1 week at 4°C	34.3	0.8694	-
aq/DNA stored for 1 week at RT	37.6	0.8608	-
aq/DNA stored for 1 month at 4°C	33.9	0.8733	-
IL/DNA stored for 1 day at RT	30.2	0.8650	-
IL/DNA stored for 1 week at RT	30.6	0.8653	-
IL/DNA stored for 1 month at RT	30.7	0.8654	-
IL/DNA stored for 2 months at RT	30.8	0.8655	-
IL/DNA stored for 3 months at RT	30.8	0.8655	-
Method 2			
aq/DNA, after extraction	26.47	0.8551	3.47
aq/DNA stored for 1 week at 4°C	31.66	0.8558	3.05
aq/DNA stored for 1 week at RT	12.21	0.8745	1.68
aq/DNA stored for 1 month at 4°C	42.94	0.8407	2.14
IL/DNA stored for 1 day at RT	17.47	0.8763	3.00

Table 4.28, continued.

Electronic Parameters	Ideality Factor, n	Barrier Height, $Ø$ (eV)	Series Resistance, R_s (kΩ)
IL/DNA stored for 1 week at RT	17.36	0.8732	3.07
IL/DNA stored for 1 month at RT	17.54	0.8775	3.03
IL/DNA stored for 2 months at RT	17.45	0.8779	3.11
IL/DNA stored for 3 months at RT	17.41	0.8782	3.15

Tables 4.26 to 4.28 compare the values of barrier height, ideality factor and series resistance of the DNA samples stored at different temperatures and time intervals calculated using Methods 1 and 2. Values of barrier height were observed to be consistent between 0.82 to 0.86 eV for *Pleurotus eryngii*; 0.83 to 0.87 eV for *Pleurotus floridanus*; 0.84 to 0.87 eV for *Pleurotus pulmonarius*.

Profiles for other DNA samples of *P. giganteus* (KLU-M 1227), *P. giganteus* (KLU-M 1385) and *P. cystidiosus* (KLU-M 1388) were shown as in Appendix B (Figure S1-S3) as the results are followed the same trends.

4.6.3 Gel Electrophoresis Analysis for the PCR-amplified DNA of ITS region Stored at Different Temperatures and Time intervals

Figures 4.37 to 4.39 show the low quality of DNA samples stored at RT for 1 to 3 months in aqueous solution (lanes 11-13), whereas the DNA samples in IL stored at RT for 1 day to 3 months remained intact. The existence of fade band in line 11 (Figure 4.37) lines 10 and 11 (Figure 4.39) and double bands in line 11 (Figure 4.38) shows the low quality of DNA stored at RT. The physical properties of ILs can be finely adjusted through the cautious selection of cations which are significant towards DNA stabilization. The

basic understandings of interaction between cations with the major and minor grooves of DNA depend on both the type of cations and DNA sequence (electrostatic property of grooves and the specific position of electronegative groups in grooves). Cations tend to move close to the DNA main chain due to strong electrostatic interactions with the phosphate groups in the DNA strands. Based on the results discussed in this thesis, the addition of [BMIM][Ace] in the DNA solution have led to long-term stability of DNA (up to 4 months, limited to the period of this current experiment) in RT.

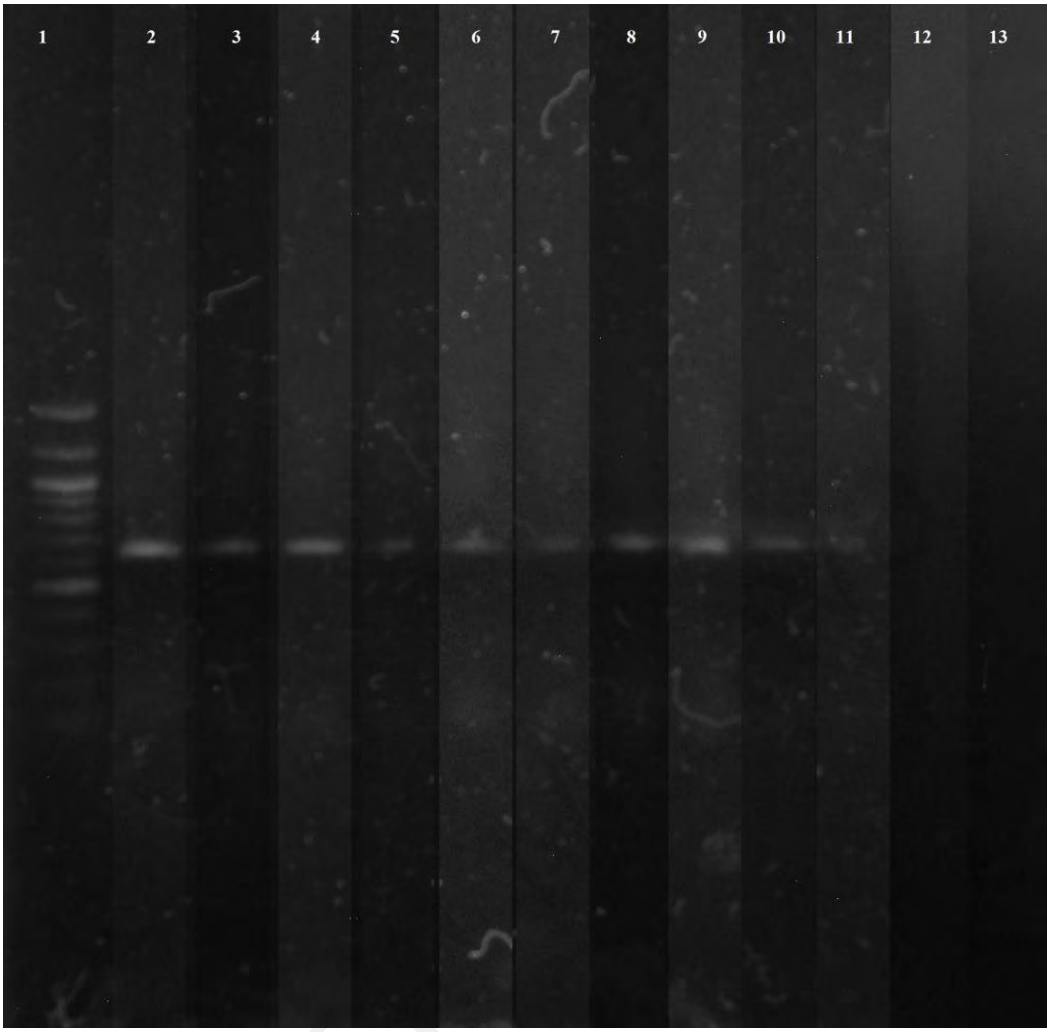

Figure 4.37: Gel electrophoresis of *Pleurotus eryngii* (KLU-M 1380) for the PCR-amplified DNA of ITS region stored at different temperatures and time intervals, obtained on amplification with primers, ITS1 and ITS4, lane 1: DNA Ladder molecular weight marker, lane 2: IL/DNA stored for 3 months at RT, lane 3: IL/DNA stored for 2 months at RT, lane 4: IL/DNA stored for 1 month at RT, lane 5: IL/DNA stored for 1 week at RT, lane 6: IL/DNA stored for 1 day at RT, lane 7: aq/DNA stored for 1 week at RT, lane 8: aq/DNA stored for 1 week at 4°C, lane 9: aq/DNA stored for 1 month at 4°C, lane 10: aq/DNA, after amplification, lane 11: aq/DNA stored for 1 month at RT, lane 12: aq/DNA stored for 2 months at RT, and lane 13: aq/DNA stored for 3 months at RT. The size of the PCR fragments was on average about 700 bp in length for all DNA samples stored at different temperatures and time intervals.

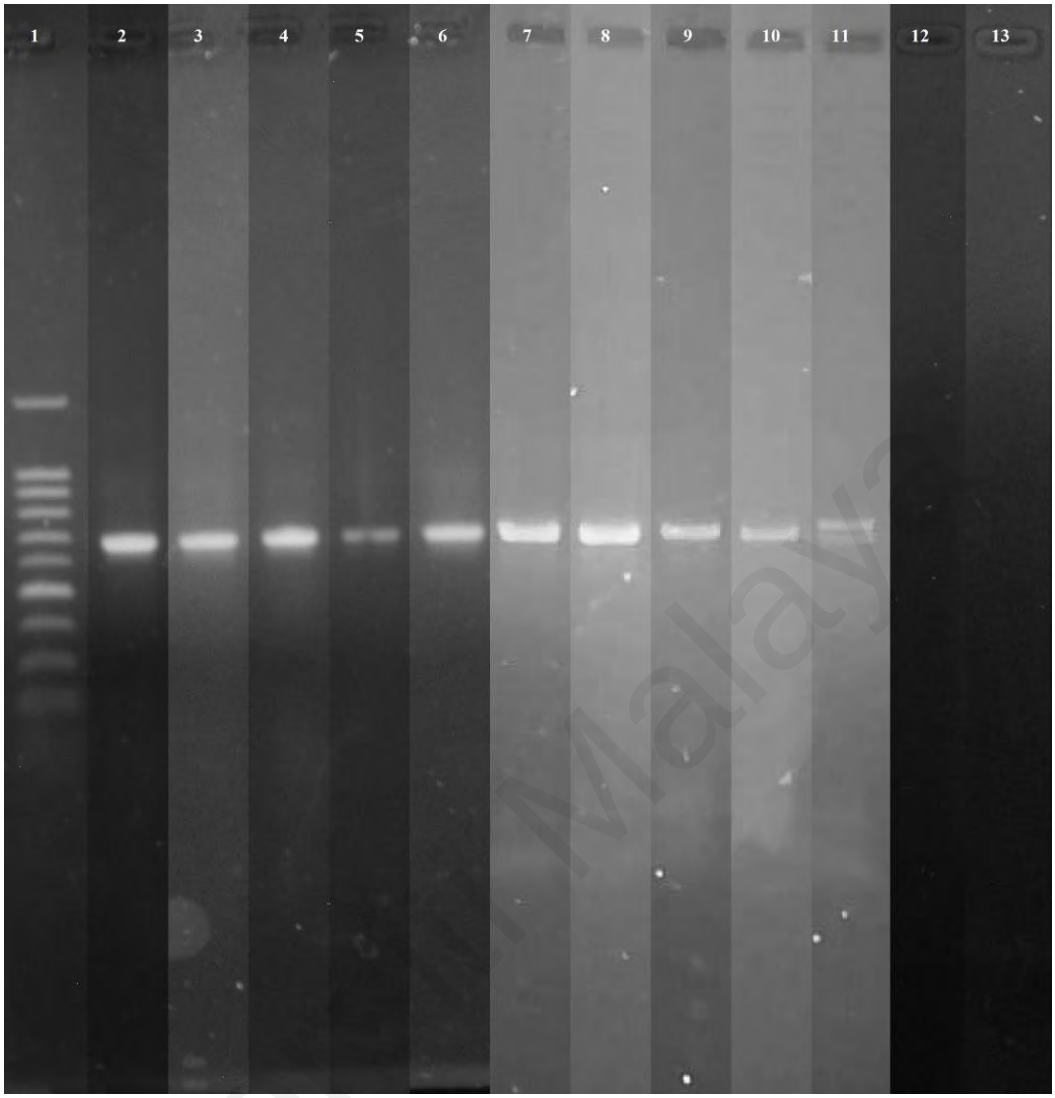

Figure 4.38: Gel electrophoresis of *Pleurotus floridanus* (KLU-M 1382) for the PCR-amplified DNA of ITS region stored at different temperatures and time intervals, obtained on amplification with primers, ITS1 and ITS4, lane 1: DNA Ladder molecular weight marker, lane 2: aq/DNA, after amplification, lane 3: aq/DNA stored for 1 week at 4°C, lane 4: aq/DNA stored for 1 month at 4°C, lane 5: aq/DNA stored for 1 week at RT, lane 6: IL/DNA stored for 1 day at RT, lane 7: IL/DNA stored for 1 week at RT, lane 8: IL/DNA stored for 1 month at RT, lane 9: IL/DNA stored for 2 months at RT, lane 10: IL/DNA stored for 3 months at RT, lane 11: aq/DNA stored for 1 month at RT, lane 12: aq/DNA stored for 2 months at RT, and lane 13: aq/DNA stored for 3 months at RT. The size of the PCR fragments was on average about 800 bp in length for all DNA samples stored at different temperatures and time intervals.

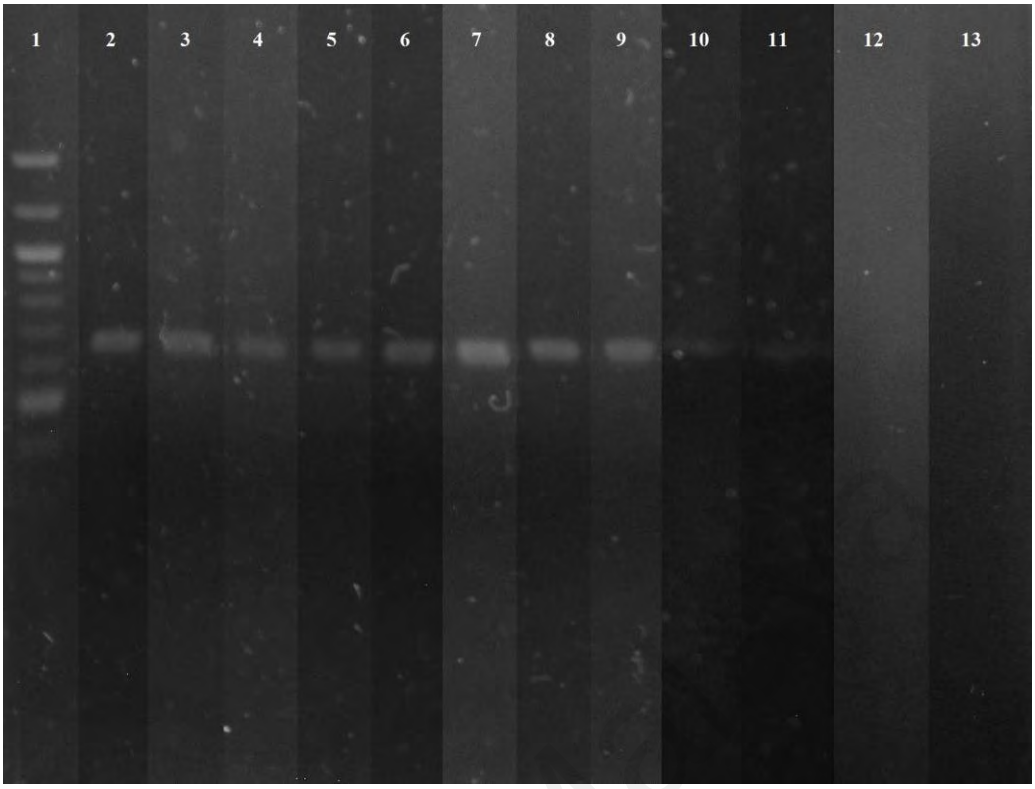

Figure 4.39: Gel electrophoresis of *Pleurotus pulmonarius* (KLU-M 1384) for the PCR-amplified DNA of ITS region stored at different temperatures and time intervals, obtained on amplification with primers, ITS1 and ITS4, (L) DNA Ladder molecular weight marker, (1) aq/DNA, after amplification, (2) aq/DNA stored for 1 week at 4°C, (3) aq/DNA stored for 1 month at 4°C, (4) IL/DNA stored for 1 day at RT, (5) IL/DNA stored for 1 week at RT, (6) IL/DNA stored for 1 month at RT, (7) IL/DNA stored for 2 months at RT, (8) IL/DNA stored for 3 months at RT, (9) aq/DNA stored for 1 week at RT, (10) aq/DNA stored for 1 month at RT, (11) aq/DNA stored for 2 months at RT, and (12) aq/DNA stored for 3 months at RT. The size of the PCR fragments was on average about 700 bp in length for all DNA samples stored at different temperatures and time intervals.

Gel electrophoresis Analysis for other DNA samples isolated from *P. giganteus* (KLU-M 1227), *P. giganteus* (KLU-M 1385) and *P. cystidiosus* (KLU-M 1388) shows the same trends and are shown as Supplementary profiles to avoid repetition in Appendix B (Figure S4-S6).

CHAPTER 5: CONCLUSIONS AND FUTURE WORKS

5.1 Conclusions

The classification and taxonomic identification of species among the genus *Pleurotus* is difficult and unreliable because phenotypic variation can be affected by wide geographic ranges, geographic overlap of species and continuing evolution, and speciation (Vilgarys & Sun, 1994). Most taxa have different morphology from other taxa. Usually, the morphological differences within closely related species are much less than more distantly related ones. Some species look very similar or maybe even outwardly identical but are reproductively isolated. On the other hand, sometimes unrelated species obtain a similar look as a result of convergent evolution or even mimicry.

In addition, when relying solely on the morphological data, some species which were earlier determined to be different species would in fact turn out to be two distinct species. It would require further longer and more expensive DNA analysis to conclude that it is actually a single species. Current method proposed in this thesis however involves directly acquiring characteristic or "fingerprinting" electronic signature signals from the respective semiconducting DNA sequence from different genus of a closely related species. Quantitative measurements such as (but not limited to) analysis of different parameters such as turn-on voltage, ideality factor, barrier height, series resistance, shunt resistance, knee-voltage and breakdown voltage can be utilized for rapid, simple and low-cost DNA/RNA identification. This electronic sensor is highly reproducible and sensitive, which requires only low amount and concentration of DNA for sensor preparation.

Generally, electrochemical properties of mushroom species are possible parameters available for identifying different mushroom species, for example, conductivity of mushrooms would be a possible parameter. However, this is practically a hard task owing to the negligibly small differences among the mushroom species. On the other hand, the

focusing parameter is injection properties of mushroom species. As such, a novel method is presented that provides significant alternative quantitative data to clearly distinguish between different species and genus and between species in the same genus, in contrast to the limitations. Between two methods that used in this study, Cheung and Cheung's method (method 2) was suggested to be the most reliable method to extract diode parameters in this case.

The use of this electronic technique for identification of genomic DNA is easier and can also be used to detect PCR-amplified DNA. Potential DNA markers vary from species to species. ITS has showed better results with less overlapping profiles for most of DNA samples due to high degree of interspecific variability, conserved primer sites and multiple copy nature in the genome. Therefore, *I-V* profiles and electronic parameters of DNA samples using ITS region may be effective for finer-scale species-level identification of *Pleurotus* mushrooms. LSU and RPB2 regions may be accepted as secondary choice for *Pleurotus* mushroom DNA samples for electronic method.

In this study, the *I-V* profiles of the forward bias region for genomic DNA sample under different pH conditions were examined. Results showed that variation in pH values can have significant changes in the DNA conductivity, where strong acidic conditions (pH 1 to 2) have higher conductivity compared to strong alkaline conditions (pH 13 to 14). Variation in the pH values can affect the conformation of the biomolecule and alter its electronic structure, causing the variation in the amount of conductivity. However, values of barrier height for DNA in alkaline conditions remain stable unlike in acidic conditions where decreasing trend was observed with increasing acidity. The ideality factor values are in general smaller for both acidic and alkaline conditions when calculated using Cheung and Cheung's method, which is indicative of the effects of series resistance. Although DNA is considered to be reasonably stable in aqueous solution, the

present study demonstrates the pH-dependent stability of DNA, which causes denaturation of its structure accompanied by ionization of the bases and disorganization of their arrangement of the secondary, tertiary and quaternary structures. Stable values and profiles were obtained for the pH 8 to 9 which suggests, it is the best pH for DNA detection.

The *I-V* profiles of the forward bias region for DNA samples under different temperatures and time intervals were also examined. Results showed that variation in temperature and time can have significant changes in the stability of DNA samples. Variations in the storage time and temperature can affect the conformation of the DNA and alter its electronic structure, causing the variation in its solid-state parameters. However, values of the electronic parameters for DNA mixed with IL remain stable. The ideality factor values are in general smaller for both the DNA and IL/DNA solutions when calculated using Cheung and Cheung's method indicative of the effects of series resistance. It is important to realize that the ion interaction with DNA is not the determining factor of DNA structure but contributes to the heterogeneity of DNA structure. The major contributor to the DNA-IL interaction is the electrostatic attraction of organic cations and DNA phosphate backbone, followed by the hydrophobic and polar interactions between ILs and the major and minor grooves of the DNA. It can be concluded that IL, [BMIM][Ace] is a potential solvent that ensures long-term stability of DNA at room temperature for more than three months.

The main benefits of the electronic method proposed in this research includes cost-effective, rapid detection, non-invasive and small-scale device design besides requiring only low amount and concentration of the sample to operate as a potential alternative to more complex and costlier tools. This simple technique could be used to provide reliable, rapid and low-cost DNA diagnostic device for the quick identification of species from

trace amounts of biological material. Moreover, the study of sequence-specific electronic properties of DNA is one such analysis that could be employed as a tool to understand its charge transfer mechanism useful for integration into functional DNA-based devices.

5.2 Future Works

This research is considered to be as a motivational precursor for future works and experiments in the field of DNA electronics. It could be used for other purposes in biology or any other science using other types of DNA or other substrates or electrodes. The current research has been extensively carried out for an in-depth electronic profiling, which includes an application of suitable semiconductor models to investigate the various solid-state parameters. These parameters could in turn be utilized to relate to its biological consequences and therefore provide the pre-requisites necessary to understand the physical significance. Further characterizations and experiments, especially on the biological aspect may in future correspond and relate strongly to the various solid-state parameters generated through this pioneering research. Moreover, studying the specific behaviors of *I-V* profiles helps in thoroughly understanding the mechanism of charge transfer in DNA base sequences. This may become a useful tool in discovering the causes of the variation among organisms, the effects of certain conditions or environmental changes or mutations and detecting or predicting any disruption or disease that the organisms can suffer from. These methods of profiling can therefore be carried out for trace diagnosis of DNAs, including pathogenic organisms by establishing a database from where quick and rapid identification could be achieved. It should be noted that due to the ongoing process of evolution subjected to its corresponding environmental conditions, it is possible for slight variations in the electronic signals to be progressively measured and studied.

The initial results discussed in this current study may demonstrate the possibility of utilizing DNA-specific Schottky barrier diodes as a kit to detect unknown DNAs by providing characteristic rectifying profiles and as an alternative way to discriminate closely related species. These could be then used to justify the importance of various solid-state parameters towards in-depth understanding of various fundamental physical, biological and biochemical phenomena in DNAs with different base pair sequences. The DNA-specific Schottky diodes may also be utilized as a tool for interrogating the underlying processes that could provide insights into DNA's damage and repair mechanism.

As expected, the stability of DNA structures in ILs have a profound impact on the future advances in various applications such as DNA storage and DNA preparation. It is therefore of great interest to understand the effect of different ILs on DNA structural changes and binding properties. This would enable us to clarify the compatibility of ILs with DNA and to rationally design ILs for DNA-based applications. These could be then used to understand the DNA stability in ILs and to stimulate further research on DNA-based applications in ILs.

From this novel method of utilization of the specific properties of DNA especially the semiconducting behavior, many other future devices can be fabricated and used in different applications. In this study, DNA-specific Schottky diodes were used for the first time to find the electronic parameters related to different species of selected mushrooms. Thus, DNA can be considered as an alternative organic semiconducting material which in the near future will be utilized in the fabrication and development of unique next generation biomedical devices.

REFERENCES

Aanen, D. K., Kuyper, T. W., & Hoekstra, R. F. (2001). A widely distributed ITS polymorphism within a biological species of the ectomycorrhizal fungus *Hebeloma velutipes*. *Mycological Research, 105*, 284-290.

Acar, I., Dizkirici Tekpinar, A., Kalmer, A., & Uzun, Y. (2017). Phylogenetic relationships and taxonomical positions of two new records *Melanoleuca* species from Hakkari province, Turkey. *Biological Diversity and Conservation, 10*(3), 79-87.

Ageno, M., Dore, E., & Frontali, C. (1969). The alkaline denaturation of DNA. *Biophysical Journal, 9*, 1281-1311.

Alberts, B., Johnson, A., Lewis, J., Walter, P., Raff, M., & Roberts, K. (2002). Molecular biology of the cell 4th edition. *Annals of Botany, 91*(3), Article#401.

Al-Ghamdi, A., Al-Hartomy, O., Gupta, R., El-Tantawy, F., Taskan, E., Hasar, H., & Yakuphanoglu, F. (2012). A DNA biosensor based interface states of a metal-insulator-semiconductor diode for biotechnology applications. *Acta Physica Polonica A, 121*, 673-677.

Altschul, S. F., Gish, W., Miller, W., Myers, E.W., & Lipman, D. J. (1990). Basic local alignment search tool. *Journal of Molecular Biology, 215*, 403-410.

Al-Ta'ii, H. M. J., Amin, Y. M. & Periasamy, V. (2015). Calculation of the electronic parameters of an Al/DNA/p-Si Schottky Barrier Diode influenced by alpha radiation. *Sensors, 15*, 4810-4822.

Al-Ta'ii, H. M. J., Amin, Y. M. & Periasamy, V. (2015). Investigations of electrical properties of structures Al-DNA-ITO-Al exposed to alpha particles. *Radiation Measurements, 72*, 85-94.

Al-Ta'ii, H. M. J., Periasamy, V. & Amin, Y. M. (2015). Detection of alpha particles using DNA/Al Schottky junctions. *Journal of Applied Physics, 118*, Article#114502.

Al-Ta'ii, H. M. J., Periasamy, V., & Amin, Y. M. (2016). Electronic characterization of Au/DNA/ITO metal-semiconductor-metal diode and its application as a radiation sensor. *PLoS ONE, 11*(1), Article#e0145423.

Al-Ta'ii, H. M. J., Periasamy, V. & Amin, Y. M. (2015). Electronic properties of DNA-based schottky barrier diodes in response to alpha particles. *Sensors, 15*(5), 11836-11853.

Al-Ta'ii, H. M. J., Periasamy, V. & Amin, Y. M. (2016). Humidity-dependent characteristics of DNA thin film-based Al/DNA/Al surface-type cell. *Sensors and Actuators B, 232*, 195-202.

Al-Ta'ii, H. M. J., Periasamy, V. & Amin, Y. M. (2016). Humidity influenced capacitance and resistance of an Al/DNA/Al Schottky diode irradiated by alpha particles. *Scientific Reports, 6*, Article#25519.

An, R., Jia, Y., Wan, B., Zhang, Y., Dong, P., Li, J., & Liang, X. (2014). Non-enzymatic depurination of nucleic Acids: Factors and mechanisms. *PLoS ONE, 9*(12), 1-17.

Anderson, J. L., Ding, J., Welton, T., & Armstrong, D. W. (2002). Characterizing ionic liquids on the basis of multiple solvation interactions. *Journal of the American Chemical Society, 124*(47), 14247-14254.

Araujo, R. (2014). Towards the genotyping of fungi: methods, benefits and challenges. *Current Fungal Infection Reports, 8*(3), 203-210.

Armand, M., Endres, F., MacFarlane, D. R., Ohno, H., & Scrosati, B. (2009). Ionic-liquid materials for the electrochemical challenges of the future. *Nature Materials, 8*, 621-629.

Artés, J. M., López-Martínez, M., Díez-Pérez, I., Sanz, F., & Gorostiza, P. (2014). Nanoscale charge transfer in redox proteins and DNA: Towards biomolecular electronics. *ElectrochimicaActa, 140*, 83-95.

Avery, O. T., MacLeod, C. M., & McCarty, M. (1944). Studies on the chemical nature of the substance inducing transformation of pneumococcal types: induction of transformation by a desoxyribonucleic acid fraction isolated from pneumococcus type III. *The Journal of Experimental Medicine, 79*(2), Article#137.

Avery, T. D., Jenkins, N. F., Kimber, M. C., Lupton, D. W., & Taylor, D. K. (2002). First examples of the catalytic asymmetric ring-opening of meso 1,2-dioxines utilising cobalt(ii) complexes with optically active tetradentate Schiff baseligands: formation of enantio-enriched cyclopropanes. *Chemical Communications, 1*, 28-29.

Avin, F. A., Bhassu, S., Shin, T. Y., & Sabaratnam, V. (2012). Molecular classification and phylogenetic relationships of selected edible Basidomycetes species. *Molecular Biology Reports, 39*, 7355-7346.

Avin, F. A., Bhassu, S., Shin, T. Y., Braukmann, T. W. A., Sabaratnam, V., & Hebert, P. D. N. (2017). Escaping introns in COI through cDNA barcoding of mushrooms: *Pleurotus* as a test case. *Ecology and Evolution, 7*, 6972-6980.

Aydoğan, Ş., Sağlam, M., & Türüt, A. (2005). Characterization of capacitance–frequency features of Sn/polypyrrole/n-Si structure as a function of temperature. *Polymer, 46*(16), 6148-6153.

Bagci, V. M. K., & Krokhin, A. A. (2007). Metal–insulator transition in DNA molecules induced by long-range correlations in the sequence of nucleotides. *Chaos, Solitons & Fractals, 34*(1), 104-111.

Bao, D. P., Ishihara, H., Mori, N., & Kitamoto, Y. (2004). Phylogenetic analysis of oyster mushrooms (*Pleurotus* spp.) based on restriction fragment length polymorphisms of the 5′ portion of 26S rDNA. *Journal of Wood Science, 50*, 169-176.

Bao, X., Duan, J., Fang, X., & Fang, J. (2001). Chemical modifications of the (1→3)-α-D-glucan from spores of Ganoderma lucidum and investigation of their physicochemical properties and immunological activity. *Carbohydrate Research, 336*, 127-140.

Barh, A., Sharma, V. P., Kamal, S., Shirur, M., Annepu, S. K., Kumar, A., & Upadhyay, R. C. (2019). Speciation of cultivated temperate and tropical *Pleurotus* species – An in silico prediction using conserved sequences. *Mushroom Research, 28*(1), 31-37.

Baryeh, K., Takalkar, S., Lund, M., & Liu, G. (2017). Introduction to medical biosensors for point of care applications. *Medical Biosensors for Point of Care (POC) Applications*, 3-25.

Baum, D. A., Smith, S. D., & Donovan, S. S. S. (2005). The tree-thinking challenge. *Science, 310*(5750), 979-980.

Beaven, G. H., Holiday, E. R., & Johnson, E. A. (1955). Optical properties of nucleic acids and their components. Eds. Chargaff, E. and Davidson, J. N., New York: Academic Press. *The Nucleic Acids, 1*, 493-553.

Begerow, D., Nilsson, H., Unterseher, M., & Maier, W. (2010). Current state and perspectives of fungal DNA barcoding and rapid identification procedures. *Applied Microbiology and Biotechnology, 87*, 99-108.

Ben-Jacob, E., Hermon, Z., & Caspi, S. (1999). DNA transistor and quantum bit element: Realization of nano-biomolecular logical devices. *Physics Letters A, 263*(3), 199-202.

Bergerová, E., godálová, Z., & Siekel, P. (2011). Combined effects of temperature, pressure and low pH on the amplification of DNA of plant derived foods. *Czech Journal of Food Sciences*, *29*(4), 337-345.

Beyer, A., & Gölzhäuser, A. (2010). Low energy electron point source microscopy: beyond imaging. *Journal of Physics: Condensed Matter, 22*(34), 1-13.

Bhalla, V., Bajpai, R. P., & Bharadwaj, L. M. (2003). DNA electronics. *European Molecular Biology Organization, 4*(5), 442-445.

Binnig, G., Quate, C. F., & Gerber, C. (1986). Atomic force microscope. *Physical Review Letters, 56*(9), Article#930.

Bipasha, C. (2011). Trends in Mushroom cultivation and breeding. *Australian Journal of Agricultural Engineering, 2*(4), 102-109.

Blanchard, L. A., & Brennecke, J. F. (2001). Recovery of organic products from ionic liquids using supercritical carbon dioxide. *Industrial & Engineering Chemistry Research, 40*, 287-292.

Blanchard, L., Hancu, D., Beckman, E., & Brennecke, J. (1999). Green processing using ionic liquids and CO_2. *Nature, 399*, 28-29.

Bonner, G., & Klibanov, A. M. (2000). Structural stability of DNA in nonaqueous solvents. *Biotechnology & Bioengineering, 68*(3), 339-44.

Bonnet, J., Colotte, M., Coudy, D., Couallier, V., Portier, J., Morin, B., & Tuffet, S. (2009). Chain and conformation stability of solid-state DNA: implications for room temperature storage. *Nucleic Acids Research, 38*(5), 1531-1546.

Braun, E., Eichen, Y., Sivan, U., & Ben-Yoseph, G. (1998). DNA-templated assembly and electrode attachment of a conducting silver wire. *Nature, 391*(6669), 775-778.

Brennecke, J. F., & Maginn, E. J. (2001). Ionic liquids: innovative fluids for chemical processing. *aIChE Journal, 47*, 2384-2389.

Brown, S. P., Rigdon-Huss, A. R., & Jumpponen, A. (2014). Analyses of ITS and LSU gene regions provide congruent results on fungal community responses. *Fungal Ecology, 9*, 65-68.

Brun, S., & Silar, P. (2010). Concepts, Molecular and Morphological Evolution. In P. Pontarotti (Eds.), *evolutionary biology* (pp. 317-328). Springer: Berlin Heidelberg.

Bruns, T. D., White, T. J., & Taylor, J. W. (1991). Fungal molecular systematics. *Annual Review of Ecology, Evolution, and Systematics, 22*, 525-564.

Buchanan, P. K. (1993). Identification, names, and nomenclature of common edible mushrooms. In S. Chang, J. A. Buswell, S. Chiu (Eds.), *In Mushroom Biology and Mushroom Products* (pp. 21-32). Hong Kong, Chinese University Press.

Burnham, N., Cruceanu, F., Dong, Q., & Thompson, N. (2004). An introduction to atomic force microscopy. *Computer, 10*, Article#800.

Butt, H.-J., Cappella, B., & Kappl, M. (2005). Force measurements with the atomic force microscope: Technique, interpretation and applications. *Surface Science Reports, 59*(1), 1-152.

Calladine, C. R., Drew, H., Luisi, B., & Travers, A. (2004*). Understanding DNA: The Molecule and How it Works* (3rd ed.). London, *Elsevier Academic Press*.

Carlson, A. L., Justo, A., & Hibbett, D. S. (2014). Species delimitation in *Trametes*: A comparison of ITS, RPB1, RPB2 and TEF1 gene phylogenies. *Mycologia, 106*, 735-745.

Chakrapani, V., Eaton, S. C., Anderson, A. B., Tabib-Azar, M., & Angus, J. C. (2005). Studies of adsorbate-induced conductance of diamond surfaces. *Electrochemical and Solid-State Letters, 8*(1), E4-E8.

Chan, Z., Ahgilan, A., Sabaratnam, V., Tan, Y. S., & Periasamy, V. (2015). Rectification of DNA films self-assembled in the presence of electric field. *Applied Physics Express, 8*(4), Article#047002.

Chang, S. T. (2008). Training manual on mushroom cultivation technology. *United Nations, economic and social commission for Asia and the Pacific, Beijing, China*, 5-65.

Chargaff, E. (1950). Chemical specificity of nucleic acids and mechanism of their enzymatic degradation. *Cellular and Molecular Life Sciences, 6*(6), 201-209.

Chargaff, E. (1971). Preface to a grammar of biology. *Science, 172*(3984).

Chen, J., Moinard, M., Xu, J., Wang, S., & Foulongne-Oriol, M. (2016). Genetic analyses of the internal transcribed spacer sequences suggest introgression and duplication in the medicinal mushroom *Agaricus subrufescens*. *PloS ONE, 11*(5), Article#e0156250.

Chen, M. J. (2014). Metal-semiconductor system: Contact. *DEE Semiconductor Device Physics, 6*(14), 331-338.

Chen, S. H., Chuang, Y. C., Lu, Y. C., Lin, H. C., Yang, Y. L., & Lin, C. S., (2009). A method of layer-by-layer gold nanoparticle hybridization in a quartz crystal microbalance DNA sensing system used to detect dengue virus. *Nanotechnology, 20*(21), Article#215501.

Cheng, D. H., Chen, X. W., Wang, J. H., & Fang, Z. L. (2007). An abnormal resonance light scattering arising from ionic-liquid/dna/ethidium interactions. *Chemistry (Weinheim an der Bergstrasse, Germany), 13*, 4833-9.

Cheng, Y. K., & Pettitt, B. M. (1992). Stabilities of double- and triple-strand helical nucleic acids. *Progress in Biophysics and Molecular Biology, 58*, 225-257.

Cheung, S. K., & Cheung, N. W. (1986). Extraction of Schottky diode parameters from forward current–voltage characteristics. *Applied Physics Letters, 49*, 85-87.

Cheung, S. T. (1999). World production of cultivated edible and medicinal mushrooms in 1997 with emphasis on *Lentinus edodes* (Berk.) Sing, in China. *International Journal of Medicinal Mushrooms, 1*, 291-300.

Chun, S., Dzyuba, S. V., & Bartsch, R. A. (2001). Influence of structural variation in room-temperature ionic liquids on the selectivity and efficiency of competitive alkali metal salt extraction by a crown ether. *Analytical Chemistry, 73*(15), 3737-41.

Crous, P. W., Hawksworth, D. L., & Wingfield, M. J. (2015). Identifying and naming plant-pathogenic fungi: past, present, and future. *The Annual Review of Phytopathology, 53*, 247-267.

Cole, J. R., Wang, Q., Fish, J. A., Chai, B., & McGarrell, D. M. (2014). Ribosomal Database Project: data and tools for high throughput rRNA analysis. *Nucleic Acids Research, 42*, D633-D642.

Coleman, A., Gould, M., & Stephano, J. L. (2013). Biochemical Techniques, Laboratory Manual. *Hayden McNeil Publishing,103*, 13-26.

Costantino, L., & Vitagliano, V. (1966). pH-induced conformational changes of DNA. *Biopolymers, 4*, 521-528.

Dahm, R. (2005). Friedrich Miescher and the discovery of DNA. *Developmental Biology, 27*8, 274-288.

Dentinger, B. T. M., Didukh, M. Y., & Moncalvo, J. M. (2011). Comparing COI and ITS as DNA barcode markers for mushrooms and allies (*Agaricomycotina*). *PLoS ONE, 6*, Article#e25081.

D'Errico, M., Parlanti, E., & Dogliotti, E. (2008). Mechanism of oxidative DNA damage repair and relevance to human pathology. *Mutation Research, 659*, 4-14.

Deepalakshmi, K., & Mirunalini, S. (2014). *Pleurotus ostreatus*: an oyster mushroom with nutritional and medicinal properties. *Journal of Biochemical Technology, 5*(2), 718-726.

De Pablo, P. J., Moreno-Herrero, F., Colchero, J., Herrero, J. G., Herrero, P., Baró, A. M., & Artacho, E. (2000). Absence of dc-conductivity in λ-DNA. *Physical Review Letters, 85*(23), Article#4992.

Dilhari, A., Sampath, A., Gunasekara, C., Fernando, N., Weerasekara, D., Sissons, C., & Weerasekera, M. (2017). Evaluation of the impact of six different DNA extraction methods for the representation of the microbial community associated with human chronic wound infections using a gel-based DNA profiling method. *AMB Express, 7*(179), 1-11.

Ding, Y., Zhang, L., Xie, J., & Guo, R. (2010). Binding characteristics and molecular mechanism of interaction between ionic liquid and DNA. *The Journal of Physical Chemistry B, 114*, 2033-43.

Di Ventra, M., & Zwolak, M. (2004). DNA Electronics. *Encyclopedia of Nanoscience and Nanotechnology, 2*, 475-493.

Dulla, E. L., Kathera, C., Gurijala, H. K., Mallakuntla, T. R., & Srinivasan, P. (2016). Highlights of DNA barcoding in identification of salient microorganisms like fungi. *Journal de Mycologie Medicale, 26*, 291-297.

Durmanov, N. N., Guliev, R. R., Eremenko, A. V., Boginskaya, I. A., Ryzhikov, I. A., Trifonova, E. A., … Kurochkin, I. N. (2017). Non-labeled selective virus detection with novel SERS-active porous silver nanofilms fabricated by electron beam physical vapor deposition. *Sensors and Actuators, B: Chemical, 257*, 37-47.

Earle, M. J., & Seddon, K. R. (2000). Ionic liquids. Green solvents for the future. *Pure and Applied Chemistry, 72*, 1391-1398.

Eberhardt, U., Beker, H. J., Vila, J., Vesterholt, J., Llimona, X., & Gadjieva, R. (2009). *Hebeloma* species associated with *Cistus*. *Mycological Research, 113*, 153-162.

Ehrlich, P., & Doty, P. (1958). The alkaline denaturation of deoxyribose nucleic acid. *Journal of the American Chemical Society, 80*, 4251-4255.

Eley, D. D., & Spivey, D. I. (1962). Semiconductivity of organic substances. Part 9. Nucleic acid in the dry state. *Transactions of the Faraday Society, 58*, 411-415.

Endres, R. G., Cox, D. L., & Singh, R. R. (2004). Colloquium: The quest for high-conductance DNA. *Reviews of Modern Physics, 76*(1), Article#195.

Feynman, R. (1963). Feynman Lectures on Physics. Basic Books. Volume 1, chapter 26.

Fink, H. W., & Schönenberger, C. (1999). Electrical conduction through DNA molecules. *Nature, 398*(6726), 407-410.

Fitch, J. P. (2002). An engineering introduction to biotechnology. *SPIE Press, 55*, Article#21.

Frenken, T., Elisabet, A., Berger, S. A., Bourne, E. C., & Mélanie, G. (2017). Integrating chytrid fungal parasites into plankton ecology: Research gaps and needs. *Environmental Microbiology, 19*(10), 3802-3822.

Frøslev, T. G., Matheny, P. B., & Hibbett, D. S. (2005). Lower level relationships in the mushroom genus *Cortinarius* (Basidiomycota, Agaricales): A comparison of RPB1, RPB2, and ITS phylogenies. *Molecular Phylogenetics and Evolution, 37*(2), 602-618.

Fujita, K., Forsyth, M., MacFarlane, D. R., Reid, R. W., & Elliott, G. D. (2006). Unexpected improvement in stability and utility of cytochrome c by solution in biocompatible ionic liquids. *Biotechnology and Bioengineering, 94*, 1209-1213.

Fujita, K., MacFarlane, D. R., & Forsyth, M. (2005). Protein solubilising and stabilising ionic liquids. *Chemical Communications*, 38, 4804-4806.

Fujita, K., MacFarlane, D. R., Forsyth, M., Yoshizawa-Fujita, M., Murata, K., Nakamura, N., & Ohno, H. (2007). Solubility and stability of cytochrome c in hydrated ionic liquids: effect of oxo acid residues and kosmotropicity. *Biomacromolecules, 8*, 2080-2086.

Fujita, K., & Ohno, H. (2010). Enzymatic activity and thermal stability of metallo proteins in hydrated ionic liquids. *Biopolymers, 93*, 1093-1099.

Fukumoto, K., Yoshizawa, M., & Ohno, H. (2005). Room temperature ionic liquids from 20 natural amino acids. *Journal of the American Chemical Society, 127*(8), 2398-2399.

García-Martinez, G., Alonso Bustabad, E., Perrot, H., Gabrielli, C., Bucur, B., Lazerges, M., … Arnau Vives, A. (2011). Development of a mass sensitive quartz crystal microbalance (QCM)-based DNA biosensor using a 50 MHz electronic oscillator circuit. *Sensors (Basel)*, 11(8), 7656-7664.

Gates, K. S. (2009). An overview of chemical processes that damage cellular dna: spontaneous hydrolysis, alkylation, and reactions with radicals. *Chemical Research in Toxicology, 22*(11), 1747-1760.

Ge, Z. W., Jacobs, A., Vellinga, E. C., Sysouphanthong, P., & van der Walt, R. (2018). A multigene phylogeny of *Chlorophyllum* (Agaricaceae, Basidiomycota): new species, new combination and infrageneric classification. *MycoKeys, 32*, 65-90.

Geiser, D. M. (2004). In advances in fungal biotechnology for industry, agriculture, and medicine. *Springer*, 3-14. date of access: 11/06/2019.

Geml, J., Laursen, G. A., Timling, I., McFarland, J. M., & Booth, M. G. (2009). Molecular phylogenetic biodiversity assessment of arctic and boreal ectomycorrhizal *Lactarius* Pers. (Russulales; Basidiomycota) in Alaska, based on soil and sporocarp DNA. *Molecular Ecology, 18*, 2213-2227.

Genereux, J. C., & Barton, J. K. (2010). Mechanisms for DNA charge transport. *Chemical Reviews, 110*, 1642-1662.

Giese, B., Amaudrut, J., Köhler, A. K., Spormann, M., & Wessely, S. (2001). Direct observation of hole transfer through DNA by hopping between adenine bases and by tunnelling. *Nature, 412*(6844), 318-320.

Giudicelli, G. C., Mäder, G., & Brandaode Freitas, L. (2015). Efficiency of ITS sequences for DNA barcoding in *Passiflora* (Passifloraceae). *International Journal of Molecular Sciences, 16*, 7289-7303.

Gomez-Navarro, C., Moreno-Herrero, F., de Pablo, P. J., Colchero, J., Gomez-Herrero, J., & Baro, A. M. (2002). Contactless experiments on individual DNA molecules show no evidence for molecular wire behavior. *Proceedings of the National Academy of Sciences, 99*(13), 8484-8487.

Gorodetsky, A. A., Buzzeo, M. C., & Barton, J. K. (2009). DNA-mediated electrochemistry. *Bioconjugate Chemistry*, 19(12), 2285-2296.

Güllü, Ö. (2010). Ultrahigh (100%) barrier modification of n-InP Schottky diode by DNA biopolymer nanofilms. *Microelectronic Engineering, 87*(4), 648-651.

Güllü, Ö., Çankaya, M., Barış, Ö., & Türüt, A. (2008a). DNA-based organic-on-inorganic devices: Barrier enhancement and temperature issues. *Microelectronic Engineering, 85*(11), 2250-2255.

Güllü, Ö., Cankaya, M., Barış, Ö., Biber, M., Özdemir, H., Güllüce, M., & Türüt, A. (2008b). DNA-based organic-on-inorganic semiconductor Schottky structures. *Applied Surface Science, 254*(16), 5175-5180.

Güllü, Ö., Çankaya, M., Barış, Ö., & Türüt, A. (2008c). DNA-modified indium phosphide Schottky device. *Applied Physics Letters, 92*(21), Article#212106.

Güllü, Ö., Pakma, O., & Türüt, A. (2012). Current density-voltage analyses and interface characterization in Ag/DNA/p-InP structures. *Journal of Applied Physics, 111*(4), Article#44503.

Güllü, Ö., & Türüt, A. (2011). Electronic properties of Al/DNA/p-Si MIS diode: Application as temperature sensor. *Journal of Alloys and Compounds, 509*(3), 571-577.

Güllü, Ö., & Türüt, A. (2015). Electronic parameters of MIS Schottky diodeswith DNA biopolymer interlayer. *Materials Science, 33*(3), 593-600.

Guo, C., Song, Y., Wei, H., Li, P., Wang, L., Sun, L., … Li, Z. (2007). Room temperature ionic liquid doped dna network immobilized horseradish peroxidase biosensor for amperometric determination of hydrogen peroxide. *Analytical and Bioanalytical Chemistry, 389*, 527-32.

Gupta, R., & Yakuphanoglu, F. (2012) Photoconductive Schottky diode based on Al/p-Si/SnS2/Ag for optical sensor applications. *Solar Energy, 86*, 1539-1545.

Gupta, R. K., Yakuphanoglu, F., Hasar, H., & Al-Khedhairy, A. A. (2011). p-Si/DNA photoconductive diode for optical sensor applications. *Synthetic Metals, 161*(17), 2011-2016.

Hall, I. R., Wang, Y., & Amicucci, A. (2003). Cultivation of edible ectomycorrhizal mushrooms. *Trends in Biotechnology, 21*(10), 433-438.

Hall, T.A. (1999). BioEdit: a user-friendly biological sequence alignment editor and analysis program for Windows 95/98/NT. *Nucleic Acids Symposium Series, 41*, 95-98.

Hamann, T. W., Gstrein, F., Brunschwig, B. S., & Lewis, N. S. (2006). Measurement of the driving force dependence of interfacial charge-transfer rate constants in response to pH changes at n-ZnO/H2O interfaces. *Chemical Physics, 326*(1), 15-23.

Hammouda, B., & Worcester, D. (2006). The denaturation transition of dna in mixed solvents. *Biophysical Journal, 91*(6), 2237-2242.

Harrower, E., Ammirati, J. F., Cappuccino, A. A., Ceska, O., & Kranabetter, J. M. (2011). *Cortinarius* species diversity in British Columbia and molecular phylogenetic comparison with European specimen sequences. *Botany, 89*, 799-810.

Haugstad, G. (2012). Atomic force microscopy: understanding basic modes and advanced applications: John Wiley & Sons.

He, Y., Li, Z., Simone, P., & Lodge, T. P. (2006). Self-Assembly of Block Copolymer Micelles in an Ionic Liquid. *Journal of the American Chemical Society, 128*(8), 2745-2750.

Heeger, F., Bourne, E. C., Baschien, C., Yurkov, A., Bunk, B., Spröer, C., … Monaghan, M. T. (2018). Long-read DNA metabarcoding of ribosomal rRNA in the analysis of fungi from aquatic environments. *Molecular Ecology Resources, 18*(6), 1500-1514.

Heim, T., Deresmes, D., & Vuillaume, D. (2004). Conductivity of DNA probed by conducting-atomic force microscopy: Effects of contact electrode, DNA structure, and surface interactions. *Journal of Applied Physics, 96*(5), 2927-2936.

Herbert, B. M. (1977). The work function of the elements and its periodicity. *Journal of Applied Physics, 48*, 4729-4733.

Hebert, P. D., Cywinska, A., Ball, S. L., & Dewaard, J. R. (2003). Biological identifications through DNA barcodes. *Proceedings of the Royal Society B: Biological Sciences, 270*(1512), 313-321.

Hey, J. (2001). The mind of the species problem. *Trends in Ecology & Evolution, 16*, 326-329.

Hillis, D. M., & Moritz, C. (1990). Molecular Systematics. Sunderland, Massachussets: Sinaeur Associates, Inc.

Holbrey, J. D., & Seddon, K. R. (1999). Ionic liquids. *Clean Technologies and Environmental Policy, 1*, 223-236.

Hu, C. (2009). Modern Semiconductor Devices for Integrated Circuits. *Chenming C., Hu (1ed.). Chapter 4*, 89-156.

Huddleston, J. G., Visser, A. E., Reichert, W. M., Willauer, H. D., Broker, G. A., & Rogers, R. D. (2001). Characterization and comparison of hydrophilic and hydrophobic room temperature ionic liquids incorporating the imidazolium cation. *Green Chemistry, 3*(4), 156-164.

Huddleston, J. G., Willauer, H. D., Swatloski, R. P., Visser, A. E., & Rogers, R. D. (1998). Room temperature ionic liquids as novel media for 'clean' liquid-liquid extraction. *Chemical Communications, 16*, 1765-1766.

Hussein, J. M., Tibuhwa, D. D., Mshandete, A. M., & Kivaisi, A. K. (2014). Molecular phylogeny of saprophytic wild edible mushroom species from Tanzania based on ITS and nLSU rDNA sequences. *Current Research in Environmental & Applied Mycology, 4*(2), 250-260.

Huzefa, A. R., Andrew, N. M., Cedric, J. P., & Nicholas, H. O. (2017). Fungal Identification Using Molecular Tools: A Primer for the Natural Products Research Community. *Journal of Natural Products, 80*, 756-770.

Hwang, J. S., Hwang, S. W., & Ahn, D. (2003). Electrical conduction measurement of thiol modified DNA molecules. *Superlattices and Microstructures, 34*(3), 433-438.

Hyde, K. D., Bahkali, A. H., & Moslem, M. A. (2010). Fungi - an unusual source for cosmetics. *Fungal Diversity, 43*, 1-9.

Iqbal, A., Sadia, B., Khan, A. I., Awan, F. S., Kainth, R. A., & Sadaqat, H. A. (2010). Biodiversity in the sorghum (Sorghum bicolor L. Moench) germplasm of Pakistan. *Genetics and Molecular Research, 9*, 756-764.

Jin, H., Wei, M., & Wang, J. (2013). Electrochemical DNA biosensor based on the BDD nanograss array electrode. *Chemistry Central Journal*, 7, Article#65.

Johnson, A. D. (2010). An extended IUPAC nomenclature code for polymorphic nucleic acids. *Bioinformatics, 26*(10), 1386-1389.

Johansson, E., Boettcher, S. W., O'Leary, L. E., Poletayev, A. D., Maldonado, S., Brunschwig, B. S., & Lewis, N. S. (2011). Control of the pH-Dependence of the band edges of Si (111) surfaces using mixed Methyl/Allyl monolayers. *The Journal of Physical Chemistry C, 115*, 8594-8601.

Joseph, S. W., Colwell, R. R., & Kaper, J. B. (1982). Vibrio parahaemolyticus and related halophilic vibrios. *CRC Critical Reviews in Microbiology, 10*, 77-124.

Juma, I., Mshandete, A. M., Tibuhwa, D. D., & Kivaisi, A. K. (2016). Identification of Tanzanian saprophytic edible mushrooms by amplification and sequencing of ITS/LSU regions of ribosomal RNA operon. *Tanzania Journal of Science, 42*, 109-121.

Jumbri, K., Abdul Rahman, M. B., Abdulmalek, E., Ahmad, H., & Micaelo, N. M. (2014). An insight into structure and stability of DNA in ionic liquids from molecular dynamics simulation and experimental studies. *Physical Chemistry Chemical Physics, 16*, 14036-14046.

Junior, N. M., Asai, T., Capelari, M. & Paccola Meirelles, L. D. (2010). Morphological and molecular identification of four Brazilian commercial isolates of *pleurotus* spp. and cultivation on corncob. *Brazilian Archives of Biology and Technology, 53*, 397-408.

Kasumov, A. Y., Kociak, M., Gueron, S., Reulet, B., Volkov, V. T., Klinov, D. V., & Bouchiat, H. (2001). Proximity-induced superconductivity in DNA. *Science, 291*(5502), 280-282.

Kelley, S. O., & Barton, J. K. (1999). Electron transfer between bases in double helical DNA. *Science, 283*(5400), 375-381.

Kharel, G. P., & Hashinaga, F. (1999). Changes of pH and electrical conductivity of water treated under high-voltage electric field. *Nepal Journal of Science and Technology, 2*, 1-4.

Khatir, N. M., Banihashemian, S. M., Periasamy, V., Ritikos, R., Majid, W. H. A., & Rahman, S. A. (2012). Electrical characterization of Gold-DNA-Gold structures in presence of an external magnetic field by means of IV curve analysis. *Sensors, 12*(3), 3578-3586.

Kim, K. S., Demberelnyamba, D. & Lee, H. (2004). Size-selective synthesis of gold and platinum nanoparticles using novel thiol-functionalized ionic liquids. *Langmuir, 20*(3), 556-560.

Kim, Y. T., Choi, E. H., Son, B. K., Seo, E. H., Lee, E. K., Ryu, J. K., … Lee, K. R. (2011). Effects of storage buffer and temperature on the integrity of human DNA. *Korean Journal of Clinical Laboratory Science, 44*, 24-30.

Kimura, M. (1968). Evolutionary rate at the molecular level. *Nature, 217*, 624-626.

Kiss, L. (2012). Limits of nuclear ribosomal DNA internal transcribed spacer (ITS) sequences as species barcodes for Fungi. *Proceedings of the National Academy of Sciences, 109*(27), Article#E1811.

Kittel, C. (1995). Introduction to solid state physics, 7th ed. Wiley, ISBN 0-471-11181-3.

Kiuru, T., Mallat, J., Raisanen, A. V., & Narhi, T. (2011). Schottky diode series resistance and thermal resistance extraction from S-parameter and temperature controlled *I-V* measurements. *IEEE Transactions on Microwave Theory and Techniques, 59*(8), 2108-2116.

Klug, A. (2004). The discovery of the DNA double helix. *Journal of Molecular Biology, 335*, 3-26.

Landeweert, R., Hoffland, E., Finlay, R. D., Kuyper, T. W., & Breemen, N. V. (2001). Linking plants to rocks: ectomycorrhizal fungi mobilize nutrients from minerals. *Trends in Ecology & Evolution, 16*(5), 248-254.

Lando, D. Y., Haroutiunian, S. G., Kul'ba, A. M., Dalian, E. B., Orioli, P., Mangani, S., & Akhrem, A. A. (1994). Theoretical and experimental study of DNA helix-coil transition in acidic and alkaline medium. *Journal of Biomolecular Structure & Dynamics, 12*(2), 355-366.

Larkin, M. A., Blackshields, G., Brown, N. P., Chenna, R., McGettigan, P. A., McWilliam, H., … Higgins, D. G. (2007). Clustal W and Clustal X version 2.0. *Bioinformatics, 23*(21), 2947-8.

Lawrence, A. J., & Smith, G. M. (1974). Measurement of gastric acid secretion by conductivity. *European Journal of Pharmacology, 25*(3), 383-389.

Lee, H. Y., Tanaka, H., Otsuka, Y., Yoo, K. H., Lee, J. O., & Kawai, T. (2002). Control of electrical conduction in DNA using oxygen hole doping. *Applied Physics Letters, 80*(9), 1670-1672.

Legoff, J., Tanton, C., Lecerf, M., Gresenguet, G., Nzambi, K., Bouhlal, H., Weiss, H., & Belec, L. (2006). Influence of storage temperature on the stability of HIV-1 RNA and HSV-2 DNA in cervicovaginal secretions collected by vaginal washing. *Journal of Virological Methods, 138*, 196 -200.

Lents, N. H. (2010). DNA III: The Replication of DNA. *Vision learning Vol. BIO-3*: (2). Retrieved on 12 June 2018 from http://www.visionlearning.com/en/library/Biology/2/DNA-III/180.

Leone, A. M., Weatherly, S. C., Williams, M. E., Thorp, H. H., & Murray, R. W. (2001). An ionic liquid form of DNA: redox-active molten salts of nucleic acids. *Journal of the American Chemical Society, 123*(2), 218-22.

Lerman, L. S. (1964). Acridine mutagens and DNA Structure. *Journal of Cellular Physiology, 64*(1), 1-18.

Leveling, T. (2002). The relationship between pH and conductivity in a lithium contaminated, de-ionized water system. *Fermilab-Pbar-Note, 674*, 1-11.

Li, J., He, X., Liu, X. B., Yang, Z. L., & Zhao, Z. W. (2017). Species clarification of oyster mushrooms in China and their DNA barcoding. *Mycological Progress, 16*, 191-203.

Li, Y., Xiang, L., Palma, J. L., Asai, Y., & Tao, N. (2016). Thermoelectric effect and its dependence on molecular length and sequence in single DNA molecules. *Nature Communications,* 7, Article#11294.

Liimatainen, K. (2013). Towards a better understanding of the systematics and diversity of *Cortinarius*, with an emphasis on species growing in boreal and temperate zones of Europe and North America. Academic dissertation, Faculty of Biological and Environmental Sciences of the University of Helsinki. pp 5-7.

Lin, X., Jiang, X., & Lu, L. (2005). DNA deposition on carbon electrodes under controlled dc potentials. *Biosensors and Bioelectronics, 20*(9), 1709-1717.

Lindahl, T., & Nyberg, B. (1972). Rate of depurination of native deoxyribonucleic acid. *Biochemistry, 11*, 3610-3618.

Lindner, D. L., & Banik, M. T. (2011). Intragenomic variation in the ITS rDNA region obscures phylogenetic relationships and inflates estimates of operational taxonomic units in genus *Laetiporus*. *Mycologia, 103*, 731-740.

Liu, K. L., Porras-Alfaro, A., Kuske, C. R., Eichorst, S. A., & Xie, G. (2012). Accurate, rapid taxonomic classification of fungal large-subunit rRNA genes. *Applied and Environmental Microbiology, 78*, 1523-1533.

Liu, Y. J., Hodson, M. C., & Hall, B. D. (2006). Loss of the flagellum happened only once in the fungal lineage: phylogenetic structure of kingdom Fungi inferred from RNA polymerase II subunit genes. *BMC Evolutionary Biology, 6*, Article#74.

Liu, Y. J., Whelen, S., & Hall, B. D. (1999). Phylogenetic relationships among Ascomycetes: Evidence from an RNA polymerse II subunit. *Molecular Biology and Evolution, 16*(12), 1799-808.

Loewe, L., & Hill, W. G. (2010). The population genetics of mutations: good, bad and indifferent. *Philosophical Transactions of the Royal Society B: Biological Sciences, 365*(1544), 1153-1167.

Luck, G., Zimmer, C., Snatzke, G., & Soendgerath, G. (1970). Optical rotatory dispersion and circular dichroism of DNA from various sources at alkaline pH. *European Journal of Biochemistry, 17*, 514-522.

Lyon, L. A., 7 Hupp, J. T. J. (1999). Energetics of the nanocrystalline titanium dioxide/aqueous solution interface: Approximate conduction band edge variations between H0 = −10 and H- = +26. *The Journal of Physical Chemistry B, 103*, 4623 - 4628.

Maciel, M. J. M., Silva, A. C., & Ribeiro, H. C. T. (2010). Industrial and biotechnological applications of ligninolytic enzymes of the Basidiomycota: A review. *Electronic Journal of Biotechnology, 13*(6), 1-13.

Macquet, J., & Butour, J. (1978). Modifications of the DNA secondary structure upon platinum binding: a proposed model. *Biochimie, 60*(9), 901-914.

Maftoun, P., Johari, H., Soltani, M., Malik, R., Othman, N. Z., & Enshasy, H. A. (2015). The edible mushroom *Pleurotus* spp.: I. biodiversity and nutritional values.). *International Journal of Biotechnology for Wellness Industries, 4*, 67-83.

Manoylov, K. M. (2014). Taxonomic identification of algae (morphological and molecular): species concepts, methodologies, and their implications for ecological bioassessment. *Journal of Phycology, 50*(3), 409-424.

Mäntele, W., & Deniz, E. (2017). UV–VIS absorption spectroscopy: Lambert-Beer reloaded: Elsevier.

Manzi, P., Aguzzi, A., &. Pizzoferrato, L. (2001). Nutritional value of mushrooms widely consumed in Italy. *Food Chemistry, 73*, 321-325.

Mark, K., Cornejo, C., Keller, C., Fluck, D., & Scheidegger, C. (2016). Barcoding lichen-forming fungi using 454 pyrosequencing is challenged by artifactual and biological sequence variation. *Genome, 59*(9), 685-704.

Martin, F., Cullen, D., Hibbett, D., Pisabarro, A., & Spatafora, J. W. (2011). Sequencing the fungal tree of life. *New Phytologist, 190*, 818-821.

Matheny, P. B. (2005). Improving phylogenetic inference of mushrooms with RPB1 and RPB2 nucleotide sequences (*Inocyb*e; Agaricales). *Molecular Phylogenetics and Evolution, 35*(1), 1-20.

Matheny, P. B., Liu, Y. J., Ammirati, J. F., & Hall, B. D. (2002). Using RPB1 sequences to improve phylogenetic inference among mushrooms (*Inocybe*, Agaricales). *American Journal of Botany, 89*, 688-698.

Matheny, P. B., Wang, Z., Binder, M., Curtis, J. M., and Lim, Y. W. (2007). Contributions of RPB2 and Tef1 to the phylogeny of mushrooms and allies (Basidiomycota, Fungi). *Molecular Phylogenetics and Evolution, 43*, 430-451.

McFail-Isom, L., Sines, C. C., & Williams, L. D. (1999). DNA Structure: Cations in Charge. *Current Opinion in Structural Biology, 9*, 298-304.

Menhaj, A. B., Smith, B. D., & Liu, J. (2012). Exploring the thermal stability of dna-linked gold nanoparticles in ionic liquids and molecular solvents. *Chemical Science, 3*, Article#3216.

Michelson, A. M., Massoulie, J., & Guschlbauer, W. (1967). Synthetic polynucleotides. *Progress in Nucleic Acid Research and Molecular Biology, 6*, 83-141.

Millanes, A. M., Diederich, P., & Wedin, M. (2016). *Cyphobasidium* gen. nov., a new lichen inhabiting lineage in the Cystobasidiomycetes (Pucciniomycetes, Basidiomycetes, Fungi). *Fungal Biology, 120*, 1468-1477.

Mishra, U., & Singh, J. (2007). Semiconductor Device Physics and Design. Springer Netherlands. Retrieved on 1 November 2017 from https://books.google.com.my/books?id=7WKOfUR-.

Mortimer, P. E., Karunarathna, S. C., Li, Q., Gui, H., Yang, X., Yang, X., … Hyde, K. D. (2012). Prized edible Asian mushrooms: ecology, conservation and sustainability. *Fungal Diversity, 56*, 31-47.

Murphy, C. J., Arkin, M. R., Jenkins, Y., Ghatlia, N. D., Bossmann, S. H., Turro, N. J., & Barton, J. K. (1993). Long-range photoinduced electron transfer through a DNA helix. *Science, 262,* 1025-1029.

Natarajan, T. S. (2012). Functional nanofibers in microelectronics applications. *Woodhead Publishing Series in Textiles*, 371-410

Natarajan, A., Devi, K. S., Raja, S. & Senthil Kumar, A. (2017). An elegant analysis of white spot syndrome virus using a graphene oxide/methylene blue based electrochemical immunosensor platform. *Scientific Report, 7*, 1-11.

Neamen, D. (2003). Semiconductor Physics and Devices: 3rd ed. New York: McGraw-Hill.

Nelson, D. L., & Cox, M. M. (2008). Lehninger Principles of Biochemistry. New York: W.H. Freeman and Company. 5th edition. Chapter 2. 60-74.

Nilsson, R. H., Kristiansson, E., Ryberg, M., Hallenberg, N., & Larsson, K. H. (2008). Intraspecific ITS variability in the Kingdom Fungi as expressed in the international sequence databases and its implications for molecular species identification. *Evolutionary Bioinformatics Online, 4*, 193-201.

Niranjan, R. B. P. (2011). Basics for the construction of phylogenetic trees. *WebmedCentral*, *2*(12), 1-11.

Nishimura, N., Nomura, Y., Nakamura, N., & Ohno, H. (2005). DNA strands robed with ionic liquid moiety. *Biomaterials, 26*, 5558-63.

Nishimura, N., & Ohno, H. (2002). Design of successive ion conduction paths in dna films with ionic liquids. *Journal of Materials Chemistry*, *12,* 2299-2304.

Ohayon, Y. P., Sha, R., Flint, O., & Seeman, N. C. (2011). Topological bonding of DNA nanostructures. *Journal of Biomolecular Structure and Dynamics, 8* (6), 1046-1046.

Ohno, H., & Nishimura, N. (2001). Ion conductive characteristics of DNA film containing ionic liquids. *Journal of The Electrochemical Society, 148*, Article#E168.

Ohsowski, B. M., Zaitsoff, D. P., Öpik, M., & Hart, M. M. (2014). Where the wild things are: Looking for uncultured Glomeromycota. *New Phytologist, 204*(1), 171-179.

Okur, S., Yakuphanoglu, F., Ozsoz, M., & Kadayifcilar, P. K. (2009). Electrical and interface properties of Au/DNA/n-Si organic-on-inorganic structures. *Microelectronic Engineering, 86*(11), 2305-2311.

Ordynets, A., Scherf, D., Pansegrau, F., Denecke, J., & Lysenko, L. (2018). Short-spored *Subulicystidium* (Trechisporales, Basidiomycota): high morphological diversity and only partly clear species boundaries. *MycoKeys, 35*, 41-99.

Page, R. D. M. (1996). TREEVIEW: An application to display phylogenetic trees on personal computers. *Computer Applications in the Biosciences, 12*, 357-358.

Pánek, M., Wiesnerová, L., Jablonský, I., Novotný, D., & Tomšovský, M. (2019). What is cultivated oyster mushroom? Phylogenetic and physiological study of *Pleurotus ostreatus* and related taxa. *Mycological Progress, 18*, 1173-1186.

Pereira, F., Carneiro, J., & Amorim, A. (2008). Identification of species with DNA-based Technology: Current progress and challenges. *Recent Patents on DNA & Gene Sequences, 2*, 187-200.

Periasamy, V., Rizan, N., Al-Ta'ii, H. M. J., Tan, Y. S., Annuar Tajuddin, H., & Iwamoto, M. (2016). Measuring the electronic properties of DNA-specific schottky diodes towards detecting and identifying basidiomycetes DNA. *Scientific Report, 6*, 1-9.

Perrin, C. L., & Nielson, J. B. (1997). "Strong" hydrogen bonds in chemistry and biology. *Annual Review of Physical Chemistry, 48*, 511-544.

Philip, G. M., & Shu-Ting, C. (2004). Mushrooms: Cultivation, nutritional value, medicinal effect, and environmental impact. (2nd edition). *CRC Press,* 315-325.

Plechkova, N. V., & Seddon, K. R. (2008). Applications of ionic liquids in the chemical industry. *Chemical Society Reviews, 37*, 123-50.

Poltronieri, P., D'Urso, O. F., Blaiotta, G., & Morea, M. (2008). DNA arrays and membrane hybridization methods for screening of six *Lactobacillus* species common in food products. *Food Analytical Methods, 1*, 171-180.

Porath, D., Bezryadin, A., De Vries, S., & Dekker, C. (2000). Direct measurement of electrical transport through DNA molecules. *Nature, 403*(6770), 635-638.

Porath, D., Lapidot, N., & Gomez-Herrero, J. (2006). Charge transport in DNA-based devices. *Introducing Molecular Electronics, Springer Berlin Heidelberg,* 411-444.

Porras-Alfaro, A., Liu, K. L., Kuske, C. R., & Xiec, G. (2014). From genus to phylum: large-subunit and internal transcribed spacer rRNA operon regions show similar classification accuracies influenced by database composition. *Applied and Environmental Microbiology, 80*, 829-840.

Pray, L. (2008). Discovery of DNA structure and function: Watson and Crick. *Nature Education, 1*(1), Article#100.

Privalov, P. L., & Ptitsyn, O. B. (1969). Determination of stability of the DNA double helix in an aqueous medium. *Biopolymers, 8*, 559-571.

Qin, W., & Li, S. F. Y. (2003). Electrophoresis of DNA in Ionic liquid coated capillary. *The Analyst, 128*, 37-41.

Raja, H. A., Miller, A. N., Pearce, C. J., & Oberlies, N. H. (2017). Fungal identification using molecular tools: a primer for the natural products research community. *Journal of Naturel Products, 80*(3), 756-770.

Reddy, V. R., Reddy, M. S. P., Lakshmi, B. P., & Kumar, A. A. (2011). Electrical characterization of Au/n-GaN metal–semiconductor and Au/SiO2/n-GaN metal–insulator–semiconductor structures. *Journal of Alloys and Compounds, 509*, 8001–8007.

Riley, M., Maling, B., & Chamberlin, M. J. (1966). Physical and chemical characterization of two- and three-stranded adenine-thymine and adenine-uracil homopolymer complexes. *Journal of Molecular Biology, 20*, 359-389.

Rizan, N., Yew, C.Y., Niknam, M.R., Krishnasamy, J., Bhassu, S., Hong, G.Z., … Periasamy, V. (2018). Electronic properties of synthetic shrimp pathogens-derived DNA schottky diodes. *Scientific Report, 8*(896), 1-9.

Robert, B., & Louis, N. (1995). Electronic devices and circuit theory. 7th-Edition. 810-813.

Robert, V., Szöke, S., Eberhardt, U., Cardinali, G., Meyer, W., Seifert, K. A., & Lewis, C. T. (2011). The quest for a general and reliable fungal DNA barcode. *Open Applied Informatics Journal, 5*, 45-61.

Robles- Hernandez, L., Cecilia- Gonzalez-Franco, A., Soto- Parra, J. M., & Montes-Dominguez, F. (2008). Review of agricultural and medicinal applications of Basidiomycete mushrooms. *Mayo- Agosto, 2*(2), 95-107.

Rockett, A. (2007). The materials science of semiconductors. *Springer, NY, USA. University of Illinois, 622*, 395-446.

Röder, B., Frühwirth, K., Vogl, C., Wagner, M., & Rossmanith, P. (2010). Impact of long-term storage on stability of standard DNA for nucleic acid-based methods. *Journal of Clinical Microbiology, 48*(11), 4260-4262.

Rodríguez-Laguna, N., Rojas-Hernández, A., Ramírez-Silva, M. T., Hernández-García, L., & Romero-Romo, M. (2015). An exact method to determine the conductivity of aqueous solutions in acid-base titrations. *Journal of Chemistry, 15*, 1-13.

Rogers, R. D., & Seddon, K. R. (2003). Chemistry. Ionic Liquids: solvents of the Future. *Science, 302*, 792-3.

Rokas, A. (2006). Genomics and the tree of life. *Science, 313*(5795), 1897-1899.

Rosenberg, M. S., & Kumar, S. (2001). Incomplete taxon sampling is not a problem for phylogenetic inference. *Proceedings of the National Academy of Sciences of the United States of America, 98*, 10751-10756.

Rossman, A. Y. (2007). Report of the planning workshop for all fungi DNA Barcoding. *Inoculum, 58*, 1-5.

Rychła, A., Benndorf, J., & Buczyński, P. (2011). Impact of pH and conductivity on species richness and community structure of dragonflies (Odonata) in small mining lakes. *Fundamental and Applied Limnology, 179*(1), 41-50.

Sadler, M. (2003). Nutritional properties of edible fungi. *British Nutrition Foundation, Nutrition Bulletin, 28*, 305-308.

Sainz, M. I., & Alfonso, R. P. (2012). DNA biosensors that reason. *Biosystems*, 109(2), 91-104.

Samanman, S., Kanatharana, P., Chotigeat, W., Deachamag, P., & Thavarungkul, P. Highly sensitive capacitive biosensor for detecting white spot syndrome virus in shrimp pond water. *Journal of Virological Methods, 173*, 75-84.

Samanta, A., & Medintz, I. L. (2016). Nanoparticles and DNA - a powerful and growing functional combination in bionanotechnology. *Nanoscale, 8*, 9037-9095.

Samiya, M. K., Aamir, N., Waqas, M., Nazir, J., Tahira, Y., Mehboob, R., … Azhar, A. K. (2011). Morphological and molecular characterization of oyster mushroom (*Pleurotus* spp.). *African Journal of Biotechnology*, *10*(14), 2638-2643.

Sanghita, D., & Bibhas, D. (2015). DNA barcoding of fungi using Ribosomal ITS Marker for genetic diversity analysis: A Review. *International Journal of Pure & Applied Bioscience, 3* (3), 160-167.

Sasaki, Y., Miyoshi, D., & Sugimoto, N. (2007). Regulation of DNA nucleases by molecular crowding. *Nucleic Acids Research, 35*, 4086-4093.

Sauer, P., Müller, M., & Kang, J. (1998) Quantitation of DNA. *Qiagen News, 2*, 23-26.

Scheeren, C. W., Machado, G., Dupont, J., Fichtner, P. F. P., & Ribeiro Texeira, S. (2003). Nanoscale Pt(0) particles prepared in imidazolium room temperature ionic liquids: synthesis from an organometallic precursor, characterization, and catalytic properties in hydrogenation reactions. *Inorganic Chemistry, 42*(15), 4738-4742.

Schoch, C. L., Robbertse, B., Robert, V., Vu, D., & Cardinali, G. (2014). Finding needles in haystacks: linking scientific names, reference specimens and molecular data for Fungi. Database Oxford University Press, 21p.

Schoch, C. L., Seifert, K. A., Caldeira, K., Myhrvold, N. P., Alvarez, R. A., Pacala, S. W., & Mullins, R. D. (2012b). Limits of nuclear ribosomal DNA internal transcribed spacer (ITS) sequences as species barcodes for Fungi. *Proceedings of the National Academy of Sciences, 109*, 10741-10742.

Schoch, C. L., Seifert, K. A., Huhndorf, S., Robert, V., & Spouge, J. L. (2012a). Nuclear ribosomal internal transcribed spacer (ITS) region as a universal DNA barcode marker for Fungi. *Proceedings of the National Academy of Sciences of the United States of America, 109*(16), 6241-6246.

Seddon, K. R. (1997). Review ionic liquids for clean technology. *Journal of Chemical Technology and Biotechnology, 50,* 1-6.

Seifert, K. A. (2009). Progress towards DNA barcoding of fungi. *Molecular Ecology Resources, 9,* 83-89.

Seifert, K. A., Samson, R. A., DeWaard, J. R., Houbraken, J., Levesque, C. A., Moncalvo, J. M., & Hebert, P. D. N. (2007). Prospects for fungus identification using CO1 DNA barcodes, with *Penicillium* as a test case. *Proceedings of the National Academy of Sciences, 104,* 3901-3906.

Segel, I. H. (1976). *Biochemical calculations* (2nd edn.). John Wi-ley & Sons, *Inc., New York.*

Selçuk, A. B., Ocak, S. B., Aras, F. G., & Orhan, E. O. (2014). Electrical characteristics of Al/poly (methyl methacrylate)/p-Si Schottky device. *Journal of Electronic Materials, 43,* 3263-3269.

Sharma, M., Mondal, D., Singh, N., Trivedi, N., Bhatt, J., & Prasad, K. (2015). High concentration DNA solubility in bio-ionic liquids with long-lasting chemical and structural stability at room temperature. *RSC Advances, 5,* 40546-40551.

Shnyreva, A. A., & Shnyreva, A. V. (2014). Phylogenetic analysis of *Pleurotus* Species. *Russian Journal of Genetics, 51*(2), 148-157.

Shockley, W. (1949). "The Theory of p-n Junctions in Semiconductors and p-n Junction Transis- tors,". *The Bell System Technical Journal, 28,* Article#435.

Shockley, W. (1950). Electrons and holes in semiconductors: with applications to transistor electronics. R. E. Krieger Pub. Co. ISBN 0-88275-382-7.

Singh, N., Sharma, M., Mondal, D., Pereira, M. M. & Prasad, K. (2017). Very high concentration solubility and long-term stability of DNA in an ammonium-based ionic liquid: A suitable medium for nucleic acid packaging and preservation. *ACS Sustainable Chemistry & Engineering, 5*, 1998-2005.

Smietana, M., & Mioskowski, C. (2001). Preparation of silyl enol ethers using (Bistrimethylsilyl) acetamide in ionic liquids. *Organic Letters, 3*, 1037-1039.

Smith, M. E., Henkel, T. W., Uehling, J. K., Fremier, A. K., Clarke, H. D., & Vilgalys, R. (2013). The ectomycorrhizal fungal community in a neotropical forest dominated by the endemic dipterocarp *Pakaraimaea dipterocarpacea*. *PLoS ONE, 8*(1), Article#e55160.

Sönmezoğlu, S., Sönmezoğlu, Ö. A., Çankaya, G., Yıldırım, A., & Serin, N. (2010). Electrical characteristics of DNA-based metal-insulator-semiconductor structures. *Journal of Applied Physics, 107*(12), Article#124518.

Sorokin, V. A., Gladchenko, G. O., & Valeev, V. A. (1986). DNA Protonation at low ionic strength of solution. *Macromolecular Chemistry, 187*, 1053-1063.

Spectronic, T. (2012). Basic UV-Vis Theory, Concepts and Applications. *Thermo Spectronic, 10*(12), *1*-28.

Stajich, J. E., Berbee, M. L., Blackwell, M., Hibbett, D. S., James, T. Y., Spatafora, J. W., & Taylor, J. W. (2009). The Fungi. *Current Biology, 19*, 840-845.

Staniaszek, M., Marczewski, W., Szudyga, K., Maszkiewicz, J., Czaplicki, A., & Qian, G. (2002). Genetic relationship between Polish and Chinese strains of the mushroom *Agaricus bisporus* (Lange) Sing., determined by the RAPD method. *Journal of Applied Genetics, 43*, 43-47.

Stielow, J. B., Lévesque, C. A., Seifert, K. A., Meyer, W., & Irinyi, L. (2015). One fungus, which genes? development and assessment of universal primers for potential secondary fungal DNA barcodes. *Persoonia, 35*, 242-263.

Stiller, J. W., & Hall, B. D. (1997). The origin of red algae: implications for plastid evolution. *Proceedings of the National Academy of Sciences of the United States of America, 94*, 4520-4525.

Stockinger, H., Peyret-Guzzon, M., Koegel, S., Bouffaud, M. L., & Redecker, D. (2014). The Largest Subunit of RNA Polymerase II as a New Marker Gene to Study Assemblages of Arbuscular Mycorrhizal Fungi in the Field. *PLoS ONE, 9*(10), Article#e107783.

Storm, A. J., Van Noort, J., De Vries, S., & Dekker, C. (2001). Insulating behavior for DNA molecules between nanoelectrodes at the 100 nm length scale. *Applied Physics Letters, 79*(23), 3881-3883.

Summerbell, R. C., Moore, M. K., Starink-Willemse, M., & Van Iperen, A. (2007). ITS barcodes for *Trichophyton tonsurans* and *T. equinum*. *Medical Mycology, 45*, 193-200.

Sun, W., Li, Y., Duan, Y., & Jiao, K. (2008). Direct electrocatalytic oxidation of adenine and guanine on carbon ionic liquid electrode and the simultaneous determination. *Biosensors & bioelectronics, 24*, 994-9.

Sun, W., Li, Y., Yang, M., Liu, S., & Jiao, K. (2008). Direct electrochemistry of single-stranded dna on an ionic liquid modified carbon paste electrode. *Electrochemistry Communications, 10*, 298-301.

Sun, Y., & Kiang, C. H. (2005). DNA-based artificial nanostructures: Fabrication, properties, and applications. *Handbook of Nanostructured Biomaterials and Their Applications in Nanobiotechnology, 1*(2), 1-33.

Suzuki, T., Ohsumi, S., & Makino, K. (1994). Mechanistic studies on depurination and apurinic site chain breakage in oligodeoxyribonucleotides. *Nucleic Acids Research, 22*, 4997-5003.

Sze, S. M., & Ng, K. K. (2006). Physics of semiconductor devices. John Wiley & Sons.

Tahir, M., Sayyad, M. H., Shahid, M., Chaudry, J. A., & Munawar, A. (2012). Fabrication of Al/N-BuHHPDI/ITO Schottky barrier diode and investigation of its electrical properties. *International Conference on Advances in Electrical and Electronics Engineering (ICAEEE'2012), 4*.

Tamura, K., & Nei, M. (1993). Estimation of the number of nucleotide substitutions in the control region of mitochondrial DNA in humans and chimpanzees. *Molecular Biology and Evolution, 10*, 512-526.

Tanabe, Y., Watanabe, M. M., & Sugiyama, J. (2002). Are Microsporidia really related to Fungi?: A reappraisal based on additional gene sequences from basal fungi. *Mycological Research, 106*, 1380-1391.

Tanabe, Y., Saikawa, M., Watanabe, M. M., & Sugiyama, J. (2004). Molecular phylogeny of Zygomycota based on EF-1alpha and RPB1 sequences: limitations and utility of alternative markers to rDNA. *Molecular Phylogenetics and Evolution, 30*, 438-449.

Tataurov, A. V, You, Y., & Owczarzy, R. (2008). Predicting ultraviolet spectrum of single stranded and double stranded deoxyribonucleic acids. *Biophysical Chemistry*, *133*(1), 66-70.

Tateishi-Karimata, H., & Sugimoto, N. (2014). Structure, stability and behaviour of nucleic acids in ionic liquids. *Nucleic Acids Research, 42*(14), 8831-8844.

Taubert, A. (2004). CuCl nanoplatelets from an ionic liquid-crystal precursor. *Angewandte Chemie, 43*(40), 5380-5382.

Taylor, D. L., Booth, M. G., McFarland, J. W., Herriott, I. C., & Lennon, N. J. (2008). Increasing ecological inference from high throughput sequencing of fungi in the environment through a tagging approach. *Molecular Ecology Resources, 8*, 742-752.

Tekpinar, A. D., & Kalmer, A. (2019). Utility of various molecular markers in fungal identification and phylogeny. *Nova Hedwigia, 109* (2), 187-224.

Telleria, M. T., Dueñas, M., & Martín, M. P. (2017). Three new species of *Hydnophlebia* (Polyporales, Basidiomycota) from the Macaronesian Islands. *MycoKeys, 27*, 39-64.

Tembe, S., Karve, M., Inamdar, S., Haram, S., Melo, J., & D'Souza, S. F. (2006). Development of electrochemical biosensor based on tyrosinase immobilized in composite biopolymeric film. *Analytical Biochemistry*, 349(1), 72-77.

Tibuhwa, D. D., Savic, S., Tibell, L., & Kivaisi, A. K. (2012). *Afrocantharellus* gen. stat. nov. is part of a rich diversity of African *Cantharellaceae*. *IMA Fungus, 3*, 25-38.

Tissue, B. M. (2002). Ultraviolet and Visible Absorption Spectroscopy Characterization of Materials: John Wiley & Sons, Inc.

Todd, A. R. (1954). Chemical structure of the nucleic acids. *Proceedings of the National Academy of Sciences of the United States of America, 40*, 748-755.

Trincao, J., Johnson, R. E., Wolfle, W. T., Escalante, C. R., Prakash, S., Prakash, L., & Aggarwal, A. K. (2004). Dpo4 is hindered in extending a G.T mismatch by a reverse wobble. *Nature Structural & Molecular Biology, 11*, 457-462.

Tuğluoğlu, N. & Karadeniz, S. (2012). Analysis of current–voltage and capacitance–voltage characteristics of perylene-monoimide/n-Si Schottky contacts. *Current Applied Physics, 12*, 1529-1535.

Turner, A., Karube, I., & Wilson, G. S. (1987). Biosensors: fundamentals and applications. Oxford University Press, Oxford. ISBN: 0198547242, 770p.

Varga, J., Kocsubé, S., Tóth, B., Frisvad, J. C., Perrone, G., Susca, A., … Samson, R. A. (2007). *Aspergillus brasiliensis* sp. nov., a biseriate black *Aspergillus* species with world-wide distribution. *International Journal of Systematic and Evolutionary Microbiology, 57*, 1925-1932.

Venkatramani, R., Keinan, S., Balaeff, A., & Beratan, D. N. (2011). Nucleic acid charge transfer: Black, white and gray. *Coordination Chemistry Reviews, 255*(7), 635-648.

Ventra, M. D., & Zwolak, M. (2004). Encyclopedia of Nanoscience and Nanotechnology, edited by Hari Singh Nalwa. *American Scientific Publishers, 2*, 475-493.

Vesty, A., Biswas, K., Taylor, M. W., Gear, K., & Douglas, R. G. (2017). Evaluating the impact of DNA extraction method on the representation of human oral bacterial and fungal communities. *PLoS ONE, 12*(1), Article#e0169877.

Vidyasagar, D. (2019). Use of silicon over germanium in the manufacturing of semiconductor in LSI & VLSI Technology. DOI: 10.13140/RG.2.2.31045.81121. Research proposal.

Vijayaraghavan, R., Izgorodin, A., Ganesh, V., Surianarayanan, M., & MacFarlene, D. R. (2010). Long-term structural and chemical stability of DNA in hydrated ionic liquids. *Angewandte Chemie, 49*(9), 1631-3.

Vilgalys, R., & Hester, M. (1990). Rapid genetic identification and mapping of enzymatically amplified ribosomal DNA from several *Cryptococcus* Species. *Journal of Bacteriology, 172*(8), 4238-4246.

Vilgarys, R., & Sun, B. L. (1994). Ancient and recent patterns of geographic speciation in the oyster mushroom *Pleurotus* revealed by phylogenetic analysis of ribosomal DNA sequences. *Proceedings of the National Academy of Sciences of the United States of America, 91*, 4599-4603.

Vizzini, A., Angelini, C., Losi, C., & Ercole, E. (2018). Diversity of polypores in the Dominican Republic: *Pseudowrightoporia dominicana* sp. nov. (Hericiaceae, Russulales). *MycoKeys, 34*, 35-45.

Vizzini, A., Consiglio, G., Setti, L., & Murat, C. (2010). The agaricoid genus *Kinia* is a new member of the Pluteoid clade subordinate to *Melanoleuca*. *Mycosphere, 1*(2), 141-145.

Vydryakova, G. A., Van, D. T., Shoukouhi, P., Psurtseva, N. V., & Bissett, J. (2012). Intergenomic and intragenomic ITS sequence heterogeneity in *Neonothopanus nambi* (Agaricales) from Vietnam. *Mycology, 3*, 89-99.

Wang, X., Lim, H. J., & Son, A. (2014). Characterization of denaturation and renaturation of DNA for DNA hybridization. *Environmental Health and Toxicology, 29*, 1-8.

Wang, Z., Binder, M., Dai, Y. C. & Hibbett, D. S. (2004). Phylogenetic relationships of *Sparassis* inferred from nuclear and mitochondrial ribosomal DNA and RNA polymerase sequences. *Mycologia, 96*, 1015-1029.

Wang, Z., Nilsson, R. H., James, T. Y., Dai, Y., & Townsend, J. P. (2016). Future Perspectives and Challenges of Fungal Systematics in the Age of Big Data. In: Li DW. (Eds.), *Biology of Microfungi. Fungal Biology*. Springer, Cham.

Wasserscheid, P., & Keim, W. (2000). Ionic liquids-lew "Solutions" for transition metal catalysis. *Angewandte Chemie, 39*(21), 3772-3789.

Watanabe, H., Manabe, C., Shigematsu, T., Shimotani, K., & Shimizu, M. (2001). Single molecule DNA device measured with triple-probe atomic force microscope. *Applied Physics Letters, 79*(15), 2462-2464.

Watkinson, S.C. (2008). Basidiomycota. *Encyclopedia of life sciences, 8*, 1-9.

Watson, J. D., & Crick, F. H. C. (1953). A structure for deoxyribose nucleic acid. *Nature, 171*, 737-738.

Watson, S. J., Smallwood, R. H., Brown, B. H., Cherian, P., & Bardhan, K. D. (1996). Determination of the relationship between the pH and conductivity of gastric juice. *Physiological Measurement, 17*(1), 21-27.

Welton, T. (1999). Room-temperature ionic liquids. Solvents for synthesis and catalysis. *Chemical Reviews, 99*, 2071-2084.

Welton, T. (2011). Room-temperature ionic liquids: solvents for synthesis and catalysis.2. *Chemical Reviews, 111*, 3508-76.

White, T. J., Bruns, T., Lee, S., & Taylor, J. (1990). Amplification and direct sequencing of fungal ribosomal RNA genes for phylogenetics. In: PCR Protocols: a guide to methods and applications. *Academic Press, New York, USA* 315-322.

Williams, M. C., Wenner, J. R., Rouzina, I., & Bloomfield, V. A. (2001). Effect of pH on the overstretching transition of double-stranded DNA: evidence of force-induced DNA melting. *Biophysical Journal, 80*, 874-881.

Wilfinger, W. W., Mackey, K., & Chomczynski, P. (1997). Effect of pH and ionic strength on the spectrophotometric assessment of nucleic acid purity. *BioTechniques, 22*, 474-481.

Wyler, S. C., & Naciri, Y. (2016). Evolutionary histories determine DNA barcoding success in vascular plants: seven case studies using intraspecific broad sampling of closely related species. *BMC Evolutionary Biology, 16*(103), 1-11.

Xie, Y. N., Wang, S. F., Zhang, Z. L., & Pang, D. W. (2008). Interaction between room temperature ionic liquid [bmim]BF4 and DNA investigated by electrochemical micromethod. *The Journal of Physical Chemistry B, 112*, 9864-9868.

Xu, B., Zhang, P., Li, X., & Tao, N. (2004). Direct conductance measurement of single DNA molecules in aqueous solution. *Nano letters, 4*(6), 1105-1108.

Xu, J. (2016). Fungal DNA barcoding. *Genome, 59*, 913-932.

Yacobi, B. G. (2003). Semiconductor Materials: An Introduction to Basic Principles. (pp. 1-3). Springer. ISBN 0-306-47361-5.

Yang, Z., & Rannala, B. (2012). Molecular phylogenetics: principles and practice. *Genetics, 13*, 303-313.

Zang, D. Y. & Grote, J. G. (2007). Photoelectrical effect and current-voltage characteristics in DNA-metal Schottky barriers. *SPIE Proceedings Organic Photonic Materials and Devices IX, 6470*, 1-10.

Zervakis, G. (2004). Molecular systematics, evolution and speciation in higher fungi: the oyster-mushroom genus *Pleurotus*. *Plant Genome: Biodiversity and Evolution, 2*, 99-128.

Zervakis, G., & Balis, C. (1996). A pluralistic approach in the study of *Pleurotus* species with emphasis on compatibility and physiology of the European morphotaxa. *Mycological Research, 100*(6), 717-731.

Zhang, W., Yang, T., Zhuang, X., Guo, Z., & Jiao, K. (2009). An ionic liquid supported CeO2 nanoshuttles-carbon nanotubes composite as a platform for impedance DNA hybridization sensing. *Biosensors & Bioelectronics, 24*, 2417-22.

Zhang, Z. C. (2006). Catalysis in ionic liquids. *Advances in Catalysis, 49*,153-237.

Zhao, H. (2014). DNA stability in ionic liquids and deep eutectic solvents. *Journal of Chemical Technology & Biotechnology, 90*, 19-25.

Zhao, P., Luo, J., & Zhuang, W. (2011a). Practice towards DNA barcoding of the nectriaceous fungi. *Fungal Divers, 46*, 183-191.

Zhao, P., Luo, J., Zhuang, W., Liu, X., & Wu, B. (2011b). DNA barcoding of the fungal genus *Neonectria* and the discovery of two new species. *Science China Life Sciences, 54*(7), 664-674.

Zhou, Y., & Antonietti, M. (2003).Synthesis of Very Small TiO2 Nanocrystals in a room-temperature ionic liquid and their self-assembly toward mesoporous spherical aggregates. *Journal of the American Chemical Society, 125*(49), 14960-14961.

Zon, J. (2015). DNA's forgotten discoverer: Swiss scientist Friedrich Miescher. Retrieved on 17 June 2018 from http://zon.trilinkbiotech.com/2015/04/13/dnas-friedrich-miescher/.

LIST OF PUBLICATIONS

1. **Rizan**, **N**., Anuar Tajuddin, H., Tan, Y. S., Abdullah, Z., Idris, A., and Periasamy, V. (2021). Effect of ionic liquid on the long-term structural and chemical stability of basidiomycetes DNAs integrated within Schottky-like junctions. *Applied Physics A, 127*(142), 1-14.

2. **Rizan**, **N.**, Tan, Y. S., Annuar Tajuddin, H., Georgepeter Gnana, k., and Periasamy, V. (2020). Effect of pH on the conductivity of basidiomycetes DNAs integrated within schottky-Like junctions. *ChemistrySelect, 5*, 601-609.

3. Nazarudin, N. F. F. B., **Rizan**, **N**., Periasamy, V., Rahman, S. A, Goh, B. T. (2019). Physical, optical and electrical studies on hybrid Ag NPs/NiSi NWs electrode as a DNA template for biosensor. *Materials Research Express, 6*(095039), 1-13.

4. **Rizan**, **N**., Yew, C.Y., Niknam, M.R., Krishnasamy, J., Bhassu, S., Hong, G.Z., Devadas, S., Shariff Mohd Din, M., Annuar Tajuddin, H., Othman, R. Y., Phang, S.M., Iwamoto, M., and Periasamy, V. (2018). Electronic properties of synthetic shrimp pathogens-derived DNA schottky diodes. *Scientific Report, 8*(896), 1-9.

5. Azmi, S. Z., Vello, V., **Rizan**, **N**., Krishnasamy, J., Phang, S. M., Iwamoto, M., Periasamy, V., Talebi, S., Gunaselvam, P., Mohamed Iqbal, S. N. and Chan, Y. Y. (2018). Electronic profiling of Algae-Derived DNA using DNA-Specific schottky diode. *Journal of Applied Physics A, 124*(8), Article#559.

6. Shakir, S., Foo, Y. Y., **Rizan**, **N**., Abd-ur-Rehman, H. M., Yunus, K., Moi, P. S., and Periasamy, V. (2018), Electro-catalytic and structural studies of DNA templated gold wires on platinum/ITO as modified counter electrode in dye sensitized solar cells. *Journal of Materials Science: Materials in Electronics, 29*(6), 4602-4611.

7. Shakir, S., Saravanan, J., **Rizan**, **N**., Babu, K. J., Aziz, M. A., Moi, P. S., and Periasamy, V. (2018), Fabrication of capillary force induced DNA template Ag nanopatterns for sensitive and selective enzyme-free glucose sensors. *Sensors and Actuators B: Chemical, 256*, 820-827.

8. Periasamy, V., **Rizan**, **N**., Al-Ta'ii, H. M. J., Tan, Y. S., Annuar Tajuddin, H., and Iwamoto, M. (2016). Measuring the electronic properties of DNA-Specific schottky diodes towards detecting and identifying basidiomycetes DNA. *Scientific Report, 6*, 1-9.

PAPERS PRESENTED

1. 6th International Conference on Functional Materials and Devices (ICFMD, 2017). DNA/Specific Schottky Diodes for Application in DNA Detection. Melaka, Malaysia. Oral Presentation.

2. ASEAN Emerging Researchers Conference (2018). Sunway University, Malaysia. Oral Highlights Presentation.